A PEDOT BY ANY OTHER NAME: TUNING THE ELECTROACTIVITY OF DIOXY-HETEROCYCLES FOR REDOX AND SOLID STATE APPLICATIONS

A Dissertation
Presented to
The Academic Faculty

by

James F. Ponder Jr.

In Partial Fulfillment
of the Requirements for the Degree
Doctor of Philosophy in the
School of Chemistry and Biochemistry

Georgia Institute of Technology
August 2017

A PEDOT BY ANY OTHER NAME: TUNING THE ELECTROACTIVITY OF DIOXY-HETEROCYCLES FOR REDOX AND SOLID STATE APPLICATIONS

Approved by:

Dr. John R. Reynolds, Advisor
School of Chemistry and Biochemistry
School of Materials Science
Georgia Institute of Technology

Dr. Lawrence A. Bottomley
School of Chemistry and Biochemistry
Georgia Institute of Technology

Dr. Seth R. Marder
School of Chemistry and Biochemistry
Georgia Institute of Technology

Dr. Elsa Reichmanis
School of Chemical and Biomolecular Engineering
Georgia Institute of Technology

Dr. Stefan France
School of Chemistry and Biochemistry
Georgia Institute of Technology

Date Approved: [June 14, 2017]

“The trouble with having an open mind, of course, is that people will insist on coming along and trying to put things in it.”

- Terry Pratchett, Diggers

“I may not have gone where I intended to go, but I think I have ended up where I needed to be.”

- Douglas Adams, The Long Dark Tea-Time of the Soul

For Laura

ACKNOWLEDGEMENTS

I came to Georgia Tech in 2011, thinking I knew quite a bit about chemistry and how to do research based on my undergraduate experience. Six years later, I now know how little I knew then and how much there is still to learn. The past six years have been a time of personal and scientific growth and have been both the best and worst time of my life. While I am grateful for my time at Georgia Tech, I am happy to be moving on. Obtaining a Ph.D. is not a simple task and both my projects and I have made it more difficult. My first project lost funding after I had spent a year working on it and my second project has never reached completion or even a publishable point. Fortunately, Dr. Anna Österholm made an observation during a group meeting regarding the CV of a specific polymer prepared by Justin Kerszulis. I prepared a few polymers based on her observation and everything else proceeded from there. The work presented in this thesis represents only a part of what I have done. While many of the experiments I performed and a significant amount of time spent never resulted in publishable work, the experience I have gained from my failures has made me a better chemist.

First, I would like to thank my parents. My mother home-schooled me until I was 16 and then I started community college. She has always tried to help and encourage me in whatever I do. My father taught me from a young age the joy of tearing things apart to see how they work. Both my parents have supported my education even when I switched majors, out of nowhere, from criminal justice to... something else to be determined

involving science or computers. My lack of direction did not hamper their support and for that I am truly grateful.

I would also like to thank my Ph.D. research advisor, Dr. John R. Reynolds. He provided me with the time, space, and funding I needed to complete my Ph.D. work. He has always been willing to discuss my (sometimes crazy) ideas and let me take my research where it interested me. Together we have worked on two book chapters, two patents, seven (and counting) pear reviewed papers, and many grant proposals. From working together, I have learned how to design and, more importantly, complete projects. Additionally, I thank my thesis committee members, Dr. Stefan France, Dr. Lawrence Bottomley, Dr. Elsa Reichmanis, and Dr. Seth Marder for their teaching and willingness to answer questions.

Next, I would like to thank my coworkers. My discussions with them have covered everything from the nature of science, to trouble shooting reaction conditions, to new books and TV shows, to who would win in a fight between Superman and Goku. I have seen many other laboratories where researchers are not as helpful and friendly, and that has made me especially grateful to be in the Reynolds group. I particularly want to thank Dr. Anna Österholm and Dr. Eric Shen for their help in research over the past six years. Collaborations outside the Reynolds group have also been an important part of my time here at Tech. I would like to thank Akanksha Menon, Jing Zhou, Dr. Petr Ledin, Dr. Ju-Won Jeon, Dr. Vladimir Tsukruk, Dr. Raghunath Dasari, and Dr. Shannon Yee for their help.

Another person that requires special thanks is Professor John Hawes. In his class and laboratory I found a love and fascination with chemistry. In his lab I also met Laura N. Stewart, my future wife. Through him I have found my primary interest, my career, and my partner.

I would also like to give thanks to God, for the skills He has given me and for His strength and guidance that have sustained me during my time here at Georgia Tech.

Most importantly, I would like to thank my wife, Laura. I met her my junior year of college and she married me during my second year at Tech and has been my constant advocate over the past 5 years. She has taught me how to lay back and enjoy things as they come. She is always trying to get me to just have fun and not worry about what comes after. She has made the stress of graduate school bearable for me and I don't know how I could have made it through without her.

Finally, I want to thank you, the reader. While I imagine there will only ever be a few of you, I appreciate you taking the time to read this thesis.

-J. Ponder 5/2017

TABLE OF CONTENTS

LIST OF TABLES

LIST OF SCHEMES

LIST OF FIGURES

PAGE

LIST OF EQUATIONS

LIST OF SYMBOLS AND ABBREVIATIONS

CIE	International Commission on Illumination (Commission Internationale de l'Eclairage)
ECP	Electrochromic Polymer
$E_{g,\ opt}$	Optical Band Gap Energy
λ_{max}	Wavelength of Maximum Absorption
E_{ox}	Oxidation potential
D-A	donor-acceptor
XDOT	Dioxythiophene
XDOS	Dioxyselenophene
EC	Electrochromic
ECD	Electrochromic Device
SC	Supercapacitor
ITO	Indium tin oxide
PC	Propylene Carbonate
ACN	Acetonitrile
LiBTI	Lithium bis(trifluoromethane)sulfonamide
$TBAPF_6$	Tetrabutylammonium Hexafluorophosphate
pTSA	p-toluenesulfonic acid
GPC	gel permeation chromatography
NMR	Nuclear magnetic resonance spectroscopy
IR	Infrared
DHAP	Direct (Hetero)Arylation Polymerization
EH	2-ethylhexyl
HxDc (or HxDec)	2-hexyldecyl
OS	Organic soluble

WS	Water soluble
SR	Solvent resistant
PEDOT	poly(3,4-ethylenedioxythiophene)
PEDOT:PSS	poly(3,4-ethylenedioxythiophene):Poly(styrene sulfonate)
PProDOT	poly(3,4-propylenedioxythiophene)
ECP-M	ECP-Magenta
CV	Cyclic voltammetry (voltammogram)
DPV	Differential pulse voltammetry (voltammogram)
a*	Red-Green Balance
b*	Yellow-Blue Balance
L*	White-Black Balance

SUMMARY

Redox active conjugated polymers are actively being investigated for use in a variety of applications including electrochromism, charge storage, plasmonic resonance tuning, and electrochemical transistors. This thesis describes the development of processable, electron-rich dioxyheterocycle-based polymers for use in electrochromic and charge-storage applications. Previously, the materials used in the Reynolds Research Group for charge storage have been insoluble polymers prepared via electrochemical polymerization. This thesis reports the development of soluble polymers that can be solution processed from organic or aqueous solutions (inks) and are redox active in organic or aqueous electrolytes with variable optical and redox properties through subtle differences in the repeat units and heteroatoms used.

Materials with low onsets of oxidation and broad electroactivity over a large voltage window, as seen with electropolymerized poly(3,4-ethylenedioxythiophene) (PEDOT), are of interest for charge storage applications. Chapter 3 reports and discusses the copolymerization of alkoxy-functionalized 3,4-propylenedioxythiophenes (ProDOTs) with unfunctionalized 3,4-ethylenedioxythiophene (EDOT) in varying ratios using direct arylation to produce a series of solution processable polymers with highly tunable optical and electronic properties. Within this series, we have identified poly(ProDOT-*alt*-biEDOT) (PE_2), a copolymer containing 67% EDOT compositionally, which combines the low oxidation potential, the redox behavior, and the deep-blue neutral color that are characteristic of PEDOT with the high solubility, exceptional electrochromic contrast, and color neutrality in the oxidized state characteristic of alkoxy-functionalized

polyProDOTs. 3,4-Phenylenedioxythiophene (PheDOT) is a unit that is similar to EDOT in terms of planarity and steric interactions but has different electronic properties due to an attached phenyl ring that allows for electron delocalization away from the thiophene ring. This unit, and its use in soluble copolymers prepared via direct (hetero) arylation polymerization (DHAP), is discussed in Chapter 4. The notable C-H inactivity of the attached phenylene unit is compared to aromatic solvents used for DHAP and the redox stability of these copolymers are demonstrated. In order to decouple the effects of planarity and electron density in redox active polymers, differences in redox properties between poly(ProDOT-*alt*-biPheDOT) and PE_2 are discussed.

Dioxyselenophenes are another group of heterocycles that have significantly different properties to their thiophene counterparts; due to various factors including lowered aromatic character. The first example of a solution processable dioxythiophene-*alt*-dioxyselenophene polymer, poly(ProDOT-*alt*-EDOS), prepared via DHAP is reported and its optical and electrochemical properties are compared to the all thiophene analog and other relevant dioxythiophene polymers. By substituting the sulfur atom for a selenium atom on one of the monomers in the repeat unit, a significant red-shift of both the neutral and polaronic absorbances results, as well as a reduction in the onset of oxidation compared to the all thiophene analog.

Due to the redox and optical similarities of PE_2 and PEDOT, the solid-state electrical conductivity of the chemically doped $ProDOT_xEDOT_y$ series (discussed in Chapter 3) is studied in Chapter 6. Additional polymer structures are introduced to understand the structure property relationships and the conductivity of PE_2 is optimized to ~250 S/cm. Because of this high electrical conductivity, an oxidized PE_2 film was used

as a transparent electrode for another electrochromic polymer to switch between purple and colorless states.

Chapter 7 outlines a chemical defunctionalization method that allows for the preparation of conjugated polymer films that can be processed from both aqueous and organic solvents and used as redox active films in either organic or aqueous-based electrochemical devices. Ester-functionalized ProDOTs are polymerized and purified from organic solvents; afterwards, they can be converted to their conjugated polyelectrolyte (CPE) form via saponification, allowing them to be processed into thin films from water. Post-processing functionalization of the CPE films using dilute acid creates a solvent resistant material that is electrochemically active in both organic and aqueous electrolyte systems. The versatility and robustness of this solvent resistant polymer is shown in a series of aqueous electrolyte systems, as well as in biologically compatible electrolytes (human serum, sports drinks, etc.). To show the use of these materials in redox active devices; two applications, namely electrochromics and charge storage, were examined using environmentally benign salt water as the electrolyte. Supercapacitors using these films in NaCl/water remained operational after 175,000 charge/discharge cycles.

Finally, Chapter 8 will demonstrate how the chemical defunctionalization method outlined in Chapter 7 can be used with polymers bearing ester side chains orientated so that upon hydrolysis only alcohol groups remain, resulting in higher mass capacitances. The alcohol functionalities remaining after hydrolysis result in hydrophilic films that are redox active in organic and aqueous media and exhibit exceptionally low onsets of oxidation.

CHAPTER 1. INTRODUCTION TO ELECTROACTIVE CONJUGATED POLYMERS

Partially adapted from:

Conducting Polymers: Redox States in Conjugated Systems, Ponder, Reynolds, *The WSPC Reference on Organic Electronics*; Brédas, Marder, Ed.; World Scientific Publishing Co. Pte. Ltd., Singapore, **2016**; Vol. 2; p 1

1.1 Development of Conjugated Polymers

The modern field of π-conjugated active materials is generally considered to have started in the 1970's with the preparation of free-standing films of polyacetylene $(CH)_X$ that, upon oxidative doping, attain high levels of electrical conductivity.[1,2,3] This research, carried out in the research groups of Hideki Shirakawa, Alan MacDiarmid and Alan Heeger, provided the crucial discoveries that stimulated the field of conjugated polymers and ultimately led to the awarding of the Nobel Prize in Chemistry in 2000.[4] However, commonly overlooked is the early syntheses of polyaniline and polypyrrole and even the term "synthetic metal" is commonly misattributed to the later work on polyacetylene.[5,6] In 1934 F. F. Runge was, to the best of my knowledge, the first to report the preparation of polyaniline via the oxidation of aniline.[7] Additional experiments were performed using polyaniline in the mid 1800s and an in depth discussion of this work in a

historical context was published S. C. Rasmussen in 2011.[5] The second conjugated polymer to be developed was polypyrrole in 1963 by D. E. Weiss.[5,8] This was achieved by the dehalogenative polymerization of tetraiodopyrrole to form a structurally irregular black material that was potentially iodine doped.[8] Additionally, it was found that same year that polypyrrole was electrically conductive and that removal of the iodine, via various methods, resulted in an increased resistance of the material.[9] The oxidative polymerization of furan, pyrrole, and thiophene was then discovered in 1967 and the resulting materials were characterized via various methods.[10] The next big step in the field is the previously mentioned polyacetylene research that many believe started everything. This story has been related in many reviews, publications, and books and will not be repeated here.[4,11,12]

1.2 Development of PEDOT

In the 1980's Bayer's Central Research Department worked to commercialize polyacetylene and develop new conjugated polymers. While their research into polyacetylene did not result in a stable, commercializable material[13], it did lead them to investigate new polymers composed of heterocycles, where the oxidized forms are stabilized be the hetero atoms.[14] Dioxythiophenes (XDOTs) were ultimately invented by manipulation of the thiophene synthon into a bicyclic system containing a dioxane ring and a thiophene ring. After exploring different size dioxane rings it was found the 3,4-ethylenedioxythiophene (EDOT) could be prepared and oxidatively polymerized using ferric chloride.[15] After several years of research and development, polyEDOT (PEDOT), poly(3,4-propylenedioxythiophene) (PProDOT), and several other polymers were reported in the literature.[16] The use of PEDOT as a transparent antistatic coating and as

an anode electrolyte material in polymer aluminum electrolytic capacitors, were also reported.[16] Interestingly, PEDOT, in various doped forms, is commonly used in commercially available aluminum electrolytic capacitors from such companies as Panasonic and Jianghai, to name a couple. These capacitors are in devices ranging from uninterruptible power supplies to car airbags, making PEDOT a common household product, even if people aren't aware of it.

1.3 Development of Soluble PProDOTs and other XDOTs

The ProDOT unit was first developed, as previously discussed, by Bayer and reported on in 1992.[16] Two years later it was reported that both electropolymerized PEDOT and PProDOT are electrochromic polymers (ECPs) that reversibly switch between vibrantly colored charge neutral states and less colored (or transmissive) oxidized states.[17] In 1997, these two polymers were then investigated more fully as electrochromic materials with additional experiments e.g. chronoabsorptiometry and in situ conductivity were performed to gain a better understanding of the redox behavior.[18] It was then found that functionalizing the 2 position of the propylene bridge of the ProDOT unit allows for incorporation of solubilizing side chains without compromising the electrochromic properties.[19,20] The use of two 2-ethylhexyloxymethyl ($EtHxOCH_2$) side chains on the ProDOT unit provide excellent solubility (>40 mg/mL) for the corresponding homopolymer with EC properties that are overall superior to electropolymerized PProDOT.[20] This homopolymer became known as ECP-Magenta 1 (ECP-M) and is still used in 2017 as a model ECP.

Several other 3,4-alkylenedioxythiophene units have also been developed over the past two decades.[14] Two of relevance to this thesis are 3,4-phenylenedioxythiophene (PheDOT) and 3,4-vinylenedioxythiophene (VDOT). In 2004 the Roncali group reported the synthesis of PheDOT and several derivatives of it and later expanded on this work by preparing biPheDOT and terPheDOT.[21,22] The use of PheDOT and biPheDOT as novel monomers will be discussed further in Chapter 4. Following the development of PheDOT, the Roncali group reported VDOT in 2006.[23] Unfortunately, VDOT has not received much attention and little is know about the properties of this monomer and corresponding homopolymer.

1.4 Doping and Charged State

PEDOT is an exemplary thiophene based polymer that forms an excellent conductor in the doped state, and Figure 1.1 demonstrates it's oxidative doping.[24,25] The neutral form of this polymer can be viewed as a series of aromatic thiophene rings linked together. The aromatic stabilization energy of the repeat units causes there to be little intrinsic conjugation between rings leading to neutral polyheterocycles having lower intrinsic conductivities than polyacetylene. Interestingly, the sulfur atoms in the thiophene heterocycle interact with the pendant oxygen atoms at the 3,4-positions via a weak donor-acceptor (D-A) type interaction. This D-A interaction assists in the planarization of PEDOT, putting the repeat units into a planar conformation with a high degree of π-overlap along the polymer chain.[26,27] Oxidative doping, illustrated by the first electron transfer reaction in Figure 1.1, leads to a delocalized cation-radical in which the extent of delocalization is controlled by the somewhat higher quinoidal energy state as the radical (spin) and the cation (charge) are coupled to one another, and they can be

viewed as a polaron charge carrier. The second oxidative electron transfer shown in Figure 1.1 leads to the dication structure in which the two cations are again coupled to one another through the quinoidal state. In essence, while the cations coulombically repel one another along the polymer chain, their increased separation leads to a higher degree of quinoidal content giving them an optimal average number of double bonds across which the di-cation is delocalized. These coupled di-cationic charge carriers are termed bipolorans in comparison to such coupled charge carriers in classical semi-conductors.[28] Due to the tunability of the repeat unit structure, doping level, and the choice of dopant used, it is possible to generate conjugated polymers with electronic properties that can be described as insulating, semiconducting, semi-metallic, and even metallic in nature.[29,30] Due to its electron rich nature, PEDOT is much easier to oxidize than polyacetylene and, thus, the oxidatively doped complexes are more stable. The maximum level of doping for a polythiophene based material is ~33%, or one charge per every three rings.[31,32]

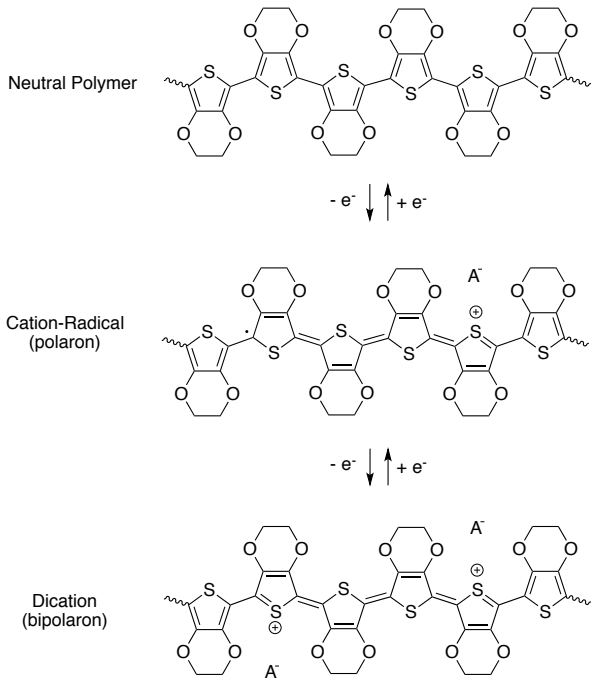

Figure 1.1. Structural scheme of the stepwise oxidation of PEDOT. Initial oxidization (from the neutral polymer) forms a cation radical (polaron) that is counter balanced by anion A^- followed by a second oxidation to form a dication (or bipolaron) with balancing charge, yielding a highly p-doped material. Figure taken from The WSPC Reference on Organic Electronics and used with permission.[33]

The introduction of charge states along the conjugated chain, via oxidation or reduction, leads to new optical transitions at the expense of the interband or π to π^* transition. This is easily monitored for films deposited on transparent electrode substrates (typically indium tin oxide, ITO, coated glass) in a spectroelectrochemical series as illustrated for PEDOT in Figure 1.2. Here, the electrochemical polymerization of PEDOT on ITO forms a film first in its oxidatively doped state which can subsequently be reduced to the neutral form at a relatively low potential (-0.9 V). This film is then placed in a monomer free electrolyte solution and its spectra probed as a function of increasing applied potential. With an onset of 750 nm (1.7 eV), a λ_{max} of 629 nm (2.0 eV), and a

broad absorption profile, this polymer film absorbs a major fraction of the long wavelength (low energy) visible light, transmitting the short wavelength, and appears deep blue to the eye. Stepwise oxidation of the film leads to depletion of this absorption and subsequent increase in absorption with a peak at ~ 1000 nm (1.2 eV) and further absorption stretching well into the near infrared. As the polymer film reached its fully oxidized state, the π to π* absorption is effectively "bleached" and absorption is transferred predominately into the near infrared with a long tail back into the red region of the spectrum. With this, the film under goes a strong blue to a faint sky-blue transmissive electrochromic switch. This electrochromic switch is fully reversible and will be discussed in detail for a series of polymers below. The faint blue color observed in this film, often referred to as tailing absorption in to the visible, is due to aggregation in the solid state and resembles the Drude absorption of metals.[34-36]

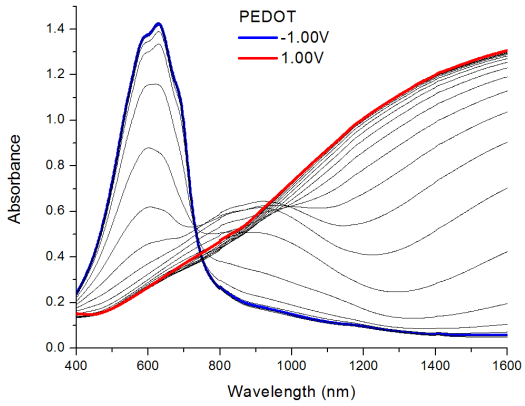

Figure 1.2. Spectroelectrochemistry of an electropolymerized PEDOT (details in Chapter 3) film on ITO. Higher energy (visible) absorbsotion is gradually suppressed as the film is electrochemically oxidized (doped). It can be seen that as the high energy absorbance decreases, the low energy absorbance increases, leaving a visibly "transparent" film.

These results can be explained using a band diagram to illustrate the electrochemically induced charge states and their optical transitions as shown in Figure 1.3 for a non-degenerate ground state polyheterocycle system.[37] Initially, the single absorption from the neutral form of the polymer can be expressed as a transition between the polymer valence band (the gray lower box) to the polymer conduction band (the white upper box), using inorganic semiconductor terminology. The magnitude of the energy (Eg) required for this absorption then determines the wavelength of absorption onset and has a significant impact on the color of the film observed, although the λ_{max} and overall transmittance profile also are critical for color control. Initial oxidation forms delocalized cation radicals (polarons in Figure 1.3) which exhibit two new absorptions of lower energy then the initial π-π^* transition. The solid arrows in Figure 1.3 illustrate the predominate electronic transitions while the dashed arrows illustrate less favored transitions due to electron-hole symmetry.[38] As the cation and the radical are coupled to one another in the polaron state, they are mobile along the chain and can move from chain to chain leading to electrical conductivity. Subsequent further oxidation, and coupling interactions between polarons, leads to the dicationic bipolarons. As Figure 1.3 shows, this leads to elimination of the spin in the intra-band state and the absorbance at 1.2 eV decreases. At the same time, the bipolarons have the long wavelength transitions (E_{b1}) and absorption in the near infrared continues to increase, ultimately leading to a band of energy states known as bipolaron bands.[39] Again, the delocalized cations of the bipolaron can move in these energy states yielding electronic conductivity.

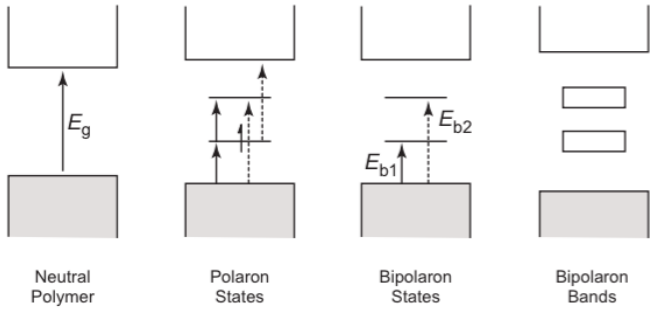

Figure 1.3. Band diagram of the possible optical transitions for a non-degenerate polyheterocycle system. Taken from the dissertation of C. A. Thomas which was adapted from Bredas, J. L., Street, G. B. *Acc. Chem. Res*. 1985, 18, 309-315.[37,39]

1.5 Control of Color and Redox Behavior

Dioxyheterocycle chemistry is highly versatile and has allowed the synthesis of a family of ECPs that provide vibrant hues of color states in their neutral form, which can be switched into their highly transmissive (bipolaron) forms.[40] The soluble ProDOT homopolymer, ECP-M, has a pinned back seven membered ring with oxygens that engage in non-bonding interactions with the sulfur atom of the adjacent thiophene ring that ultimately relaxes steric interactions along the conjugated chain and leads to a peak absorption near 550 nm, approximately in the middle of the visible spectrum. As such, this polymer film transmits both red and blue light and appears magenta/purple to the eye.[20] Changing the substituents to an acyclic derivative leads to steric twisting of the backbone, decreasing conjugation, and widening the band gap such that the polymers peak absorption shifts to ~485 nm making the polymer appear orange.[41] Copolymerization of the ProDOT unit with a 1,4-phenylene unit leads to increased twisting such that the peak absorbance is ~450 nm. In this case, all of the visible light at a

wavelength longer than 525 nm (the onset) is transmitted and the film appears yellow to the eye.[42,43] Alternatively, the introduction of electron poor units, such as BTD, in conjunction with the electron rich ProDOTs, lead to a donor-acceptor conjugated polymer with a relatively low band gap and two absorption maxima.[44] More detailed discussions on color control will follow in this thesis along with new methods of fine-tuning the perceived color or mimicking the color of a known system.

1.6 Overview of Dissertation

This thesis describes the development of processable, electron-rich dioxyheterocycle-based polymers for use in electrochromic and charge-storage applications Previously, the majority of conjugated polymers used in charge storage research have been insoluble polymers prepared via electrochemical polymerization or dispersions of an insoluble conjugated polymer in an insulating matrix. This thesis reports the development of soluble polymers that can be solution processed from organic or aqueous solutions (inks) and are redox active in organic or aqueous electrolytes with variable optical and redox properties through subtle differences in the repeat units and heteroatoms used.

Chapter 1 outlines the early development of conjugated polymers and basic principles of doping and color control in electron rich polymers. Chapter 2 then overview the development and optimization of direct (hetero)arylation polymerization, the recently developed method used to prepare the materials discussed in this thesis. Certain aspects

optical and electrochemical characterizations are then discussed followed by details regarding electrochemical supercapacitors and chemical doping of conjugated polymers.

Materials with low onsets of oxidation and broad electroactivity over a large voltage window, as seen with electropolymerized poly(3,4-ethylenedioxythiophene) (PEDOT), are of interest for charge storage applications. Chapter 3 reports and discusses the copolymerization of alkoxy-functionalized 3,4-propylenedioxythiophenes (ProDOTs) with unfunctionalized 3,4-ethylenedioxythiophene (EDOT) in varying ratios using direct arylation to produce a series of solution processable polymers with highly tunable optical and electronic properties. Within this series, we have identified poly(ProDOT-alt-biEDOT) (PE_2), a copolymer containing 67% EDOT compositionally, which combines the low oxidation potential, the redox behavior, and the deep-blue neutral color that are characteristic of PEDOT with the high solubility, exceptional electrochromic contrast, and color neutrality in the oxidized state characteristic of alkoxy-functionalized polyProDOTs. 3,4-Phenylenedioxythiophene (PheDOT) is a unit that is similar to EDOT in terms of planarity and steric interactions but has different electronic properties due to an attached phenyl ring which allows for electron delocalization away from the thiophene ring. This unit, and its use in soluble copolymers prepared via direct (hetero) arylation polymerization (DHAP), is discussed in Chapter 4. The notable C-H inactivity of the attached phenylene unit is compared to aromatic solvents used for DHAP and the redox stability of these copolymers are demonstrated. In order to decouple the effects of planarity and electron density in redox active polymers, differences in redox properties between poly(ProDOT-alt-biPheDOT) and PE_2 are discussed.

Dioxyselenophenes are another group of heterocycles that have significantly different properties to their thiophene counterparts; due to various factors including lowered aromatic character. The first example of a solution processable dioxythiophene-alt-dioxyselenophene polymer, Poly(ProDOT-alt-EDOS), prepared via DHAP is reported and its optical and electrochemical properties are compared to the all thiophene analog and other relevant dioxythiophene polymers. By substituting the sulfur atom for a selenium atom on one of the monomers in the repeat unit, a significant red-shift of both the neutral and polaronic absorbances results, as well as a reduction in the onset of oxidation compared to the all thiophene analog.

Due to the redox and optical similarities of PE_2 and PEDOT, the solid-state electrical conductivity of the chemically doped $ProDOT_xEDOT_y$ series (discussed in Chapter 3) is studied in Chapter 6. Additional polymer structures are introduced to understand the structure property relationships and the conductivity of PE_2 is optimized to ~250 S/cm. Because of this high electrical conductivity, an oxidized PE_2 film was used as a transparent electrode for another electrochromic polymer to switch between purple and colorless states.

Chapter 7 outlines a chemical defunctionalization method that allows for the preparation of conjugated polymer films that can be processed from both aqueous and organic solvents and used as redox active films in either organic or aqueous-based electrochemical devices. Ester-functionalized ProDOTs are polymerized and purified from organic solvents; afterwards, they can be converted to their conjugated polyelectrolyte (CPE) form via saponification, allowing them to be processed into thin films from water. Post-processing functionalization of the CPE films using dilute acid

creates a solvent resistant material that is electrochemically active in both organic and aqueous electrolyte systems. The versatility and robustness of this solvent resistant polymer is shown in a series of aqueous electrolyte systems, as well as in biologically compatible electrolytes (human serum, sports drinks, etc.). To show the use of these materials in redox active devices; two applications, namely electrochromics and charge storage, were examined using environmentally benign salt water as the electrolyte. Supercapacitors using these films in NaCl/water remained operational after 175,000 charge/discharge cycles. Chapter 8 will demonstrate how the chemical defunctionalization method outlined in Chapter 7 can be used with polymers bearing ester side chains orientated so that upon hydrolysis only alcohol groups remain, resulting in higher mass capacitances. The alcohol functionalities remaining after hydrolysis result in hydrophilic films that are redox active in organic and aqueous media and exhibit exceptionally low onsets of oxidation.

Chapter 9 provides perspective on this work and the impact it has on the various areas of electroactive polymer research. The potential paths forward for the materials and methods used in this thesis are then discussed along with the remaining questions raised during or brought about by this work.

CHAPTER 2. EXPERIMENTAL METHODS

Partially adapted from:

Conducting Polymers: Redox States in Conjugated Systems, Ponder, Reynolds, *The WSPC Reference on Organic Electronics*; Brédas, Marder, Ed.; World Scientific Publishing Co. Pte. Ltd., Singapore, **2016**; Vol. 2; p 1

2.1 Introduction to Conjugated Polymer Polymerizations and Metal Catalyzed Cross Coupling

The synthesis of conjugated polymers has undergone significant change over the past five decades. Electrochemical polymerization directly onto an electrode via various methods (e.g. potentiostatic or galvanostatic deposition) has been used for several decades to produce films that are typically insoluble and have strong adhesion to the electrode.[45,46] Similarly, polymer films can be prepared via vapor deposition of monomer in the presence of an oxidant, resulting in the doped polymer.[47] This technique has been successfully used to prepare highly conducting films of doped PEDOT via vapor deposition of EDOT onto a surface coated with a Fe(III) salt.[47] In some rare cases, polymerization can be achieved spontaneously in the solid state without either an electrochemical potential or an oxidant. One example of this is the solid-state polymerization of dibromoEDOT (EDOT-Br_2) to form bromine doped PEDOT.[48] As the

focus in the field has turned towards being able to coat films using high throughput techniques, and as metal-mediated cross-coupling reactions have grown more sophisticated, the focus of this thesis is the preparation and properties of soluble polymers prepared via a Pd catalyzed cross-coupling reaction.

While there are many known metal catalyzed cross-coupling reactions with unique mechanisms, several of the most used methods have common reaction steps. For example, Migita-Kosugi-Stille (Stille)[49-51], Suzuki–Miyaura (Suzuki)[52], and Negishi[53] couplings, along with several other reactions, share common mechanistic features. These coupling reactions, whether for synthesis of discrete molecules or polymers, typically use palladium (Pd) in the zero oxidation state as the catalyst with ligands to provide solubility and tune catalyst reactivity. The catalytic cycle of the Stille reaction for the synthesis of a polyProDOT from the dibromide and di(trimethylstannyl) species is shown in Figure 2.1 as a specific example of the catalytic cycles discussed. The Pd(0) ligand complex (with Pd shown in green throughout Figure 2.1) then undergoes oxidative addition with a carbon halide (or pseudohalide) bond to form a Pd(II) species with negative charges on the halide (shown in blue) and carbon species. The Pd then undergoes transmetalation with the organometallic species (the ditin in this case with the tin unit shown in red) so that both carbon species are bonded to the Pd and the halide and metal/organometallic species leave the cycle. The Pd then undergoes reductive elimination to form a carbon-carbon bond and restore the catalyst to the zero oxidation state. This mechanism has been extensively studied and reaction conditions optimized for the Stille and Suzuki reactions, although the precise details of the transmetalation step are not fully understood for the Suzuki reaction.[54]

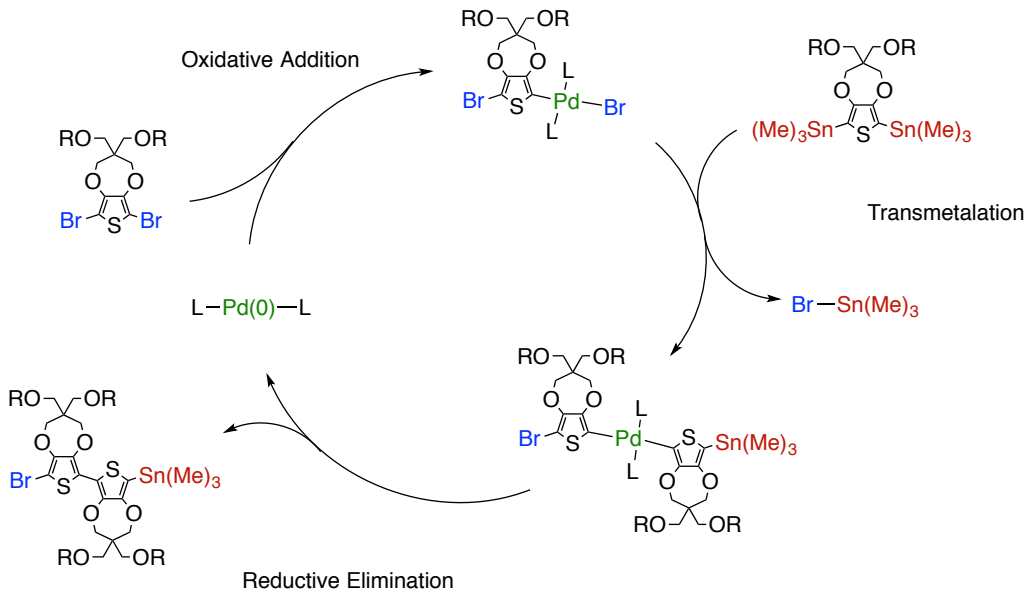

Figure 2.1. Catalytic cycle for the Stille reaction to form a substituted polyProDOT with the typical steps seen in Pd catalyzed cross-couplings outlined.

2.2 Direct (Hetero)Arylation Polymerization (DHAP)

2.2.1 Small Molecule C-H Activation/Direct Arylation

Direct Arylation (a form of C-H activation reaction) has been used for the synthesis of discrete molecules for decades.[55-57] Various C-H activation methods have been reported using a broad range of metals including Ir[58], Ru[59], Rh[60], and Pd[61], with Pd being the most common and versatile. The central problem with this method is that different aromatic systems require different conditions for C-H activation. Other methods, such as Stille and Suzuki, generally work with a range of conditions and tuning of variables (catalyst, temperature, etc.) is primarily done to optimize synthetic yield. However, despite this increased complexity, C-H activation chemistry has remained a point of interest due to the reduced number of synthetic steps and the ability to control the

point of C-H activation for various heterocycles via choice of conditions and reagents. Direct arylation is a specific example of C-H activation that has become increasingly important to build discrete molecules, oligomers, and polymers.[62]

2.2.2 Early Work on Conjugated Polymer Synthesis via DHAP

Over the past seven years C-H activation has become a common method for the synthesis of conjugated polymers. This method is typically referred to as either Direct Arylation Polymerization (DArP) or Direct (Hetero)Arylation Polymerization (DHAP) depending on the group reporting their results. The first reported synthesis of a high weight conjugated polymer via DHAP was in 2010 using a Pd based catalyst to prepare regioregular poly(3-hexylthiophene) (P3HT).[63] Other reports of homopolymers and copolymers prepared via DHAP appeared the following year. Mario Leclerc[64,65], Barry Thompson[66,67], Takaki Kanbara[68,69], and Michael Sommer[70,71] stand out as pioneers of this field, with each offering unique approaches to understanding and/or optimizing DHAP for various systems. The Reynolds group has demonstrated the synthesis of various ECPs via DHAP and that the resulting polymers have lower residual metal content than the same materials prepared via oxidative or Grignard metathesis (GRIM) polymerization.[72,73]

2.2.3 Divergence into Two Distinct Sets of Polymerization Conditions

Two different classes of conditions have developed for DHAP over the past several years, each being useful for specific syntheses. The difference is largely based on the solvent polarity and how this changes the rate and selectivity of coupling. The first report by Fumiyuki Ozawa used THF (under pressure at high temperature) with

Herrmann's catalyst as a source of Pd(II) and a phosphine ligand.[63] Soon after this, Takaki Kanbara reported a phosphine ligand free DHAP using DMAc as the solvent to produce polymers of reasonable to high molecular weight.[74] From these reports there is a clear divergence in methods. The relatively lower dielectric constants of THF, dioxane, or arylene based solvents (such as toluene or xylenes) cause the C-H activation to proceed slower, potentially due to the solvent being less able to stabilize the intermediates. Full color change, indicating the growing chains have reached the effective conjugation length of the polymer, is typically observed after 30 minutes to a few hours when using these conditions. Additionally, a phosphine ligand is typically used to tune the reactivity and assist in solubilizing the Pd species in the low polarity conditions. Conversely, the higher dielectric constants of DMAc, NMP, or HMPA accelerate the reaction and solubilize the Pd species without ligands, with full color change observed in these reactions within minutes. However, the increased polarity also increases the reactivity of C-H bonds that are not desirable for coupling and can result in branched or cross-linked polymer chains.[66] These types of polymer defects, along with others, will be further discussed in Chapter 4. The different conditions also favor different monomer types: electron rich dihalide monomers couple with increased efficiency and form higher weight polymers using the more polar conditions while some electron deficient dihalide monomers couple more efficiently in the less polar conditions. The C-H activation typically occurs in both classes of conditions for electron rich and poor species although differing reports in the literature has shown inconsistences in this. For example, in my work and the work of the Leclerc group it was found that XDOTs do undergo C-H

activation using the less polar conditions while the Kanbara group reports that they do not.[69,75] Clearly a more broadly applicable set of reaction conditions are needed.

2.2.4 Mechanistic Details of DHAP

2.2.4.1 Oxidative Addition, C-H Activation, and Reductive Elimination

When analyzing the mechanism of DHAP it is clear that it shares many of the same features previously discuss for other Pd catalyzed cross-couplings. The oxidative addition and reductive elimination steps are directly comparable to Stille or Suzuki, with the transmetalation step being replaced with C-H activation. A proposed cycle based on the literature is outlined in Figure 2.2 for the synthesis of a substituted polyProDOT.[76] After oxidative addition the halide (shown in blue in Figure 2.2) is displaced from the Pd species (shown in green in Figure 2.2) by a carboxylate (e.g. pivalate) or carbonate anion. Next is the C-H activation step. While several mechanism have been proposed, the "concerted metalation deprotonation" pathway is generally accepted and is outlined in Figure 2.3.[65,76] In this mechanism the Pd complex can coordinate with a π system to form a six membered intermediate which then simultaneously transfers a proton from the aryl (or heteroaryl) ring to the carboxylate and the electrons from the C-H bond move to form a bond between the carbon and Pd atoms, as illustrated in Figure 2.3.[76] Following this C-H activation step, reductive elimination occurs in the same manner as other Pd cross-coupling reactions, restoring the catalyst to the starting point.

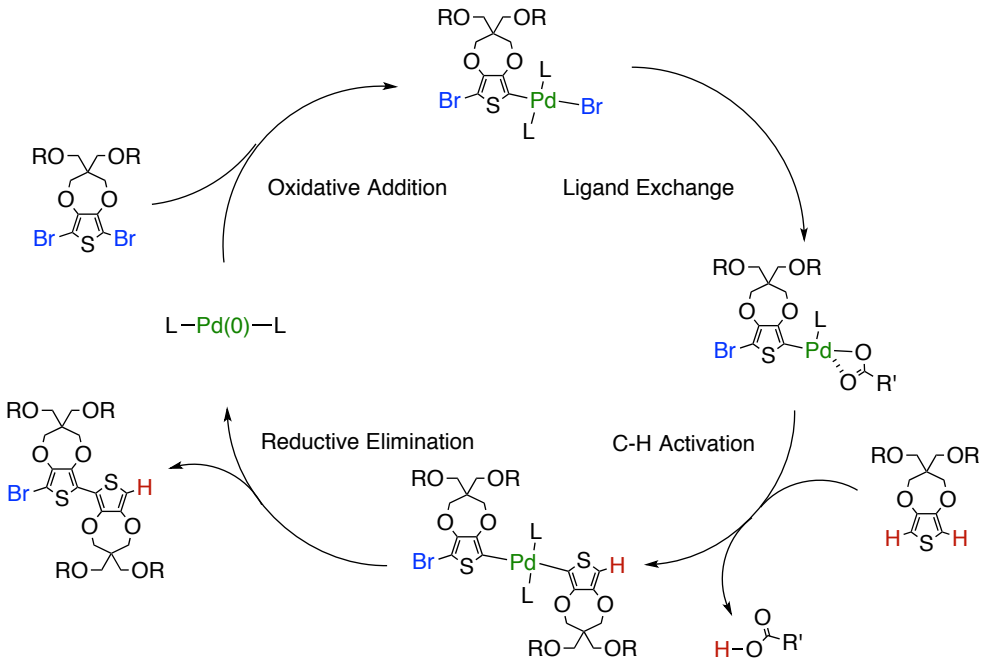

Figure 2.2. A proposed catalytic cycle for DHAP to form a substituted polyProDOT with the various steps of the cycle outlined. Based on a report cycle in the literature.[76]

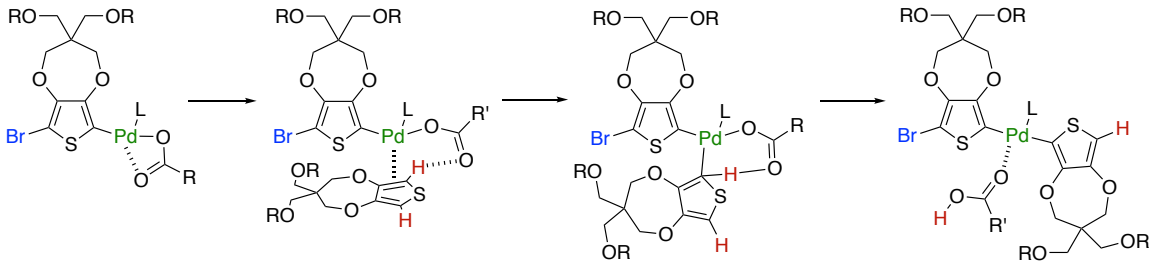

Figure 2.3. A proposed reaction pathway for the C-H activation of a ProDOT C-H bond from Pd(II) in the presence of a carboxylate. Based on a report mechanism in the literature.[76]

2.2.4.2 Catalysts & Ligands

As noted previously, Pd(0) is the required initial state of Pd for the catalytic cycle. Despite this, Pd(II) sources are often used due to their increased stability and the lower cost of many of these catalysts. $Pd(OAc)_2$ and Herrmann-Beller catalyst are the most common sources of Pd(II) but other sources have also been found to be effective. In a report by the Leclerc group it was found that the Pd source did not play any apparent role and that the other reagents (solvent, ligand, etc.) are the key factors.[64] It should be noted that a chloride-promoted DHAP was reported in 2015, showing higher molecular weights (M_n) and yields when $PdCl_2$ was used as the catalyst.[77] However, this has not been reproduced by other groups and requires more investigation. Alternatively, ligand choice can drastically change the resulting molecular weight, yield, absorbance profile, and even degree of branching.[78,79] There is currently no consensus on what ligand (or mixture of ligands) provides the highest quality materials, although P(*o*-OMePh)$_3$ and P(*o*-NMe_2Ph)$_3$ are commonly used with good results.

2.2.4.3 Formation of the Active Pd(0) Catalyst from the Precatalyst via Homocoupling

The Pd(0) species can be formed in solution from Pd(II) via a double C-H activation followed by reductive elimination to form the homocoupled aryl unit and the Pd(0) species. This is expected to alter the monomer ratio and should, therefore, reduce the molecular weight of the resulting material according to the Carothers equation.[80] This is, however, not actually observed and exceptionally high molecular weight polymers[68] can be obtained from a Pd(II) source without altering the monomer ratio to account for the stoichiometric imbalance from the catalyst reduction. What is observed are small

amounts of homocoupling defects in the polymer chains and the impact of these have been studied.[66,70]

2.2.4.4 The Role of a Bulky Proton Transfer Shuttle

Carboxylic acids, or carboxylate salts, additives are almost always added to a DHAP reaction as they assist in the catalytic cycle and transfer protons to the less soluble carbonate in solution, with the most commonly used being pivalic acid and 1-adamantanecarboxylic acid. The group of Barry Thompson performed an in depth study of the role of the proton transfer shuttle and how the steric bulkiness of the acid affects branching of the resulting polymer.[67] It was found that isomers of neodecanoic acid are sufficiently bulky to suppress branching off the main polymer chain when preparing regioregular P3HT. This was further studied by the Leclerc group and modified by the Marks group for the preparation of other polymer systems.[78,81]

2.2.4.5 Development of Oxidative DHAP (Oxi-DHAP)

The previously discussed formation of Pd(0) via homocoupling has also been exploited by the Thompson group in 2016 to produce homopolymers by continuous oxidation of the Pd(0) species.[82] This was done adding a Ag(I) species (specifically Ag_2CO_3) to the reaction so that 2 equivalents of Ag(I) converts the Pd(0) produced from the reductive elimination step back into Pd(II) that can then undergo C-H activation again. This produces the corresponding homopolymer without an organometallic or halogen species and silver metal as the byproduct. A proposed mechanism for this Oxi-DHAP is shown in Figure 2.4. Shortly after this initial report a similar method was reported using Cu(II) as the oxidant to form alternating copolymers from trimers.[83] Later

that same year it was reported that oxygen could be used as the sole oxidant for the polymerization.[84] This method has also been used for the synthesis of random copolymers of donors and acceptors.[85]

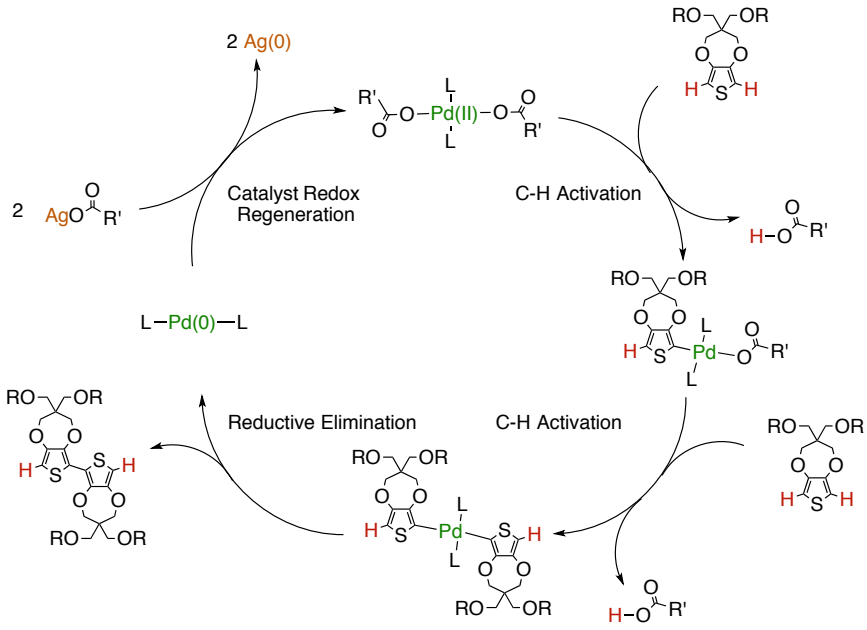

Figure 2.4. A proposed catalytic cycle for oxidative DHAP to form a substituted polyProDOT with the various steps of the cycle, including the catalyst regeneration, outlined.

2.2.4.6 Scope of DHAP

Currently, the full scope of DHAP is unknown. Most of the common monomers currently used in organic electronics undergo DHAP provided the proper conditions are used. However, some units do not appear to undergo C-H activation efficiently and therefore do not produce high molecular weight (defined for the purpose of this text as ≥ 10 kDa) polymers. Most notably, EDTT and XDOPs have not, to date, undergone C-H activation efficiently using known conditions. This topic is discussed further in Chapter 9.

One significant advantage of DHAP over Stille coupling polymerizations is its insensitivity to water and air. While this has been qualitatively observed in the DHAP community for some time the Leclerc group reported biphasic conditions open to air in 2017.[86] The addition of air and/or water did not significantly alter the molecular weights or absorbance profiles of the resulting polymers. Moreover, polymers prepared via DHAP can have properties comparable to the corresponding material prepared via Stille. While this has been demonstrated several times in the literature, work from the Marks group stands out as an in depth analysis was done on the structure and properties of several solar polymers prepared by both methods.[81] It was found that all of the polymers were approximately the same in terms of various properties, including absorbance profiles and PCEs, once reaction conditions were optimized. DHAP has also been performed in flow reactors, making large-scale production of polymers via this method practical.[75] These results show that DHAP is a realistic and practical replacement for Stille and Suzuki polymerizations.

2.3 Evaluating Redox Properties of Conjugated Polymers via Cyclic Voltammetry and Differential Pulse Voltammetry

Cyclic voltammetry is an electrochemical technique that involves cycling the potential of a working electrode at a fixed scan rate (typically ranging from a few mV/s to several V/s depending on the experiment) while monitoring the current. CV and differential pulse voltammetry are both measured using a three-electrode cell setup. In this work, the working electrode was either glassy carbon or ITO coated with a polymer film, whereas a Pt wire or flag served as the counter electrode to balance the current passed at the working electrode during the CV or DPV experiment. When using organic

electrolyte solutions for the experiments, a Ag/Ag^+ pseudoreference electrode consisting of a Ag wire immersed in a solution containing 10 mM $AgNO_3$ and 0.5 M $TBAPF_6$/ACN or 0.5 M LiBTI/ACN supporting electrolyte solution was used and calibrated vs. the ferrocene/ferrocenium (Fc/Fc^+) redox couple. For aqueous electrolyte solutions, an Ag/AgCl reference electrode is used which consists of a AgCl coated Ag wired immersed in a 1 M KCl/H_2O supporting electrolyte solution.

Discrete molecules, like ferrocene, have well-defined, reversible oxidation/reduction cyclic voltammogram (CV) traces as the one shown in Figure 2.5. From this CV we can calculate the $E_{1/2}$ for the Fc/Fc^+ redox couple in this specific electrolyte system, which, in this case, was +55 mV. In contrast to this well-defined CV of ferrocene, Figure 2.5a also shows a representative CV of a conjugated polymer, specifically that of ECP-M. From this CV it can be observed that there are several overlapping reversible redox processes that occur in the polymer chain.[32] These are due to different conjugation lengths or chain lengths, differences in aggregated and amorphous regions, or continued oxidation of partially oxidized species (such as the oxidation of a polaron to a bipolaron). For clarity, the inset in Figure 2.5a shows the orientation of the current (green) and potential (blue), as used in this thesis. Another difference between discrete molecules and CPs is a change in the CV trace over the first several cycles, as shown for ECP-M in Figure 2.5b. This phenomenon has been referred to as a memory effect, electrochemical break-in, electrochemical annealing, or electrochemical conditioning. It is caused by the reorganization of the polymer chains as the polymer oxidizes and is forced to planarize and swell with solvated ions, as discussed in Chapter 1.[32] Upon repeated cycling the polymer obtains the lowest energy

conformation in its charge neutral state for this redox cycling, resulting in stable and reversible switching.

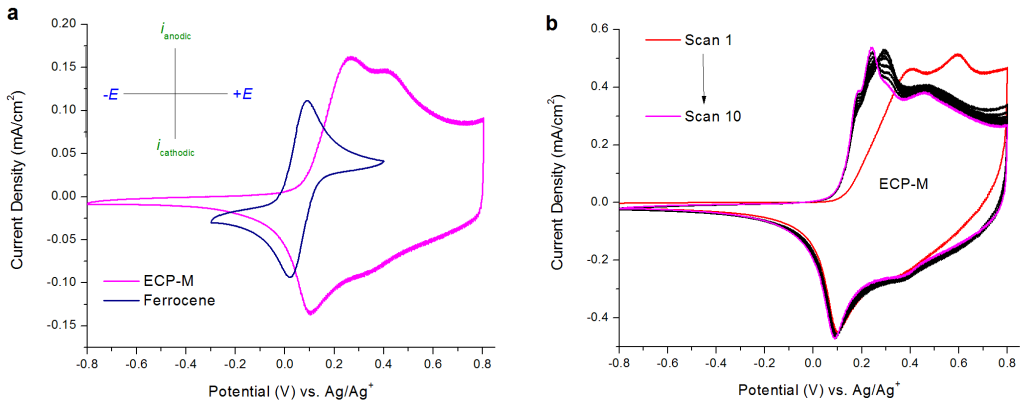

Figure 2.5. a) CV traces of ferrocene (navy trace) dissolved in 0.5 M $TBAPF_6$/PC and a drop cast film of ECP-M (magenta trace) on a glassy carbon button electrode and b) the first 10 CV traces of a ECP-M film showing the electrochemical conditioning of the film in 0.5 M $TBAPF_6$/PC at a scan rate of 50 mV/s with inset designating the direction of the potential and current as used in this thesis.

The CV of an electropolymerized (via cyclic voltammetry) PEDOT film on a glassy carbon button electrode in 0.5 M LiBTI/PC electrolyte, shown in Figure 2.6, is now discussed in order to provide a clearer understanding of the redox behavior of the polymer films discussed in this thesis. Beginning at -1.0 V, the polymer is in its charge neutral form. As the potential is scanned anodically the polymer begins to oxidize and the current increases until the first peak at ca. -0.25 V (A). Beyond that, the current plateaus (B) as the material is converted into its oxidized and conducting form. As the potential scan is reversed and the charges are neutrallized, the current is almost independent of the potential from 1.2 to -0.7 V (C). Subsequent full reduction and charge neutralization is evident (D) by the peak near -0.9V, which subsequently returns the polymer to its neutral form. A material that is able to pass a high current that is independent of the applied

potential in a relatively broad electrochemical window, is often referred to as a pseudocapacitive material.[87] This material property, along with the fact that it is reproducible over 10^5-10^6 cycles, prompted research into the use of PEDOT and its derivatives as the active layer in supercapacitors. This is nicely illustrated in the work of Österholm et al. who used PEDOT as the active material in designing thin films supercapacitors.[88] By using an ionic liquid electrolyte, these supercapacitors could be charged and discharged for over four hundred thousand cycles with minimal loss in performance.

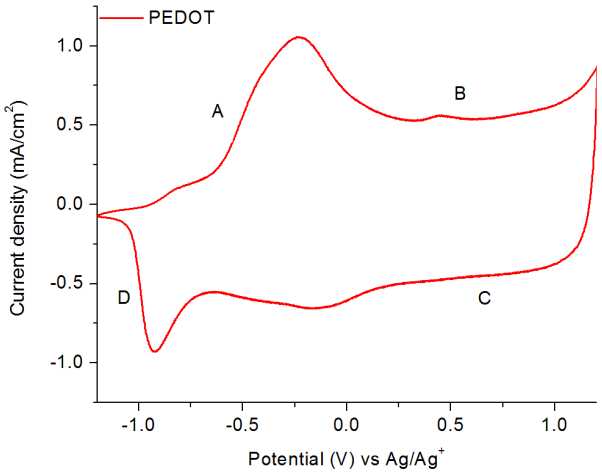

Fig 2.6. Cyclic voltammetry of an electrochemically polymerized PEDOT film cycled in 0.5 M LiBTI/PC at 50 mV/s. Adapted from Österholm et al.[88]

Another important technique is differential pulse voltammetry, which, instead of linearly sweeping the potential, uses regular voltage pulses. Using this technique the charging current is suppressed and we can selectively observe the faradaic current, which allows for a more accurate estimation of the onset of oxidation for a polymer. It should be

noted that for polymeric systems we probe the onset of oxidation/reduction and not the peak potential as one would for a discrete molecule. This is particularly important as many of the polymers discussed here are designed to have broad electrochemical responses as the polymer backbones gradually oxidize. This will be discussed using the example of PEDOT in Chapter 3. An example differential pulse voltammogram (DPV) trace for a conjugated polymer is shown in Figure 2.7, the intersection of two dotted tangent lines is referred to as the onset of oxidation for that polymer. In this particular experiment and throughout the thesis, the step size of the pulse used in DPV measurements was 2 mV with a step time of 0.1 seconds and amplitudes of + 5 mV for segment 1 and – 5 mV for segment 2 with the data point being the difference of segment 1 and 2. DPV is also often used to estimate the HOMO (and sometimes LUMO) level of conjugated polymers. However, this is inherently inaccurate and other methods, such as UPS, have been shown to give more accurate results.[89]

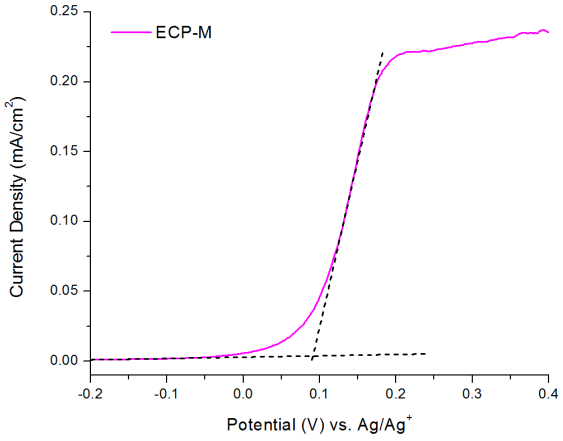

Figure 2.7. DPV trace of a drop cast film of ECP-M on a glassy carbon button electrode in 0.5 M TBAPF$_6$/PC.

2.4 Evaluating Color Properties of CPs via Spectroelectrochemistry & Colorimetry

Spectroelectrochemistry is a method where absorbance spectra are taken at various electrochemical potentials for a conjugated polymer. The electrochemical doping studied by UV-vis-NIR in this thesis is all oxidative, although reductive spectroelectrochemistry is used in the literature and other regions of the electromagnetic spectrum can be monitored.[90] Here, a three-electrode cell in a cuvette is used and the oxidation state of the polymer, that is coated on a transparent ITO slide, is set by applying a constant potential for a set period of time before recording a spectrum. The fundamental concepts of this method has been discussed in Chapter 1 and explained using the spectroelectrochemistry of PEDOT (shown in Figure 1.2). Specific experimental details are described in the experimental details of the chapters and extended discussions of this method can be found in the dissertations of Dr. Justin A. Kerszulis and Dr. Rayford H. Bulloch.[91,92]

Colorimetry is an area of color science that allows for the quantification of color relative to an observer's field of view. While various color spaces are used, this thesis will be limited to the use of the CIELAB L*a*b* color space. Briefly, a* represents the red−green balance, with positive a* values being red and negative values being green. b* is the yellow−blue balance of a given color, with positive values being yellow and negative values being blue. The L* coordinate represents the white−black balance (i.e., the lightness or darkness), with more positive values being lighter and more negative values being darker. In addition to L*a*b*, CIE has developed color-matching functions that represent average color vision in humans and these functions are called a standard

observed, shown in Figure 2.8.[93] Using the L*a*b* coordinates of a material the difference in color between two objects can be quantitatively compared using equation 2.1 to calculate the color difference (ΔE*ab).[94-96] Values of less than 2.3 are indistinguishable to a CIE standard observer.[94,95,97] This is a useful method for determining if two colors are quantitatively the same, to a representative person, or merely similar.

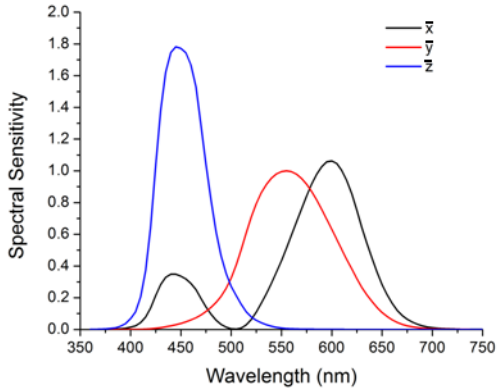

Figure 2.8. The various functions for the CIE 1931 (2°) standard colorimetric observers, approximating average human vision. Figure from the dissertation of Justin Kerszulis, which was adapted from the literature.[91,93]

$$\Delta E^*_{ab} = \sqrt{(\Delta L^*)^2 + (\Delta a^*)^2 + (\Delta b^*)^2} \qquad \text{(eq. 2.1)}$$

Another important concept for electrochromic polymers is color saturation, which defines the ratio of chromatic color to the total color sensation on a scale of 0−100, where 0 is gray and 100 is a pure color.[94] This is a metric of the "vividness of a color" given a

certain level of illuminance. Color saturation can be calculated using the CIE L*a*b* coordinates with equation 2.2, which was developed by Eva Lübbe.[98]

$$S_{ab} = \frac{\sqrt{a^{*2} + b^{*2}}}{\sqrt{a^{*2} + b^{*2} + L^{*2}}} * 100 \qquad \text{(eq. 2.2)}$$

2.5 Evaluating Supercapacitor Devices

Electrochemical supercapacitors (ESC) using conjugated polymers as the active pseudocapacitive material have recently received increased attention due to concerns regarding renewable energy and the need for energy storage systems.[99] In conjugated polymers charge can be stored in a combination of faradaic processes, oxidation and reduction reactions, as well as in in the electrochemical double layer.[87] This is distinctly different from carbon-materials used in commercial electrochemical double-layer capacitors that store charge primarily electrostatically at the electrolyte/electrode interface.[100,101] Supercapacitors (SC) have lower specific power than conventional double layer capacitors due to their longer discharge times, but higher that those of batteries. On the other hand, their specific energy density should be higher than double layer capacitors but lower than batteries.[102,103] These factors combined with the possibility of making flexible devices make polymer-based SCs useful for many low-power applications and various device types, including textile-based devices, are being investigated.[99,104] Much of the research presented in this thesis focuses on the design of new soluble polymers that could be used as active layers in SCs. For a material to be useful in a SC it should be

stable to repeated charge/discharge cycles (> 10^6), switch between oxidation states rapidly, and have a broad electroactive with current response independent of voltage over a large potential window as energy density is proportional to the square of the voltage. This relationship is shown in equation 2.3, where *C* is the film capacitance and *V* is the voltage window.

$$Energy\ Density = \frac{1}{2}CV^2 \qquad \text{(eq. 2.3)}$$

SCs can have different device architectures.[103] Type I devices are symmetrical, with the same p- or n-type polymer on both electrodes, as shown in the schematic of a in Figure 2.9. Type II devices are composed of two different active materials that can be either both p-type or both n-type. By using two different materials the voltage window of a type II device could be significantly larger than a type I device using either individual material. When charged, type I and II devices have one material in the neutral state and the other in the fully oxidized (or reduced) state and both in the half oxidized (or reduced) states when discharged. Type III devices are symmetrical, like Type I, but require the active material to be able to be both electrochemically oxidized and reduced reversibly. In the charged state one half of the device in the fully oxidized state and the other in the fully reduced state, after discharge both of the materials are in the charge neutral form. The electrolyte in these devices can be aqueous, organic, ionic liquid, or gel based. The current collectors (the electrodes) used in this thesis are made of glassy carbon, although

other materials, such as carbon fabric, carbon nanotubes, and gold on Kapton, have been investigated in XDOT and dioxypyrrole based SCs.[92,105,106]

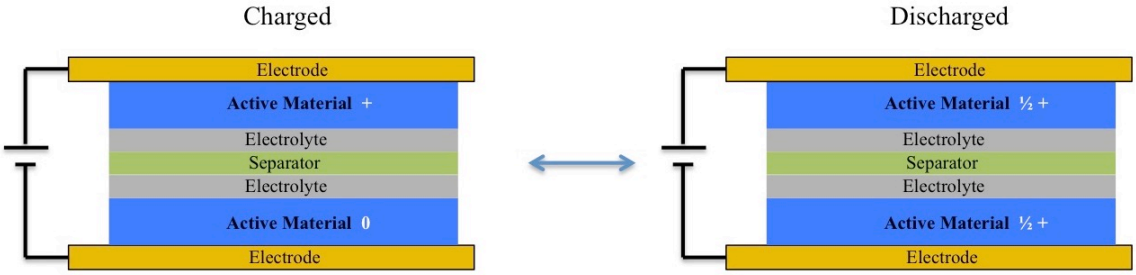

Figure 2.9. Schematic of a type I supercapacitor in the charged state on the left and the discharged state on the right.

There are many metrics that can be used to assess SC performance. These metrics include: power density (kW/kg), energy density (Wh/kg), areal capacitance (F/cm^2), mass capacitance (F/g), and fill factor (FF, %). In this thesis, the polymers are evaluated in terms of mass capacitance (from which areal capacitance can be calculated) and devices in terms of mass capacitance, energy density, power density, and FF. It should be noted that we are only considering the mass of the active polymer, as the weight of the whole device is a matter of engineering and not material design. As FF is a relatively new metric in the field of SC it should be briefly discussed. FF for s SC device was first reported in 2013 for PEDOT based Type I devices and is adapted from the organic photovoltaic (OPV) literature.[88] Its purpose is to quantitatively assess the ideality of a devices performance during discharge. An ideal capacitor (or pseudocapacitor) maintains a constant current density over the voltage window during discharge. A visual representation of the FF for a Type I XDOT-based device is shown in Figure 2.10, with

the actual area inside the blue trace (solid line) and the ideal area as the red box (dashed line). Deviation from ideal charge/discharge behavior (a rectangle) is caused by any form of resistance in the device (e.g. charge transfer resistance between the electrodes, ionic resistance between the active material and the electrolyte, resistance from the separator).

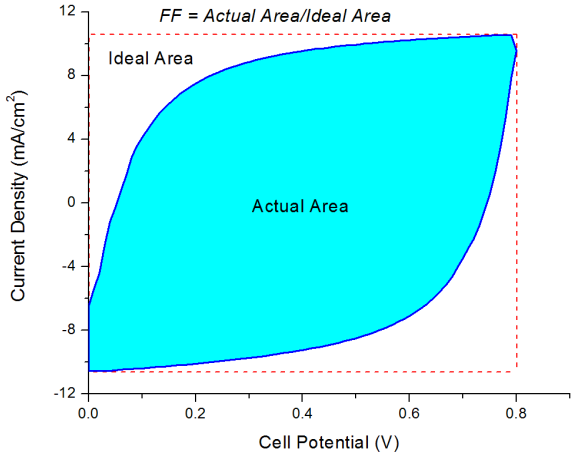

Figure 2.10. A charge/discharge CV trace of a Type I supercapacitor device showing the actual area (shaded in teal) vs. the ideal area (red box).

2.6 Electrical Conductivity & Seebeck Coefficient

The electrical conductivity of conjugated polymers has been a point of research since the initial discovery that doped films of polyacetylene can have electrical conductivity values of >500 S/cm, as previously discussed in Chapter 1.[107] In the charge neutral form, conjugated polymers have low electrical conductivities, typically < 10^{-5} S/cm. Introduction of charges to the polymer backbone via doping, as discussed in Chapter 1, can increase this conductivity by many orders of magnitude and specific

examples of this significant increase are shown in Chapter 6. To be clear, in the context of this document, unless otherwise noted, the term doping refers to a transfer of an electron (or electrons) to or from the conjugated polymer to an added small molecule or metal salt, resulting in polarons and/or bipolarons on the polymer chains and the corresponding geometric changes associated with this process. The highest conductivity solution processable polymer is currently PEDOT:PSS, with reported conductivities of several thousand S/cm.[108,109] Truly soluble polymer, and not dispersions, have also reached high conductivities. For example, the Chabinyc group has reported PBTTT to have a conductivity of 1300 S/cm when vapor doped.[110] However, these materials are outliers and the majority of CPs have significantly lower conductivities when doped. The structure property relationships needed to design new highly conductive materials have not been established and doping studies normally consist of one polymer being selected and doped without comparison to other materials and why the resulting conductivity is what it is. Films of ECPs were cast onto glass substrates (not ITO) via various methods including spray and blade coating. These films were then dipped in a solution of dopant and either heptane or PC at various concentrations for a various periods of time. The films were then washed (with either clean heptane or PC followed by methanol) and dried in air. Gold electrical contacts were deposited on the films and the electrical conductivity measurements are performed using the four-probe van der Pauw technique. A schematic of the contacts, film, and substrate is shown in Figure 2.11. Micromanipulators with tungsten tips were used to make electrical contact to the gold contact pads to obtain the in-plane resistivity. The electrical conductivity in S/cm was calculated using the

resistivity values and film thickness as determined by profilometry after the measurements.

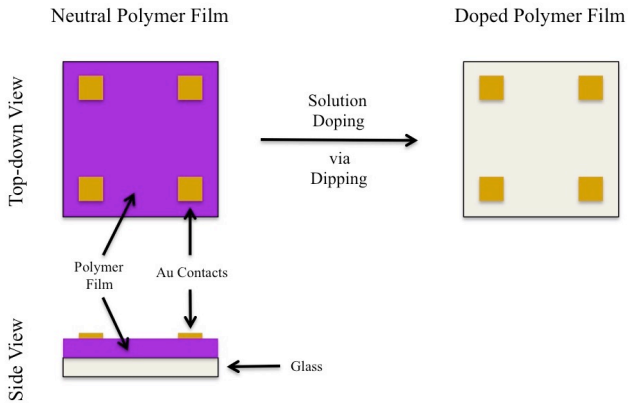

Figure 2.11. Schematic of a polymer film (before and after doping) on a glass slide with gold contacts deposited on top of the polymer.

The diffusion of mobile charge carriers (holes or electrons) in a material due to a temperature gradient (ΔT) across it is termed the Seebeck coefficient (S).[34] S is essentially the amount of entropy of the carriers in a material. This value can be positive or negative depending if the carriers move towards the hot or cold side of the material and is commonly reported in μV/K. For doped CPs the values are generally positive and small and as the doping level of a polymer increases the S value decreases.[34] There are currently no known structure property relationships for the S in CPs. For these measurements, the film was suspended between two temperature-controlled Peltier units and a series of temperature differences were applied between the stages. The thermoelectric voltage was measured between two contact pads on separate stages using

the probe tips, while the temperature of each pad was measured with thermocouple in close proximity to the probe tips. The S was extracted as the slope of the V - ΔT plot. Further details regarding the conductivity and S measurements can be found in the experimental details of Chapter 6.

CHAPTER 3. DESIGNING A SOLUBLE PEDOT ANALOGUE WITHOUT SURFACTANTS OR DISPERSANTS

Adapted from:

Ponder, J., F., Österholm, A., M., Reynolds, J. R. Designing a Soluble PEDOT Analogue without Surfactants or Dispersants. *Macromolecules* **2016**, 49, 2106–2111

&

Österholm, A., M., Ponder, J., F., Kerszulis, J., A., Reynolds, J., R. Solution processed PEDOT analogs in electrochemical supercapacitors. *ACS Applied Materials & Interfaces*, **2016**, 8 (21), 13492–13498

3.1 The Reason for a Processable PEDOT Analogue

Since its discovery in the 1980s, PEDOT has become one of the most studied and used electroactive polymers because of its redox activity, high conductivity with concurrent visible transmissivity, accompanying thermal, chemical, and environmental stability, as well as organic and, to some extent, aqueous electrolyte compatability.[14,16] Thin films of PEDOT have been evaluated for use in a variety of applications ranging from transistors to electrolytic capacitors and organic supercapacitors, solar cells, and antistatic coatings.[88,111-114] In addition, PEDOT was also one of the first cathodically

coloring electrochromic polymers, switching from a deep blue neutral form to a sky-blue transmissive oxidized form.[115,116] In the absence of surfactants or dispersants (such as poly(styrenesulfonate) (PSS^-)), PEDOT is an insoluble polymer, where the properties of the resulting PEDOT films are highly dependent on the precise polymerization method/conditions, making structural and molecular weight characterizations difficult.[117,118,46] Attempts have been made to develop a soluble version of PEDOT by functionalization of the ethylene bridge with alkyl chains, but any direct manipulation of the EDOT unit changes the electrochemical and optical properties of the resulting polymer as a result of the increased steric bulk and regioirregularity induced by the solubilizing groups.[119,120] To facilitate solution processing, EDOT can be polymerized in the presence of PSS^- or another solubilizing salt to form an aqueous dispersion (e.g., PEDOT:PSS) which allows these composites to be deposited by various methods including, but not limited to, spin-coating, slot-die coating, and inkjet printing.[14]

While PEDOT:PSS is used effectively in various solid-state applications where device operation relies on PEDOT maintaining its oxidation state, electrochemical devices such as supercapacitors and electrochromic displays rely on complete and reversible switching between two extreme redox states for optimal device performance (i.e., complete charge/discharge in supercapacitors and optimal color contrast in electrochromic devices). In the presence of an excess of an immobilized counterion, such as PSS^-, PEDOT cannot be fully reduced to its charge neutral form, limiting its use as an active material in these electrochemical devices. In addition to numerous solvent additives or post-treatment methods that have been evaluated to either remove or segregate the PSS^-, polyethylenimine (PEI) has been used to chemically reduce

PEDOT:PSS for an all-polymer battery application.[121,108,122,123,124] However, even this method was not able to fully remove polaronic charge carriers from the PEDOT backbone.[124]

3.2 Developing the ProDOT$_x$-EDOT$_y$ Series

Here, a series of soluble dioxythiophene polymers (Scheme 3.1) have been designed and prepared which are electrochemically equivalent and optically superior to PEDOT with the added advantage of being highly soluble in organic solvents without having to structurally modify the EDOT unit or use any additional surfactants or dispersants. As shown in Scheme 3.2, this is achieved by copolymerizing various ratios of EDOT with alkoxy-functionalized ProDOTs as the solubilizing unit. Alkoxy-functionalized ProDOT was chosen due to its (i) electron richness to maintain a low oxidation potential, (ii) ease of side chain manipulation to tune solubility, and (iii) high electrochromic contrast and color neutral oxidized state of the corresponding homopolymer, ECP-M.[20] We show that it is possible to combine these two model polymers, ECP-M and PEDOT, to obtain a copolymer with the high solubility and colorless oxidized state of ECP-M and the low onset of oxidation, high electrochemical activity over a broad voltage range, and vibrant blue neutral state color of PEDOT. It has been previously demonstrated in the literature that EDOT readily undergoes direct DHAP as either the dihydrogen or dihalide species, allowing us to avoid the use of more toxic cross-coupling polymerization methodologies such as the tin reagents employed in Stille couplings.[125,126]

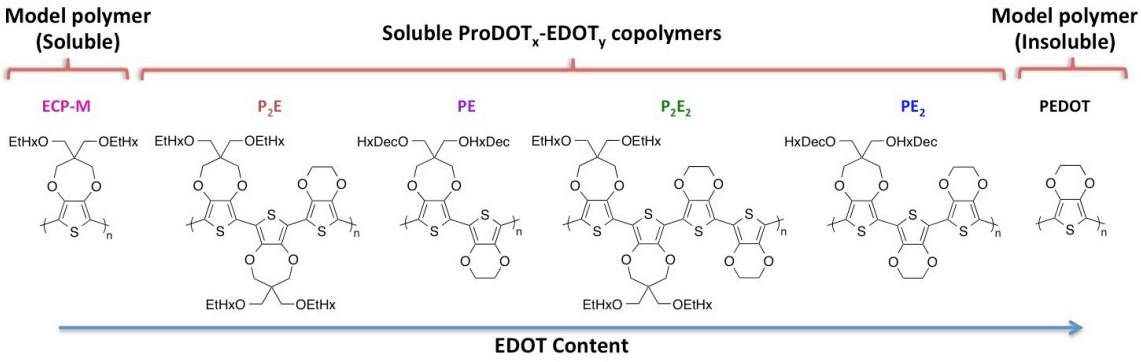

Scheme 3.1. The full series of investigated ProDOT$_x$-EDOT$_y$ (P$_x$E$_y$) copolymers as well as the parent homopolymers, beginning from the left with the soluble alkoxy-functionalized PProDOT (ECP-M) and progressing through a series of soluble copolymers (P$_x$E$_y$) with increasing EDOT content in the repeat unit, and finally ending with PEDOT on the far right.

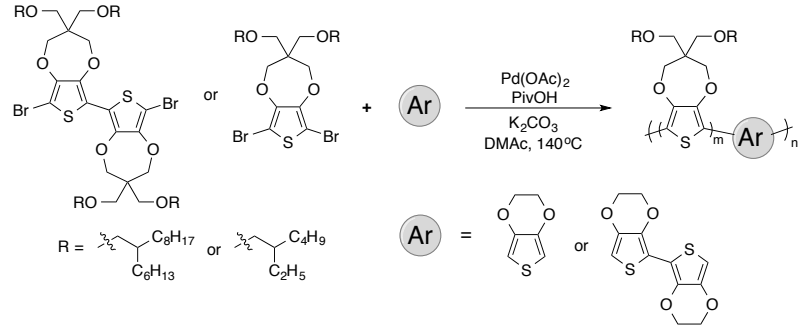

Scheme 3.2. Synthetic route to ProDOT$_x$-EDOT$_y$ (P$_x$E$_y$) copolymers via DHAP

ECP-M was prepared by Dr. Justin Kerszulis via an oxidative polymerization previously reported (M_n: 12.4 kDa, Đ: 1.8).[127] Each of the copolymers were designed to achieve a solubility in typical solvents (such as $CHCl_3$) exceeding 30 mg/ml to be suitable for a wide range of coating methods yielding films with varied thicknesses. To achieve this solubility, PE and PE_2 were synthesized with 2-hexyldecyloxymethyl (HxDec) side chains, whereas shorter 2-ethylhexyloxymethyl (EtHx) side chains were sufficient for the other copolymers. P_2E (M_n: 14.5 kDa, Đ: 2.0), and P_2E_2 (M_n: 14.1 kDa,

Đ: 4.5) were synthesized by Justin Kerszulis as previously reported using typical DHAP conditions.[72-73] PE (M_n = 43.8 kDa, Đ = 1.4) and PE_2 (M_n = 56 kDa, Đ = 1.8) were also polymerized using DHAP, with full synthetic details in section 3.7.1.

3.3 Optical and Redox Progression

From the structures shown in Scheme 3.1, PE_2 has the highest EDOT content of all the copolymers. However, even with every third heterocycle in PE_2 being an alkoxy-functionalized ProDOT unit, we found this copolymer to be optically (in the charge neutral state) and electrochemically essentially identical to electrochemically polymerized PEDOT as shown in the transmittance spectra and cyclic voltammograms in Figure 3.1. In the charge neutral state (−1.0 V in Figure 3.1a), both PE_2 and PEDOT exhibit a transmittance minimum at ~600 nm, thereby absorbing the low energy red light and resulting in giving them both a deep blue color. Despite the similarities in the neutral state color, there is a remarkable difference in the oxidized state spectra (+1.0 V in Figure 1a). PE_2 in the charge neutral state has a narrower and more defined absorbance profile in the visible range and far less tailing into the near-IR in its oxidized state when compared to PEDOT. This results in both a more neutral color and a significantly more transmissive oxidized state. A comparison of the CV traces of these two polymers (Figure 3.1b) shows a remarkable similarity between them in both the onset of oxidation and breadth of electroactivity. Such low potentials for current onsets demonstrate the highly electron-rich nature of the soluble copolymer film, as desired for applications where accessing the oxidized and conducting form of the polymer is important. In addition, both polymers exhibit high capacitive currents beyond the reversible redox process over a broad

potential range (>1.5 V), which is a desirable attribute when considering these polymers for charge storage applications, as discussed in Chapter 2. This broad redox response is not typically seen in soluble ProDOT-based polymers, as they tend to exhibit both a much higher onset of oxidation and a more defined, Faradaic redox behavior. Interestingly, even though the ProDOT moieties with their solubilizing groups (i.e., that are significantly different from unfunctionalized EDOT) make up a third of the polymer chain, the electrochemical properties and the color in the charge neutral state bare little resemblance to the ProDOT homopolymer and many similarities to unfunctionalized PEDOT.

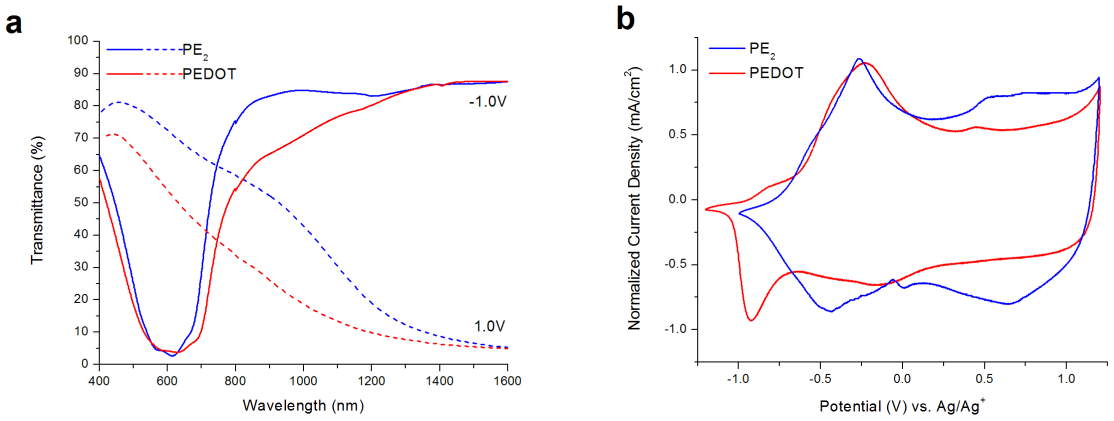

Figure 3.1. a) Transmittance spectra of PE_2 (blue curves) and electrochemically polymerized PEDOT (red curves) on ITO/glass in their charge neutral (-1.0 V vs. Ag/Ag^+, solid lines) and oxidized states (+1.0 V vs. Ag/Ag^+, dashed lines) and b) CVs of PE_2 (blue line) and PEDOT (red line) on glassy carbon electrodes at a sweep rate of 50 mV/s, with both experiments in 0.5 M $TBAPF_6$/PC.

From these results, we focused on understanding how the P_xE_y copolymers differed from the parent PProDOT and PEDOT homopolymers, as well as elucidate how

changing the ratio of the heterocycle rings affected the optical and electrochemical properties. Surprisingly, the addition of just one EDOT unit for every three heterocycles drastically altered the band gap and oxidation onset compared to the homopolymer ECP-M, as shown in Figure 3.2. P_2E has an optical band gap ($E_{g,opt}$) of 1.81 eV, which is significantly narrower than the ECP-M homopolymer with an $E_{g,opt}$ of 1.97 eV. Similarly, the onset of oxidation is lowered by 0.4 V when exchanging every third ProDOT unit for an EDOT. Increasing the amount of EDOT further from 33% to 50% and finally to 67% results in a progressive decrease in both the band gap (Figure 3.2a) and the onset of oxidation (Figure 3.2b), albeit at a more gradual rate. PE_2, with an EDOT content of 67%, has an $E_{g,opt}$ that is 0.26 eV smaller than ECP-M but only 0.05 eV larger than electrochemically polymerized PEDOT. Compared to ECP-M, the oxidation potential is almost 0.8 V lower for PE_2. The lower oxidation potential and narrower $E_{g,opt}$ is the result of reduced steric interactions between adjacent rings as the amount of solubilizing groups decrease, which leads to a planarization of the polymer backbone.[73]

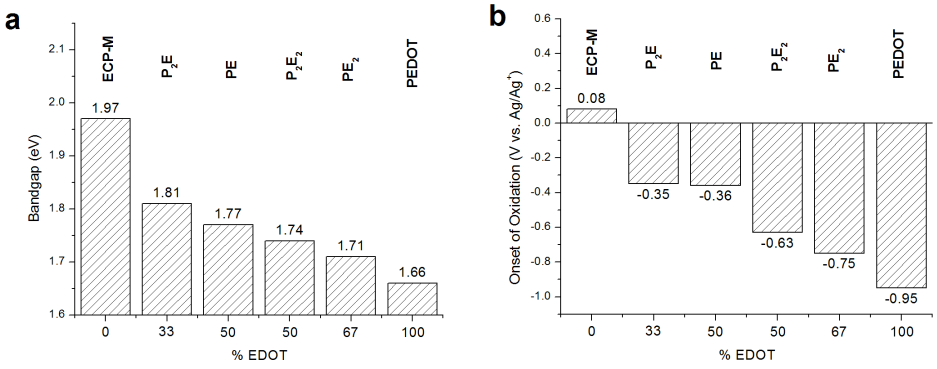

Figure 3.2. Progression of the a) optical band gap and the b) onset of oxidation (determined by differential pulse voltammetry) as a function of EDOT content in P_xE_y copolymers compared to their parent polymers ECP-M and PEDOT.

As demonstrated in Figure 3a, adding just one EDOT unit to the ProDOT system (P_2E) not only lowers the onset of oxidation, but also results in a significant, almost 5-fold, increase in the current density compared to the ProDOT homopolymer. The high current density is also maintained for the other EDOT containing copolymers. Another interesting observation is found when comparing PE and P_2E_2; even when the overall EDOT content in one repeat unit is the same (50%), the incorporation of a biEDOT unit results in a significant, almost 0.3 V decrease in the onset of oxidation. This is likely due to the planar, electron-rich nature of the biEDOT unit, which, in comparison to a single EDOT unit, is able to more efficiently stabilize the positive charge carriers formed during oxidation.

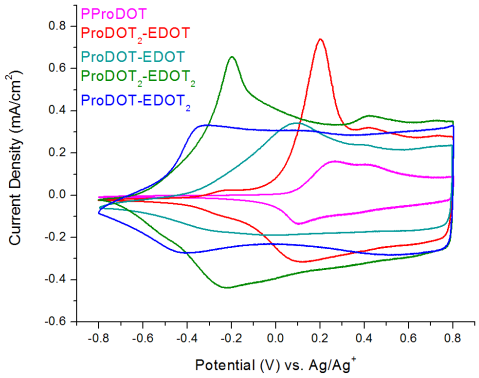

Figure 3.3: CVs of drop cast films of ECP-M and the P_xE_y copolymers on glassy carbon button electrodes, in 0.5 M TBAPF$_6$-PC at 50 mV/s.

The narrowing of the $E_{g,opt}$ and a red-shift of the λ_{max} (Figure 3.4a) that is observed as the EDOT content is increased translate into a color change that progresses from the distinct purple-magenta color of alkoxy-functionalized PProDOT to the vibrant

deep blue color of PEDOT. To accurately quantify and compare the colors, the absorbance spectra were converted to CIELAB L*a*b* coordinates. The a*b* representation in Figure 3.4b allows us to quantify both the hue and saturation of the color, as discussed in Chapter 2. All the copolymers fall in the +a* and −b* (red−magenta−purple−blue) quadrant of the color space, as shown in Figure 3.4b. The red-shift observed in both the λ_{max} and $E_{g,\ opt}$ translates into the color of the polymer becoming more blue as indicated by the high negative b* and the progressive lowering of the a* (red) component with increasing EDOT content and increased chain relaxation. The color coordinates for all the copolymers are summarized in Table 3.1. From the L*a*b* values we can determine the degree of color saturation (see equation 2.2), previously discussed in Chapter 2.[94] All the soluble copolymers, as well as PProDOT, exhibit a color saturation between 86 and 91 (see Table 3.1); these values indicate a higher degrees of color purity for the P_xE_y series compared to broadly absorbing materials, such as those used in OPV. As seen graphically in Figure 3.4b and numerically in Table 3.1, the color coordinates of the charge neutral states of PE_2 and PEDOT are very similar. The difference in color can be quantitatively compared using equation 2.1 to calculate the color difference (ΔE^*_{ab}). As shown in Table 3.1, the value of ΔE^*_{ab} for PE_2 and PEDOT is 2.2 in the colored state. Recall from Chapter 2 that a ΔE^*_{ab} value lower than 2.3 means that two colors (in this case of PE_2 and PEDOT) are indistinguishable to a C.I.E. standard observer.[94,95]

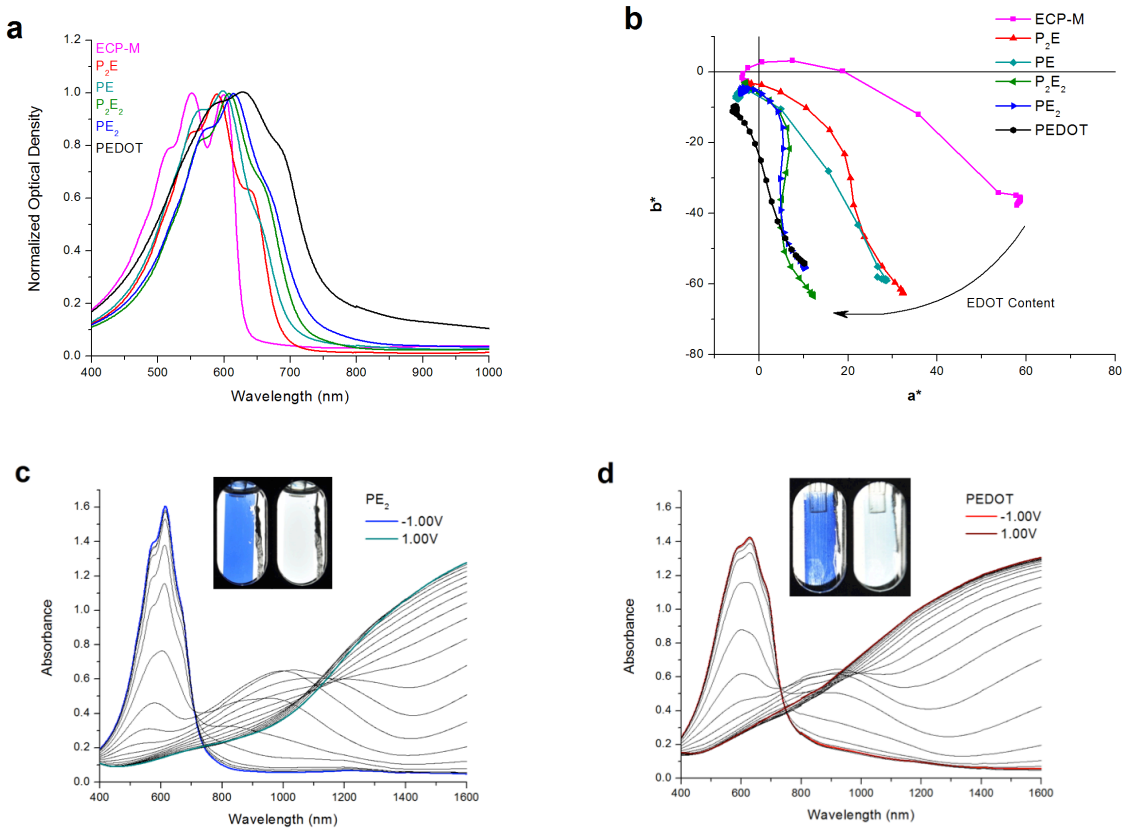

Figure 3.4. a) Normalized absorbance spectra of PProDOT and the P_xE_y copolymers on ITO glass, in 0.5 M $TBAPF_6$-PC at 50 mV/s. b) a*b* diagram showing the color change occurring during electrochemical oxidation of the polymer series from -1.0 V to 0.8 or 1.0 V vs. Ag/Ag^+ in 0.1 V increments. Absorbance as a function of potential recorded between -1.0 V and 1.0 V vs. Ag/Ag^+ of c) PE_2 and d) electrochemically polymerized PEDOT with photographs inset, in 0.5 M $TBAPF_6$/PC.

Table 3.1. Colorimetry and Optical Comparisons of P_xE_y polymer series.

Polymer	L*, a*, b* (neutral)	L*, a*, b* (oxidized)	Color Saturation (neutral)	ΔE^*_{ab} of P_xE_y vs. PEDOT (neutral)	ΔE^*_{ab} of P_xE_y vs. PProDOT (neutral)
ECP-M	42, 58, -38	89, -3, -3	86	51.1	0.0
P_2E	33, 32, -63	89, -2, -3	91	23.9	37.2
PE	30, 27, -58	87, -2, -3	91	18.2	38.8
P_2E_2	37, 12, -63	92, -3, -3	87	9.4	52.6
PE_2	34, 10, -56	83, -3, -5	86	2.2	51.9
PEDOT	35, 10, -54	81, -6, -10	84	0.0	51.1

In addition to a high color saturation and vibrancy, the copolymers all switch to a highly transmissive and color neutral state upon electrochemical oxidation as can be seen in Table 3.2 and in the color tracks in Figure 3.3b. In comparison to PEDOT, all copolymers are more color neutral in their oxidized states as indicated by the lower a*b* values and the higher L*.[128] The slightly negative a*b* values recorded for the oxidized states are due to tailing of charge carrier bands into the visible as will be discussed in more detail below.

Table 3.2. Summary of electrochemical and optical properties of P_xE_y copolymers.

Polymer	EDOT Content (%)	λ_{max} (nm)	Contrast (Δ%T)	Switching speed (sec)[a]
ECP-M	0	552 (600)[b]	71	1.1
P_2E	33	590	71	0.6
PE	50	596	71	1.1
P_2E_2	50	606	75	0.5
PE_2	67	613	71	0.5
PEDOT	100	629	46	0.7

a) 95 % of full switch from colored-to-bleached, calculated from chronoabsorptiometry, b) Secondary vibronic peak

3.4 A Closer Look at PE_2 and PEDOT

As shown in Table 3.2 and demonstrated for PE_2 in Figure 4c, all the copolymers exhibit high electrochromic contrasts (Δ%T, defined as the change in transmittance between the neutral and oxidized states measured at λ_{max}) exceeding 70% with switching times on the order of 0.5−1 s (the chronoabsorptiometry data for PE and PE_2 are shown in Figure 5 and in ref 28 for P_2E and P_2E_2). Even though comparable electrochromic contrasts could not be obtained here for PEDOT using our electrolyte system and polymerization method, a contrast of 71 Δ%T at 635 nm has been reported for electrochemically deposited PEDOT by Bendikov and co-workers using highly optimized

film thicknesses and polymerization conditions.[46] This large variation in film quality and resulting electrochromic contrast from electropolymerized films is due to the nucleation-growth mechanism and is not a concern for solution processed polymers. The main difference in the electrochromic switching performance of this family of solution processable copolymers we have developed was that with increasing EDOT content the potential at which the π–π* absorption band is completely bleached out decreases following a similar trend as observed for the $E_{g,opt}$, with PE_2 essentially reaching its fully bleached state at just 0.0 V, as shown in the spectra in Figure 3.4c. Interestingly, even if little electrochromic change is observed at higher potentials, PE_2 and P_2E_2 are still able to maintain a high redox current up to potentials exceeding 1 V vs Ag/Ag^+.

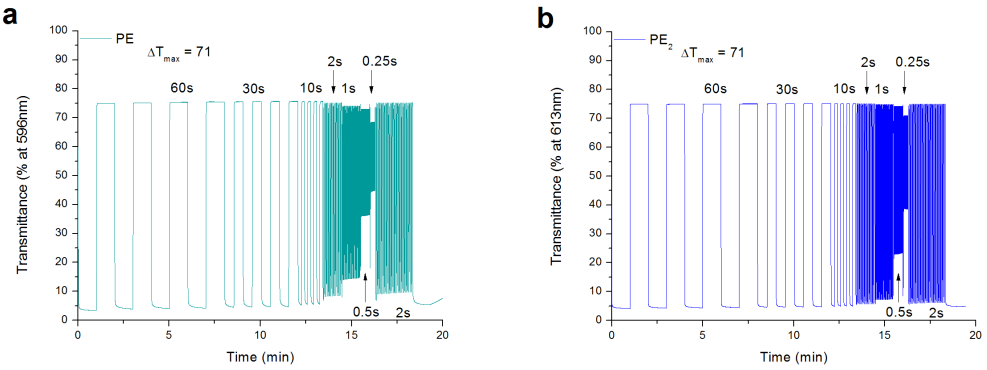

Figure 3.5. Chronoabsorptiometry of a) PE and b) PE_2 on ITO glass in 0.5 M $TBAPF_6$/PC.

A more careful comparison of the spectroelectrochemistry of PE_2 and PEDOT (Figures 3.4c and 3.4d) shows that the absorption spectra are nearly identical in the

charge neutral states including the same vibronic features, and this accounts for the similarity in the color of the two polymers as discussed above. The noticeable difference in the electrochromic contrast and in the chromaticity of the oxidized states (with a ΔE^* of ab 6.2 for PE_2 vs PEDOT in their oxidized states) is due to the charge carrier bands in PEDOT tailing into the visible, leaving more residual color while reducing optical contrast. In PE_2, the higher energy charge carrier band originating from polarons is red-shifted by >100 nm, from 923 nm to approximately 1038 nm. Also, the bipolaron absorption (λ_{max} outside the recorded wavelength range) is shifted to a lower energy in PE_2, which significantly reduces the tailing into the visible and accounts for a more color neutral oxidized state. The positions of the charge carrier bands in PE_2 are more similar to those found in alkoxy-functionalized PProDOT than those in PEDOT. This red-shift of charge carrier bands is an interesting observation as it differs from the trends observed for the $E_{g,opt}$, the color, and the oxidation potential where the copolymers exhibit properties more closely resembling those of PEDOT than those of PProDOT.

3.5 PE_2 Based Type I Supercapacitor Devices

The average mass capacitance of PE_2 films estimated from the CVs recorded at 50 mV/s is 71.4 (+/- 10.1) F/g. Considering only the mass contribution of the electroactive backbone (i.e. 46 wt %), the mass capacitance is 130.8 F/g. This is higher than typically estimated for electrodeposited PEDOT (90-120 F/g), and is close to the theoretical capacitance of PEDOT of 210 F/g (assuming a doping level of 0.33 as discussed in Chapter 1).[129,130] In order to appropriately assess this copolymer for charge storage applications, it is necessary to evaluate it in a symmetrical two-electrode device referred to as a Type I SC.[131] SC devices using PE_2 as the active material and LiBTI/PC as the

electrolyte were tested in triplicate and the specific capacitance was calculated based on the integrated area of the discharge CV using the mass of the active material on one electrode and was calculated as 31.5 (+/- 2.0) F/g at 50 mV/s. As shown in Figure 3.6a, unencapsulated PE_2 supercapacitors assembled and tested under ambient conditions are highly stable in PC-based electrolytes showing minimal loss (< 20 %) of current/capacitance/FF over the course of 50,000 charge/discharge cycles. This confirms that these polymer films are electrochemically robust and that the long-term cycling stability characteristics for electrochemically synthesized PXDOTs are maintained in these soluble analogs. In addition to the promising cycling stability, these devices also exhibit exceptional electrochemical stability over a broad voltage range, as shown in Figure 6b. PE_2 supercapacitors maintain a high FF and charge/discharge currents even at a cell voltage of 1.6 V. This increase in cell voltage results in an increased energy density (18.4 Wh/kg) and power density (3.3 kW/kg) that is almost a five-fold increase compared to earlier work on PXDOT and PXDOP devices.[105,106,132,133]

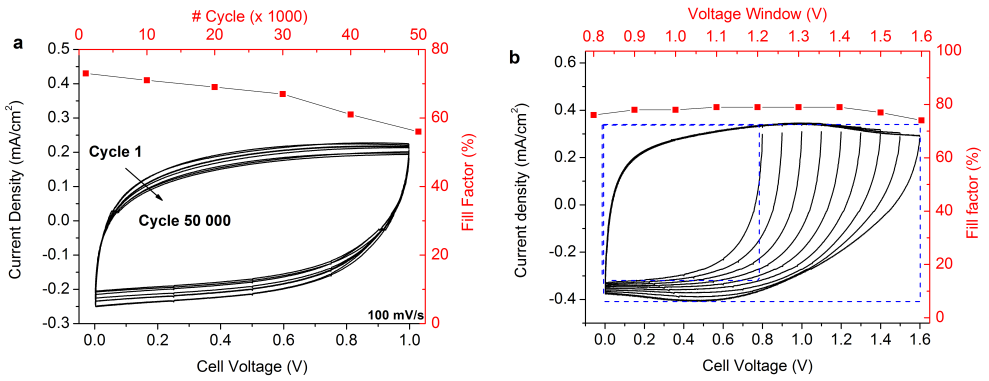

Figure 3.6. a) Cycling stability and fill factor retention of a PE_2 device over the course of 50,000 cycles at 100 mV/s and b) the effect on fill factor and redox behavior at 50 mV/s of a PE_2 type I supercapacitor (0.5 M LiBTI-PC electrolyte, polypropylene separator) with increased cell voltage.

3.6 Conclusion

In summary, we have developed a highly soluble dioxythiophene-based polymer using direct arylation copolymerization that mimics the electrochemical and optical properties of PEDOT, and we have been able to accomplish this without additional surfactants or dispersants. Using this copolymerization method, we have prepared a family of polymers that combines the attractive properties of PEDOT (low oxidation potential, broad electrochemical window) with those of alkoxy-functionalized PProDOTs (high solubility and exceptional electrochromic contrast) with a range of accessible colors. The polymer with the highest EDOT content (PE_2) possesses a neutral state color that is optically indistinguishable from electrochemically prepared PEDOT while achieving a higher contrast and a more color neutral oxidized state. This polymer also possesses the lowest oxidation potential we have observed for a soluble thiophene-based polymer and a stable electrochemical window of over 2 V. Charge storing supercapacitors of PE_2 are highly stable to repeated cycling stability with minimal capacitance loss even after 50,000 cycles and can achieve voltages up to 1.6 V, outperforming most Type I and Type II polymer-based supercapacitors. This allows us to now move away from electropolymerized films for charge storage and make solution-processed device using electrodes of varying form factor made from different materials.

3.7 Experimental Details

3.7.1 Materials & Synthesis

Materials

EDOT (97%) was purchased from Alfa Aesar and purified via vacuum distillation before use. 2-Hexyl-1-decanol (97%) and pivalic acid (99%) were purchased from Sigma and was used as received. NaH (57-63% oil dispersion, Alfa Aesar), $Pd(OAc)_2$ (98% , Strem Chemicals), K_2CO_3 (anhydrous, Oakwood Products), 18-Crown-6 (99%, Acros), diethyldithiocarbamic acid diethylammonium salt (97%, TCI America) were all used as received. 3,3-Bis(bromomethyl)-3,4-dihydro-2H-thieno[3,4-b][1,4]-dioxepine [ProDOT($CH_2Br)_2$] was prepared by Dr. B. Reeves[35] and used here without additional puricication. BiEDOT was prepared using a published method[36] and confirmed via ^{1}H NMR and GC-MS. The new monomers ProDOT(HxDec) and ProDOT(HxDec)-Br_2 were prepared as described below with their NMRs. DMF (*N,N*-dimethylformamide) (anhydrous) was purchased from EMD and used as received. DMAc (*N,N*-dimethylacetamide) (HPLC grade, Alfa Aesar) was filtered through a pad of basic alumina (Sigma Aldrich) prior to use. Chloroform (BDH, 99.8 %) was used without further purification to dissolve the polymers. ^{1}H-NMR and ^{13}C-NMR spectra were collected on either a Varian Mercury Vx 300 MHz instrument or a Bruker AVANCE III HD 500 MHz instrument using $CDCl_3$ as a solvent.

Synthesis of ProDOT(HxDec)

A dry 500 mL round-bottom flask equipped with a stir bar was filled with 240 mL of DMF and 43.0 mL (0.148 mol, 2.5 eq.) of 2-hexyldecyl alcohol. The experiment was placed under argon, and 7.49 g (0.2339 mol, 4 eq.) of NaH (57-63% in mineral oil) was

slowly added. Upon complete addition of the NaH, the reaction was then heated to 110 °C for 30 minutes. 20.0g (0.0585 mol, 1 eq.) of ProDOT($CH_2Br)_2$ was then added and the reaction was carried out at 110 °C for 20 h. Afterwards, the flask was cooled to ambient temperature and extracted with brine and 1:1 diethyl ether/ethyl acetate. The organic layer was then washed three times with deionized water and the solvent was removed by rotary evaporation under reduced pressure. The resulting crude oil was purified by column chromatography using 2% ethyl acetate in hexanes on neutral silica to give 33.1 g (85.0%) of the product as a clear, colorless oil. ^{1}H-NMR (300 MHz, $CDCl_3$, 25 ^{o}C) δ 6.43 (s, 2H), 4.00 (s, 4H), 3.46 (s, 4H), 3.26 (d, 4H, J = 5.7 Hz), 1.53 (s, 2H), 1.34-1.20 (br, 48H), 0.88 (t, 12H, J = 6.7 Hz). ^{13}C-NMR (75 MHz, $CDCl_3$, 25 ^{o}C) δ 149.7, 104.9, 74.7, 73.8, 69.8, 47.8, 38.1, 31.93, 31.90, 31.5, 30.1, 29.8, 29.7, 29.4, 26.8, 22.7, 14.1. HRMS (ESI) m/z calcd for $C_{41}H_{77}O_4S$ 665.5537, found 665.5530.

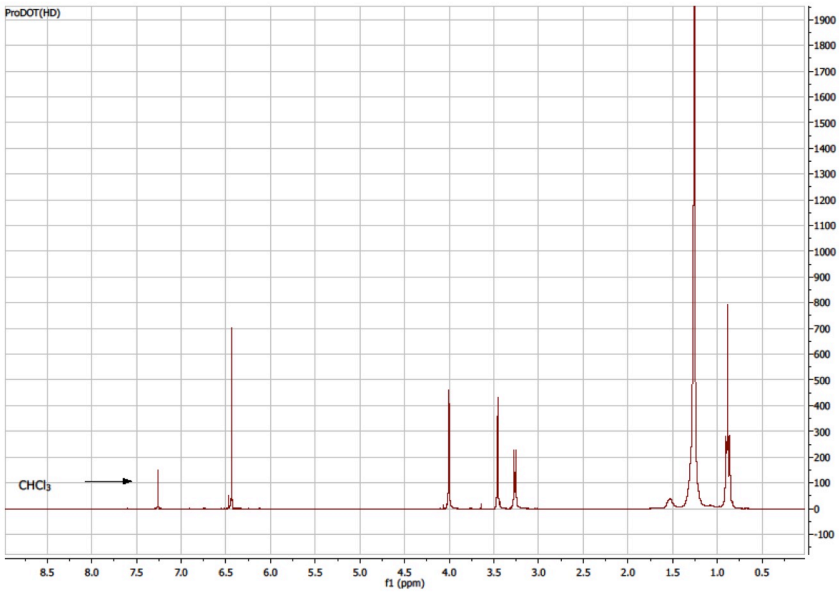

Synthesis of ProDOT(HxDec)-Br_2

A dry 250 mL round-bottom flask equipped with a stir bar was filled with 70.0 mL of $CHCl_3$ and 2.012 g (3.0 mmol, 1 eq.) of ProDOT(HxDec). Then 1.34 g (7.5 mmol, 2.5 eq.) of NBS was added and the reaction stirred under argon overnight at room temperature while cover with aluminum foil to block light. After completion, the product was extracted with brine and 200mL of 1:1 ethyl ether/ethyl acetate. The organic layer was then washed three times with deionized water and dried over magnesium sulfate. The solvent was removed by rotary evaporation under reduced pressure. The resulting crude oil was purified by column chromatography using hexanes on neutral silica to give 2.29 g (91.8%) of the product as a clear, colorless oil. ^{1}H-NMR (300 MHz, $CDCl_3$, 25 ^{o}C) δ 4.07 (s, 4H), 3.47 (s, 4H), 3.26 (d, 4H, J = 5.7 Hz), 1.54 (s, 2H), 1.35-1.20 (br, 48H), 0.88 (t, 12H, J = 6.9 Hz). ^{13}C-NMR (75 MHz, $CDCl_3$, 25 ^{o}C) δ 147.0, 90.8, 74.7, 74.3, 69.7, 48.0, 38.1, 31.93, 31.90, 31.5, 30.1, 29.8, 29.7, 29.4, 26.9, 26.8, 22.7, 14.1 HRMS (ESI) m/z calcd for $C_{41}H_{75}O_4Br_2S$ 821.3747, found 821.3745.

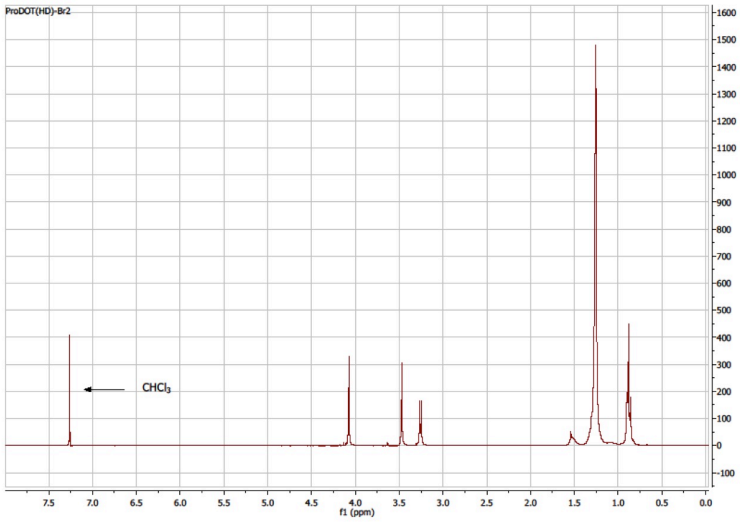

Synthesis of PE

To a 38 mL Schlenk tube equipped with a stir bar, ProDOT(HxDec)-Br_2 (0.7999 g, 1.0 eq.), EDOT (0.1379 g, 1.0 eq.), palladium acetate (0.0052 g, 2 mol%), pivalic acid (0.0292 g, 0.3 eq.), and potassium carbonate (0.3327 g, 2.5 eq.) were added. 25 mL of DMAc was added to the tube to dissolve the contents and it was sealed under argon. The reaction mixture was premixed for 2 minutes and then lowered into a hot oil bath held at 140 °C. This solution was allowed to stir vigorously overnight (~14 hours). After the flask was removed from the oil bath and allowed to cool to room temperature, a small amount of $CHCl_3$ was added. The polymer dispersion was precipitated into methanol and stirred for one hour. The precipitate was filtered into a soxhlet extraction thimble and washed with methanol, acetone, hexanes, and finally dissolved into chloroform. The washings were conducted until color was no longer observed during extraction. After dissolution from the thimble, the chloroform was removed via rotary evaporation. 50 mL of chloroform was added followed by ~40 mg of a palladium scavenger (diethylammonium diethyldithiocarbamate) and ~40 mg of 18-crown-6 and then the solution was stirred for 2 hours at 50° C followed by precipitation into 250 mL of methanol. The precipitate was vacuum filtered, using a Nylon pad (with a pore size of 20 μm) as the filter, and washed with a large volume of methanol and allowed to dry. The dried material was collected into a vial and dried under vacuum. The polymer was obtained as a dark purple solid in 60.2% yield (469 mg). ^{1}H-NMR (500 MHz, $CHCl_3$, 50 ^oC) δ 4.19 (br, 4H), 3.63 (br, 4H), 3.36 (br, 4H), 1.62 (br, 2H), 1.45-1.15 (br, 65H), 0.90 (s, 12H). Anal. calcd. for $C_{47}H_{78}O_6S_2$ C 70.28, H 9.79, S 7.98, Found C 70.09, H 9.83, S 8.23. M_n = 43.8 kDa, Đ = 1.4, vs. PS in THF at 35 °C.

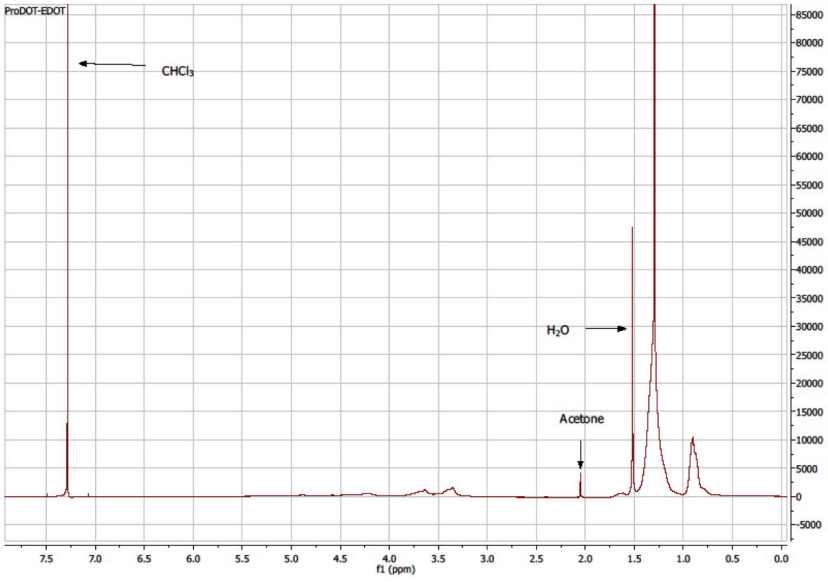

Synthesis of PE_2

To a 38 mL Schlenk tube equipped with stir bar, ProDOT(HxDec)-Br_2 (0.54505 g, 1.0 eq.), biEDOT (0.187 g, 1.0 eq.), palladium acetate (0.003 g, 2 mol%), pivalic acid (0.021 g, 0.3 eq.) and potassium carbonate (0.220 g, 2.5 eq.) were added. 20 mL of DMAc was added to dissolve the contents and the tube was sealed under argon. The reaction mixture was premixed for 2 minutes to ensure the contents dissolved before heating. The tube was lowered into a hot oil bath held at 140 °C and allowed to stir vigorously overnight (~14 hours). After the flask was removed from the oil bath and allowed to cool to room temperature, a small amount of $CHCl_3$ was added the polymer was precipitated into methanol and stirred for one hour. The precipitate was filtered into a soxhlet extraction thimble and washed with methanol, acetone, hexanes, and finally dissolved into chloroform. The washings were conducted until color was no longer observed during extraction. After dissolution from the thimble, the chloroform was removed via rotary

evaporation. 50 mL of chloroform was added followed by ~40 mg of a palladium scavenger (diethylammonium diethyldithiocarbamate) and ~40 mg of 18-crown-6 and then stirred for 2 hours at 50 °C followed by precipitation into 250 mL of methanol. The precipitate was vacuum filtered, using a Nylon pad (with a pore size of 20 μm) as the filter, and washed with a large volume of methanol and allowed to dry. The dried material was collected into a vial and dried under vacuum. The polymer was obtained as a blue/purple solid in 92.1% yield (575 mg). ^{1}H-NMR (500 MHz, $CHCl_3$, 50 ^{o}C) δ 4.41 (br, 8H), 4.20 (s, 4H), 3.55 (s, 4H), 3.46 (d, 4H), 1.59 (s, 2), 1.45-1.21 (br m, 90H), 1.00-0.84 (br m, 14H). Anal. calcd. for C53H82O8S3 C 67.48, H 8.76, S 10.19, Found C 66.94, H 8.76, S 10.34. M_n: 56 kDa, Đ: 1.8, vs. PS in trichlorobenzene at 120 °C.

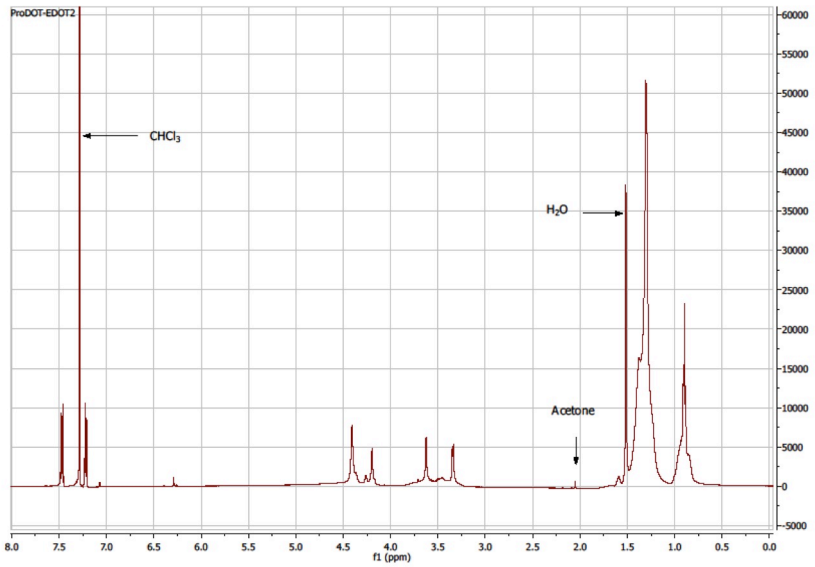

3.7.2 Film Preparation & Characterizations

In this study, the copolymers and PProDOT were spray coated onto ITO/glass (25 x 75 x 0.7 mm^3, sheet resistance: 8-12 ohm/sq, Delta Technologies) using a simple hand-held airbrush (Iwata-Eclipse HP-BC, 15 psi) from 5 mg/mL polymer-chloroform solutions (BDH, 99.8 %) to an optical density of 1.4 to 1.6. ITO coated glass slides were cleaned with toluene, acetone, and isopropanol and used as the working electrode for the spectroelectrochemical measurements. Propylene carbonate was used as the electrolyte solvent (PC, Acros Organics, 99.5 %) and was purified and dried using a solvent purification system from Vacuum Atmospheres. Tetrabutylammonium hexafluorophosphate ($TBAPF_6$, Alfa Aesar, 98 %) was used as the supporting electrolyte for the electropolymerization of EDOT, as well as the electrochemical and spectroelectrochemical measurements. $TBAPF_6$ was purified by recrystallized from hot ethanol. Glassy carbon button electrodes (0.07 cm^2) were used for the cyclic voltammetry and differential pulse voltammetry measurements. For the electrochemical measurements the polymers were drop cast on the glassy carbon electrodes with a fixed volume of 3 μl from a 2 mg/ml solution (6 μg of polymer). PEDOT was potentiostatically polymerized on ITO and glassy carbon at 1.0 V for 30 s in a solution containing 50 mM EDOT dissolved in 0.5 M $TBAPF_6$/PC.

Electrochemical measurements were performed in a three-electrode cell with a Pt flag as the counter electrode, a Ag/Ag^+ (10 mM $AgNO_3$ in 0.5 M $TBAPF_6$/ACN, $E_{1/2}$ for ferrocene: 68 mV) as the reference electrode, and a polymer coated glassy carbon button electrode as the working electrode. The voltage and current were controlled and monitored with an EG&G PAR 273A potentiostat/galvanostatic under CorrWare control.

All films were characterized via cyclic voltammetry between -0.8 V and 0.8 V at 50 mV/s for 25 cycles, the onset of oxidation was determined by differential pulse voltammetry. The in situ spectroelectrochemical measurements were carried out using the same potentiostat/galvanostatic in combination with Varian Cary 5000 UV-Vis-NIR spectrophotometer. The switching speeds were determined by square wave potential absorptiometry (chronoabsorptiometry). Change in absorption was monitored at λ_{max} for the given polymer and switched at between two potentials (-1.0 to 1.0 V in the case of PE and PE_2). All colorimetric values were quantified by converting the absorbance spectra to CIELAB L*a*b* color coordinates where the L* represents the white-black balance, a* represents the green-red balance, and the b* the blue-yellow balance of a given color. Photography was performed using a Nikon D90 SLR camera with a Nikon 18-105 mm VR lens. The photographs are presented without any manipulation apart from cropping. The degree of color saturation for the different polymers was estimated using equation S1 where the color saturation (S_{ab}) is defined as the ratio of chromatic color (C_{ab}^* to the total color sensation on a scale of 0 to 100 where 100 is the pure color).

CHAPTER 4. SOLUBLE PHEDOT COPOLYMERS VIA DIRECT (HETERO)ARYLATION POLYMERIZATION: A REVIVED MONOMER FOR ORGANIC ELECTRONICS

4.1 Electropolymerized PPheDOT and Processable PheDOT Homopolymers

Since the development of EDOT in the late 1980s, dioxythiophenes have become ubiquitous in organic electronics (OEs).[14] EDOT has been used in materials for applications ranging from electrochromism,[115,134] to hole transport,[135] to OPV[68] and its corresponding homopolymer, PEDOT, and derivative of said homopolymer have been some of the most studied materials in OEs. ProDOTs and acyclic dioxythiophene (AcDOTs) have also received much attention, albeit primarily in the field of electrochromism. Alternatively, PheDOTs have received far less attention. As discussed in Chapter 2, PheDOT and poly(PheDOT) was first reported by Roncali in 2004 in an attempt to design a material with the planarity and properties of PEDOT that could be functionalized with solubilizing chains without introducing regioirregularity or increased interring twisting as seen in functionalized PEDOT.[21,119] However, PheDOT, and derivatives of PheDOT, have unique properties and distinct differences from EDOT due to the phenylene ring. Later results further show the differences between EDOT and PheDOT and of longer oligomers of these units.[22] Due to the planarity between adjacent rings and between the three fused rings of the PheDOT unit, oligo and polyPheDOTs can form highly ordered and crystalline materials. This is exemplified in polyPheDOT

functionalized with dodecyl side chains, yielding a material that forms nanoribbons with a high degree of intra and interchain order, as determined by differential scanning calorimetry (DSC) and 2D wide-angle X-ray scattering (2D-WAXS).[136]

Comparing the PheDOT monomer unit to other dioxythiophenes, PheDOT is comparable to EDOT in terms of steric bulk, but with a significantly lower electron density on the thiophene ring due to π-electrons delocalizing into the phenylene ring.[22] This greatly improves the stability of dihydrogen or dihalogen PheDOT based materials compared to the analogous EDOT or ProDOT based materials. Additionally, like AcDOT and ProDOT, functionalization of PheDOT with solubilizing side chains does not necessarily introduce regioirregularity or chirality to the resulting polymers, as previously noted for EDOTs. The homopolymer structures of the monomers discussed are shown in Scheme 4.1.

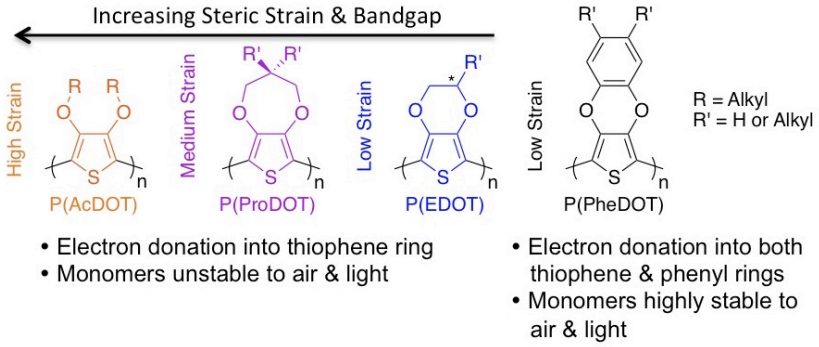

Scheme 4.1. Structures of electron-rich polymer built from common monomers used in organic electronics with varying steric strain between adjacent units and different electronic environments on the thiophene ring, leading to different redox, optical properties, and stabilities.

4.2 DHAP of PheDOTs

In spite of these promising results, PheDOTs have received minimal attention. This can be attributed to the difficult synthesis of soluble PheDOT monomers. After the several steps required alkylating catechol, the transetherification reaction to form the alkylated PheDOT unit is typically low yielding (~17 to 30%). One way to overcome this difficulty is to synthesize PheDOT directly from commercially available 3,4-dimethoxythiophene and catechol and use an alkylated comonomer for solubility. While dibromoPheDOT (PheDOT-Br_2) has been shown to undergo palladium catalyzed cross-coupling reactions, including Stille[137] and Suzuki[138], direct arylation using PheDOTs (as either the dihydrogen or dihalogen species) has not previously been demonstrated. Here I outline the synthesis of a series of soluble, alternating copolymers containing either PheDOT or biPheDOT prepared via DHAP, as shown in Scheme 4.2, where the PheDOT unit can serve as either the dihydrogen or dihalogen species.

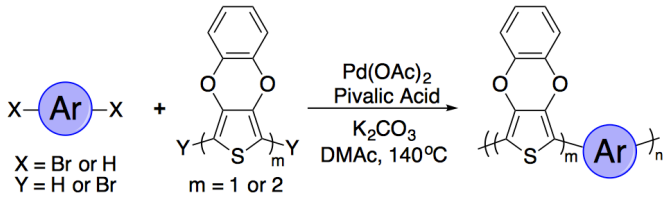

Scheme 4.2. A general outline of the copolymerization of PheDOT monomers with other aryl monomers using DHAP, with the PheDOT unit serving as either the dihydrogen or dibromide species.

4.3 NMRs of PheDOT Copolymers

PheDOT was prepared via the typical transetherification reaction, and subsequent bromination of PheDOT using NBS produced PheDOT-Br_2.[22] Lithiation of PheDOT followed by addition of copper(II) yielded biPheDOT.[22] All three monomers were purified via short silica columns using hexanes as the mobile phase, simplifying purification. One benefit of these monomers is their high stability/shelf life. PheDOT-Br_2 does not undergo a solid-state polymerization in the same manner as EDOT-Br_2,[139] and many other halogenated dioxyheterocycles,[140,141] to form the halogen-doped oligomer/polymer. After over one year of storage in the presence of oxygen and ambient light and temperature the three monomers used in this study remained pure and polymerization ready.

DHAP was performed using higher polarity conditions found to be favorable for dioxythiophene-based systems,[72] as outlined in Scheme 4.2, to yield the four soluble copolymers shown in Figure 4.1a. Interestingly, the less polar conditions used to prevent crosslinking/branching, previously optimized by the groups of Thompson[66] and Leclerc,[64] are not needed and C-H reactivity appears to be isolated to the heteroaryl (thiophene) units and not the phenylenes. NMRs of the copolymers, shown in the experimental details and magnified in Figure 4.1b, do not indicate branching off of the backbone and show that the expected repeat unit structures were obtained. This is also qualitatively observed in the high solubility of these materials in common organic solvents (THF, Toluene, $CHCl_3$, etc.) even with number average molecular weights above 50 kDa, as listed in the Table 4.1. The comparatively low reactivity of the of the attached phenylene ring is consistent with the use of toluene (or other aromatic compound) as a solvent for DHAP.

These solvents can undergo C-H activation and end-cap polymer chains,[142,71,70] however, this is slow compared to thiophene C-H activation and high quality polymers, comparable to those made via Stille or Suzuki, can be prepared using these aromatic solvents.[64] Another example of this slow aryl C-H activation compared to heteroaryls is the use of halogenated phenylenes and fluorenes units in DHAP without forming crosslinking materials.[143,68]

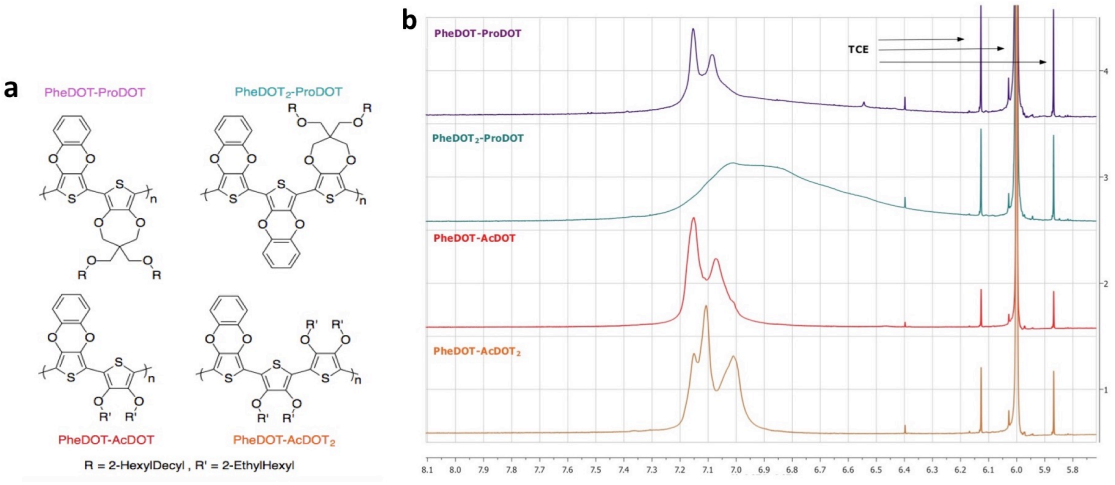

Figure 4.1. a) Structures of the PheDOT copolymer series prepared using DHAP and b) NMRs (700 MHz in TCE-D_2) of the copolymers magnified to show the region containing aromatic protons.

Table 4.1. Molecular weight, redox switching, and optical information on the copolymer series.

Polymer	M_n (kDa)[a]	Đ (M_w/M_n)[a]	Onset of Oxidation (V)[b]	$E_{g,\ opt}$ (eV)[c]	λ_{max} (nm)[c]	ΔT at λ_{max} (%)[c]	Switching Speed (95%) (s)[c]
PheDOT-ProDOT	68.2	3.7	-0.10	1.92	560, 607	74	0.8
$PheDOT_2$-ProDOT	33.8	1.4	-0.05	1.86	573	65	0.9
PheDOT-AcDOT	22.5	4.4	-0.08	1.99	541	72	0.6
PheDOT-$AcDOT_2$	51.8	2.4	0.13	2.03	530	69	1.5

a) via GPC vs. polystyrene standards in THF b) by DPV vs Ag/Ag^+ (68 mV vs. Fc/Fc^+) c) from film data on ITO glass in 0.5 M $TBAPF_6$/PC

4.4 Thermal Properties of PheDOT Copolymers

Considering the thermal properties of these systems, thermal gravimetric analysis (TGA) demonstrates that all of the copolymers are stable to over 300 °C, shown in Figure 4.2a. Introduction of a ProDOT or AcDOT unit bearing branched side chains removed the ordering previously seen in some PheDOT based systems, with DSC traces (Figure 4.2b) showing no thermal transitions. This low degree of order is useful for electrochromic applications as it can reduce the variation in films from different processing conditions and it has been theorized that amorphous films yield higher electrochromic contrast (ΔT) due to reduced light scattering from the film surface.

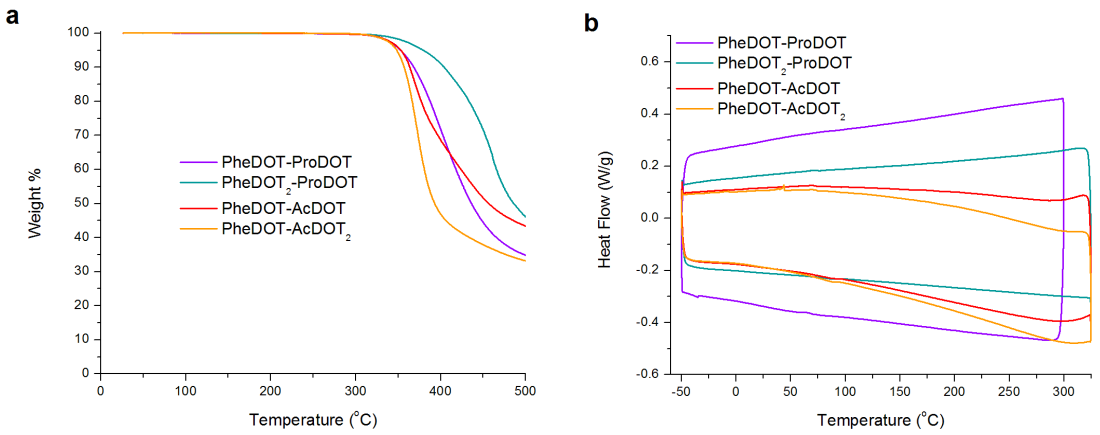

Figure 4.2. a) TGA at a rate of 10 °C/minute and b) DSC of the copolymer series.

4.5 Redox Properties

The CVs of both PheDOT-ProDOT and PheDOT$_2$-ProDOT, as seen in Figure 2a, are relatively broad and reversible from -1 to 0.8V. The CVs of these two copolymers have onsets of oxidation that are lower than the ProDOT homopolymer, ECP-M[144], and similar to electropolymerized polyPheDOT.[21] As expected, incorporation of a biPheDOT unit broadens the electroactive response and appears to lower the E_{ox} slightly. However, the DPVs, shown numerically in Table 4.1, indicate a slightly lower E_{ox} for PheDOT-ProDOT than PheDOT$_2$-ProDOT. Copolymerization with an AcDOT unit (yielding PheDOT-AcDOT) raises the E_{ox} of the resulting copolymer and also increases the current density in the CV. These two effects are observed again when changing the AcDOT for a biAcDOT unit (yielding PheDOT-AcDOT$_2$). The CV traces (Figure 4.2a and 4.2b) of PheDOT-ProDOT, PheDOT-AcDOT, and PheDOT-AcDOT$_2$ show the expected trend of increasing E_{ox} with increased steric strain between rings.

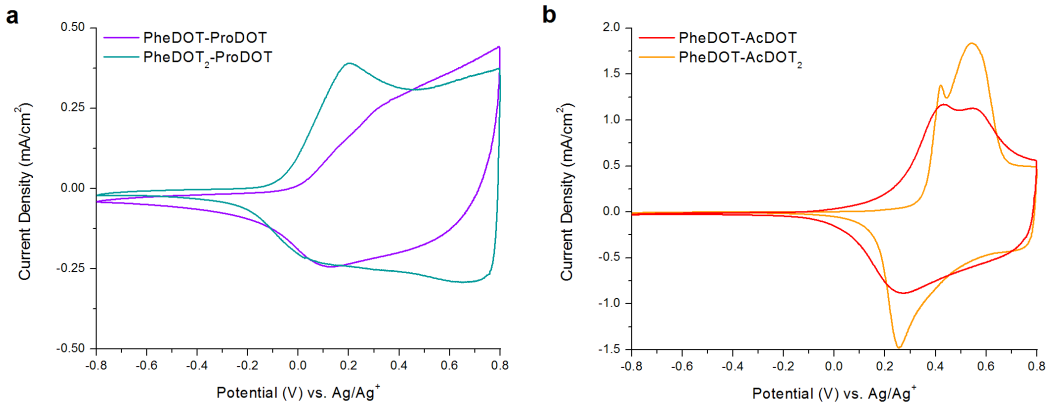

Figure. 4.3. CVs, after electrochemical breakin, of dropcast films (3 µL of a 2 mg/mL solution in $CHCl_3$) of the a) ProDOT containing copolymers and b) the AcDOT containing copolymers on glassy carbon button electrodes using a Pt flag as a counter electrode and 0.5 M $TBAPF_6$/PC as the electrolyte, sweeping at a scan rate of 50 mV/s. Current densities normalized to PheDOT-$AcDOT_2$ for clarity.

4.6 UV-vis & Spectroelectrochemistry

Film (in the charge neutral state after electrochemical conditioning) UV-vis spectra of the copolymer series, seen in Figures 4.4a, show narrow absorbance profiles with gradually lowering optical bandgaps ($E_{g,\ opt}$) as the repeat units go from most (PheDOT-$AcDOT_2$) to least (PheDOT$_2$-ProDOT) twisted. As seen in Figure 4.4b, transmittance spectra of the polymer films in the charge neutral states (solid lines) and oxidized states (dashed lines) show a large change in absorbance. From these spectra and the photos in Figure 4.4c it can be seen that all of the copolymers are high contrast electrochromic materials that go from vibrantly colored neutral states to transmissive, color neutral oxidized states. The change in transmittance (ΔT) for all four copolymers, as listed in table 4.1, is between 65 and 74% (at λ_{max}), making these materials comparable

to other solution processable, high contrast dioxyheterocycle-based electrochromic materials. It should be noted that while PheDOT-AcDOT$_2$ does reversibly switch on button electrodes, large films on ITO delaminate upon repeated cycling. Various cleaning and surface modification procedures were tested but none improved electrode adhesion for this copolymer. However, this may not be a problem in electrochromic devices using a gel or solid electrolyte. Chronoabsorptiometry experiments for the copolymers demonstrate that all of them, except for PheDOT-AcDOT$_2$, have 95% switching speeds of less than one second (listed in Table 1).

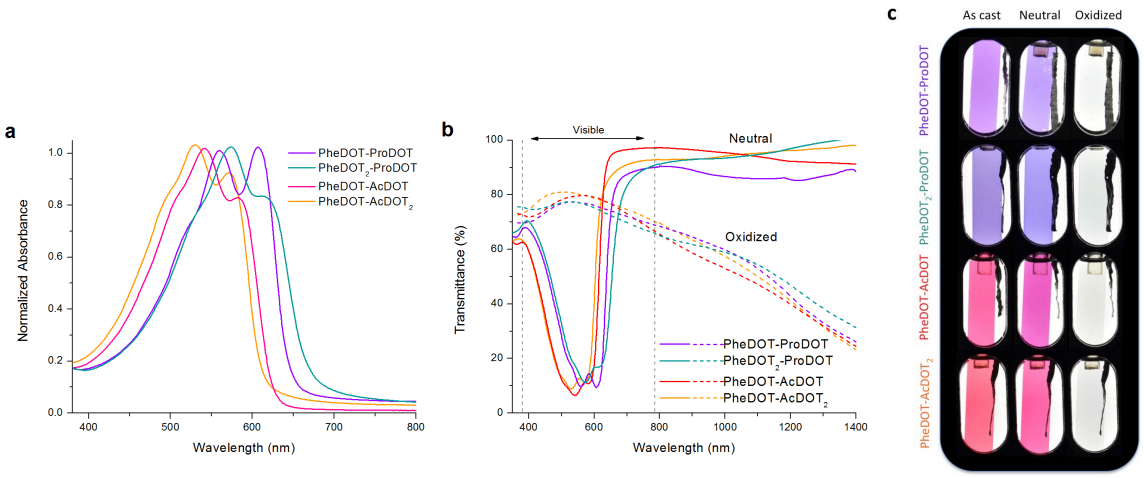

Figure 4.4. a) Normalized absorbance spectra of spray cast films (from a 4 mg/mL solution in $CHCl_3$, cast to an optical density 1 ± ~0.1) of the PheDOT copolymer series, b) transmittance spectra (without normalization) of the series in the charge neutral (solid lines) and oxidized (dashed lines) states, and c) photographs of these films in their pristine, neutral, and oxidized states, all on ITO glass in a three electrode cell setup in a quartz cuvette using a Pt flag as a counter electrode and 0.5 M $TBAPF_6$/PC as the electrolyte.

4.7 Colorimetry

By analyzing the colorimetry of these copolymer films we can better understand the color evolution during the oxidation process. In the a*b* plot (Figure 4.5a) we can see that after the spray cast films are electrochemically switched the polymer chains reorganize, leading to a change in color. Specifically, the b* (yellow/blue component) values of both AcDOT containing copolymers decrease (increased blue and decreased yellow color) upon electrochemical conditioning and the a* (red/green component) and b* values decrease (shifting from purple towards blue) for the ProDOT containing copolymers. After conditioning, electrochemical oxidation of the copolymers lead to the a*b* values approaching the origin, making the color appear to bleach out and resulting, ultimately, in the color neutral transmissive state. While this bleaching process is gradual for the ProDOT containing copolymers it is more sudden for AcDOT containing copolymers, with PheDOT-$AcDOT_2$ showing an almost complete change in a 0.1 V window. This is also observed in the change in L* (light/dark component) values as a function of potential, shown in Figure 4.5b. While the other three copolymers switch gradually between -0.2 and 0.7 V, PheDOT-$AcDOT_2$ has a sudden change from colored to bleached between 0.3 and 0.4 V. Currently, the cause of this effect is unknown but has been observed for similar systems and is being studied further.

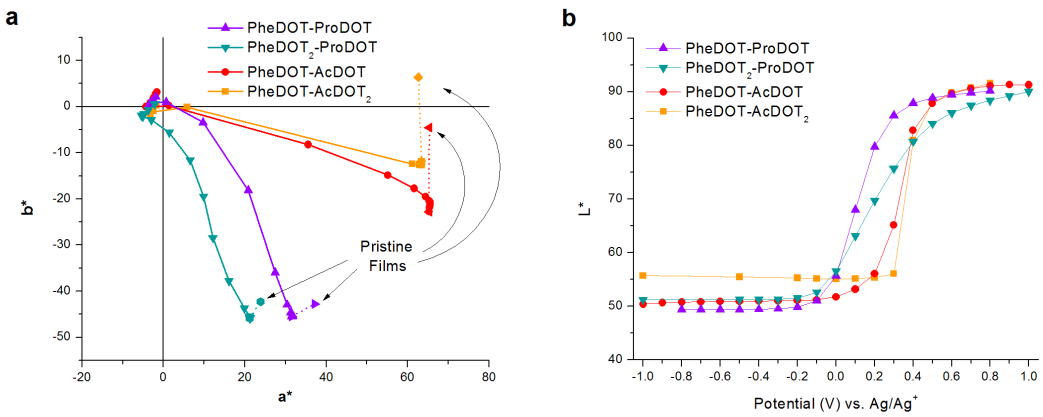

Figure 4.5. a) a*b* diagram showing the color change occurring during electrochemical oxidation of the copolymer series from the pristine films to the charge neutral states after conditioning (dotted lines) and charge neutral to oxidized states (solid lines) in 0.1 V increments and b) the change in L* as a function of potential on ITO glass in 0.5 M TBA/PF_6/PC vs. Ag/Ag^+.

The previously noted similarity in E_{ox} between PheDOT-ProDOT and $PheDOT_2$-ProDOT calls for further discussion. This similarity in E_{ox} is significantly different than what was observed with ProDOT/EDOT copolymer systems, where incorporation of a biEDOT unit in place of an EDOT resulted in a reduction in the E_{ox} of 0.4 V.[144] This was initially surprising as both the biPheDOT and biEDOT units are planar. However, while this planarity does reduce steric interactions between rings leading to a lowering of the E_{ox}, there is also a difference in the electron density of these two units. BiEDOT is highly electron rich due to the π-electron donation from the oxygen atoms into the thiophene ring while biPheDOT is comparatively less electron rich, and therefore more difficult to oxidize, due to the π-electrons being able to delocalize into either the thiophene or phenylene rings. This is also the cause of the increased stability of the PheDOT-based monomers compared to other dioxyheterocycles. With this in mind we can now

rationalize the differences in E_{ox} and breadth of electroactivity between PheDOT$_2$-ProDOT and PE$_2$, with the CVs of these two polymers shown in Figure 4.6. These differences allow for further structural tuning to design polymers for various applications. For example, in charge storage the exceptionally low E_{ox} of PE$_2$ is beneficial as energy density is a function of the voltage window. Alternatively, in polymer blending for color tuning this low E_{ox} can result in blends with intermediate colors that are undesirable, making PheDOT$_2$-ProDOT potentially a better choice.

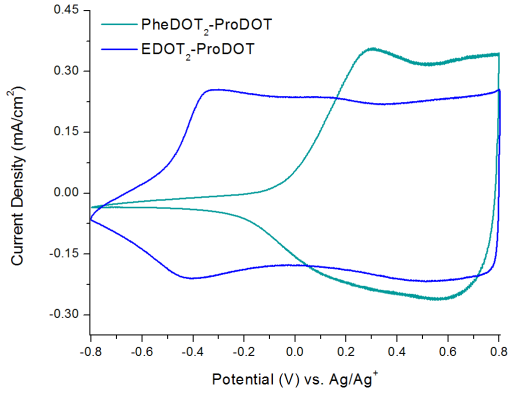

Figure 4.6. CVs of drop cast films (3µL of a 2mg/mL solution in $CHCl_3$) of PheDOT$_2$-ProDOT and PE$_2$ (or EDOT$_2$-ProDOT) on glassy carbon button electrodes using a Pt flag as a counter electrode and 0.5 M $TBAPF_6$/PC as the electrolyte, sweeping at a scan rate of 50 mV/s.

4.8 Switching Stability

Finally, the long-term cycling stability of one of the PheDOT copolymers, specifically PheDOT-ProDOT, was tested in order to determine if the phenylene unit reduces the switching lifetime of the copolymer. The reactivity of the phenylene unit was

initially a concern as some electrochromic polymers containing phenylenes in the backbone show low cycling stability, potentially due to crosslinking of the phenylenes upon oxidation.[145] A spray-cast film of PheDOT-ProDOT was prepared and placed in a three-electrode cell using the same setup as for the spectroelectrochemistry and the electrolyte solution (0.5 M $TBAPF_6$/PC) was degassed via argon bubbling for five minutes. The setup was then placed in the UV-vis instrument and left open to ambient conditions. The UV-vis specta were taken in the neutral and oxidized states. The film was then switched in a chronoabsorptiometry experiment between -0.5 and 0.7 V for 2000 cycles. Spectra of the neutral and oxidized states were taken again after the 2000 cycles and is can be seen in Figure 4.7 that there is no significant change to the absorbance profiles in either the neutral of oxidized states between the pre and post cycling spectra. Extracting the Δ%T values from the chronoabsorptiometry shows only a 1.1% decrease in contrast (from 69.2 to 68.1) at λ_{max}, with the values listed as a function of cycles in Figure 4.7. This demonstrates the high stability of these systems and their potential use in electrochromic devices and other redox active applications. This also suggests that the previously discussed poor redox stability of polymers containing phenylenes is due to the change between aromatic to quinoidal forms of the phenylene unit. This change does not occur in the PheDOT unit as the attached phenyl ring maintains its aromaticity during redox stitching.

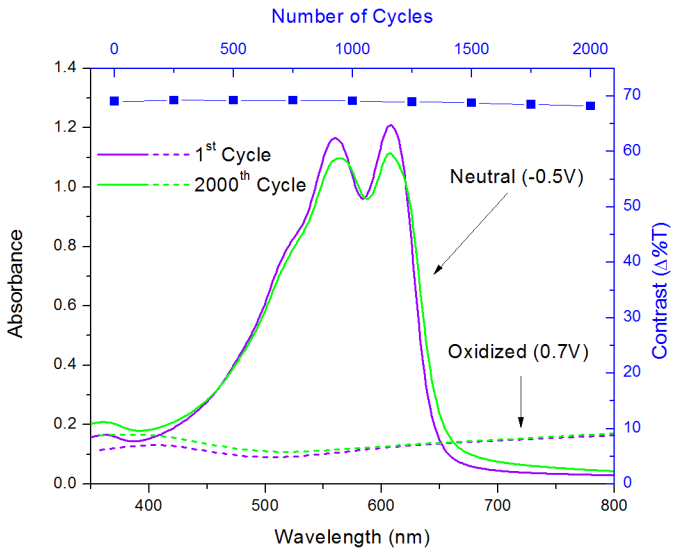

Figure 4.7. a) Absorbance spectra of a PheDOT-ProDOT film (on ITO glass) in the charge neutral (-0.5 V) and oxidized states (0.7 V) before (purple traces) and after (green traces) 2000 cycles with the contrast as a function of cycles (blue points and trace) in 0.5 M $TBAPF_6$/PC.

4.9 Conclusion

In summary, the PheDOT unit undergoes C-H activation to selectively polymerize through the thiophene ring without crosslinking from the fused phenylene. Standard DHAP conditions are effective at forming structurally well-defined, high molecular weight copolymers that are soluble and processable in common organic solvents. PheDOT containing copolymers are vibrantly colored electrochromic materials with colorless oxidized states with high contrast values (Δ%T) that are comparable to other dioxyheterocycle-based polymers. The copolymers are exceptionally stable to repeated redox switching, with only a 1% loss in contrast after 2000 switching cycles in ambient

conditions. This work demonstrates that PheDOTs are useful units for organic electronics that have been underutilized over the past decade.

4.10 Experimental Details

4.10.1 Materials

PheDOT, biPheDOT, and PheDOT-Br_2 were prepared according to literature procedures and confirmed using ^{1}H NMR and GC-MS.[22] AcDOT-Br_2 and biAcDOT-Br_2 were prepared by J. Kerszulis as reported in the literature.[73] $Pd(OAc)_2$ (98 %, Strem Chemicals), pivalic acid (99 %, Sigma), K_2CO_3 (anhydrous, Oakwood Products), 18-Crown-6 (99 %, Acros), diethyldithiocarbamic acid diethylammonium salt (97 %, TCI America), KOH (Technical Grade, Fisher Scientific), and pTSA (monohydrate, 98 %, Alfa Aesar) were used as received. DMAc (HPLC grade, Alfa Aesar) was filtered through a pad of alumina (basic, Sigma Aldrich) and degassed by argon bubbling prior to use.

4.10.2 Instrumentation

The molecular weight and dispersity of the polymer were obtained using a THF GPC at 35°C calibrated vs. polystyrene standards. The ^{1}H-NMR (64 scans) spectrum was collected on a Bruker 700 MHz instrument using $C_2D_2Cl_4$ as a solvent at a temperature of 323K The electrical potential in the three-electrode cell setup was measured using either a Ag/Ag^+ reference electrode (10 mM $AgNO_3$ in 0.5 M $TBAPF_6$-ACN, $E_{1/2}$ for ferrocene: 68 mV), and the counter electrode was a platinum flag. The CV and DPV measurements

were performed on an EG&G PAR (model 273A) potentiostat/galvanostatic under CorrWare control. Spectroelectrochemistry and chronoabsorptiometry were measured using an Agilent Technologies Cary 5000 UV-Vis-NIR Spectrophotometer under Cary WinUV control and a EG&G PAR (model 263A) potentiostat/galvanostatic under CorrWare control. All colorimetric values were quantified by converting the absorbance spectra to CIELAB L*a*b* color coordinates where the L* represents the white-black balance, a* represents the green-red balance, and the b* the blue-yellow balance of a given color. Photography was performed using a Nikon D90 SLR camera with a Nikon 18-105 mm VR lens. The photographs are presented without any manipulation apart from cropping.

4.10.3 Polymer Synthesis

PheDOT-ProDOT

To a 38 mL Schlenk tube with stir bar, PheDOT-Br_2 (0.4185 g, 1.0 eq.), ProDOT(HxDec) (0.800 g, 1.0 eq.), palladium acetate (0.006 g, 2 mol%), pivalic acid (0.036 g, 0.3 eq.), and potassium carbonate (0.4159 g, 2.5 eq.) were added. 12 mL of DMAc was added to dissolve the contents and the tube was sealed under argon. The reaction mixture was premixed for 2 minutes. The tube was then lowered into an oil bath and heated to 140 °C and allowed to stir vigorously overnight (~14 hours). After the flask was removed from the oil bath and allowed to cool to room temperature, the polymer was precipitated into methanol and stirred for one hour. The precipitate obtained from precipitation was filtered into a soxhlet extraction thimble and washed with methanol, acetone, hexanes, and finally dissolved into chloroform. The washings were conducted

until color was no longer observed during extraction. After dissolution from the thimble, the chloroform was removed using a rotary evaporator and then ~50 mL of chloroform was added followed by ~20 mg of a palladium scavenger (diethylammonium diethyldithiocarbamate) and ~20 mg of 18-crown-6 and then stirred for 2 hours at 50 °C. This solution was then precipitated into ~250 mL of methanol. The precipitate was vacuum filtered, using a Nylon pad (with a pore size of 20 μm) as the filter, and washed with a large volume of methanol and allowed to dry. The dried material was collected into a vial and dried under vacuum. The polymer was obtained as a purple solid in 46% yield (471 mg). ^{1}H-NMR (700 MHz, $C_2D_2Cl_4$, 50 ^{o}C) δ 7.11 (d, 4H), 4.28 (br, 2H), 3.65 (br, 4H), 3.38 (br, 4H), 1.30 (br), 1.01-0.84 (br). Anal. calcd. for $C_{51}H_{78}O_6S_2$ C 71.96, H 9.24, S 7.53, Found C 71.66, H 9.12, S 7.73. M_n = 68.2 kDa, Đ = 3.7, vs. PS in THF at 35 °C.

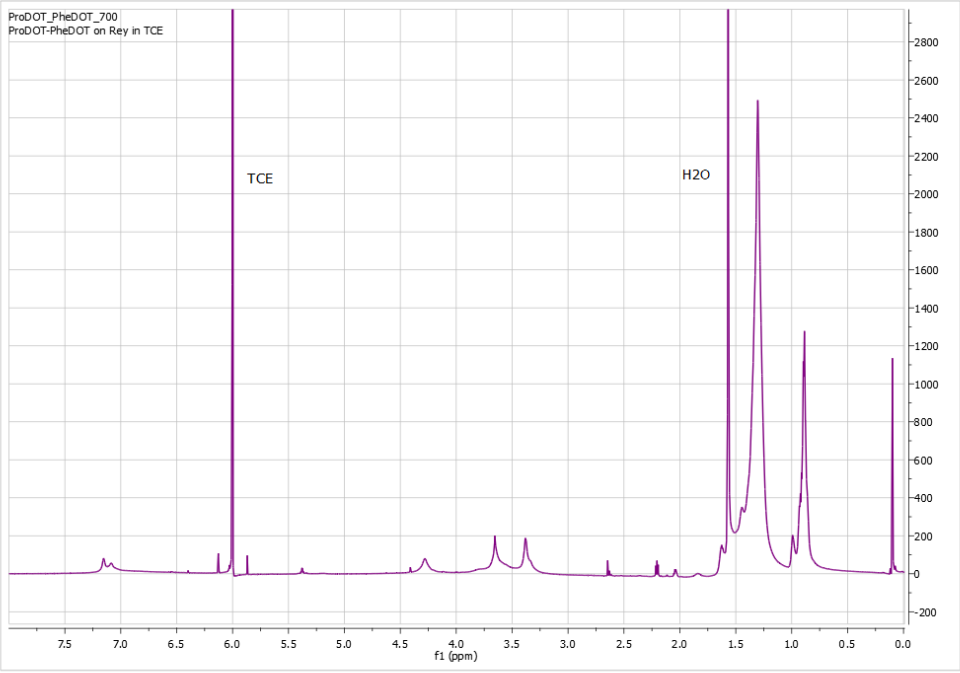

PheDOT$_2$-ProDOT

To a 38 mL Schlenk tube equipped with stir bar, ProDOT-Br_2 (0.2129 g, 1.0 eq.), biPheDOT (0.0978 g, 1.0 eq.), palladium acetate (0.0025 g, 2 mol%), pivalic acid (0.086 g, 0.3 eq.), and potassium carbonate (0.096 g, 2.5 eq.) were added. 2.6 mL of DMAc was added to dissolve the contents and the tube was sealed under argon. The reaction mixture was premixed for 2 minutes. The tube was lowered into an oil bath and heated to 140 °C and allowed to stir vigorously overnight (~14 hours). After the flask was removed from the oil bath and allowed to cool to room temperature, the polymer was precipitated into methanol and stirred for one hour. The precipitate was filtered into a soxhlet extraction thimble and washed with methanol, acetone, hexanes, and finally dissolved into chloroform. The washings were conducted until color was no longer observed during extraction. After dissolution from the thimble, the chloroform was removed using a rotary evaporator and then ~50 mL of chloroform was added followed by ~20 mg of a palladium scavenger (diethylammonium diethyldithiocarbamate) and ~20 mg of 18-crown-6 and then stirred for 2 hours at 50 °C then precipitated into 250 mL of methanol. The precipitate was vacuum filtered, using a Nylon pad (with a pore size of 20 μm) as the filter, and washed with a large volume of methanol and allowed to dry. The dried material was collected into a vial and dried under vacuum. The polymer was obtained as a purple/blue solid in 64% yield (171 mg). ^{1}H-NMR (700 MHz, $C_2D_2Cl_4$, 50 ^{o}C) δ 7.25-6.55 (br, 8H), 4.25 (br, 2H), 3.50 (br, d, 8H), 1.65-1.10 (br), 1.05-0.70 (br). Anal. calcd. for $C_{61}H_{82}O_8S_3$ C 70.48, H 7.95, S 9.25, Found C 69.67, H 7.42, S 9.88. M_n = 33.8 kDa, Đ = 1.4, vs. PS in THF at 35 °C.

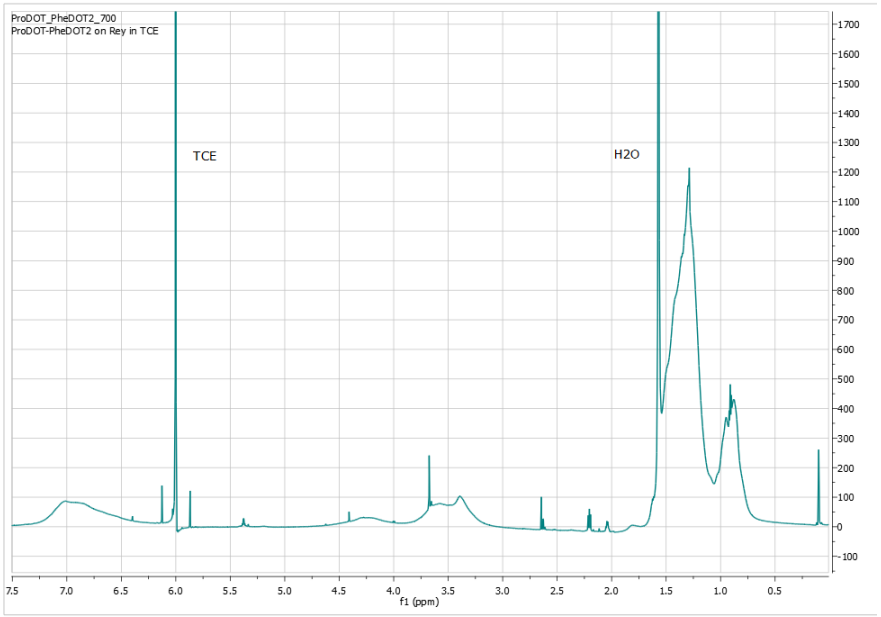

PheDOT-AcDOT

To a 38 mL Schlenk tube equipped with stir bar, AcDOT-Br_2 (0.700 g, 1.0 eq.), PheDOT (0.2672 g, 1.0 eq.), palladium acetate (0.007 g, 2 mol%), pivalic acid (0.045 g, 0.3 eq.), and potassium carbonate (0.485 g, 2.5 eq.) were added. 14.0 mL of DMAc was added to dissolve the contents and the tube was sealed under argon. The reaction mixture was premixed for 2 minutes. The tube was lowered into an oil bath and heated to 140 °C and allowed to stir vigorously overnight (~14 hours). After the flask was removed from the oil bath and allowed to cool to room temperature, the polymer was precipitated into methanol and stirred for one hour. The precipitate was filtered into a soxhlet extraction thimble and washed with methanol, acetone, and finally dissolved into hexanes. The washings were conducted until color was no longer observed during extraction. After dissolution from the thimble, the chloroform was removed using a rotary evaporator and

then ~50 mL of chloroform was added followed by ~20 mg of a palladium scavenger (diethylammonium diethyldithiocarbamate) and ~20 mg of 18-crown-6 and then stirred for 2 hours at 50 °C then precipitated into 250 mL of methanol. The precipitate was vacuum filtered, using a Nylon pad (with a pore size of 20 μm) as the filter, and washed with a large volume of methanol and allowed to dry. The dried material was collected into a vial and dried under vacuum. The polymer was obtained as a dark red solid in 41% yield (304 mg). ^{1}H-NMR (700 MHz, $C_2D_2Cl_4$, 50 ^{o}C) δ 7.12 (d, 4H), 4.08 (br, 4H), 1.95 (br, 2H), 1.70-1.48 (br, m), 1.47-1.26 (br), 1.10-0.80 (br). Anal. calcd. for $C_{30}H_{38}O_4S_2$ C 68.41, H 7.27, S 12.17, Found C 68.14, H 7.08, S 12.42. M_n = 22.5 kDa, Đ = 4.4, vs. PS in THF at 35°C.

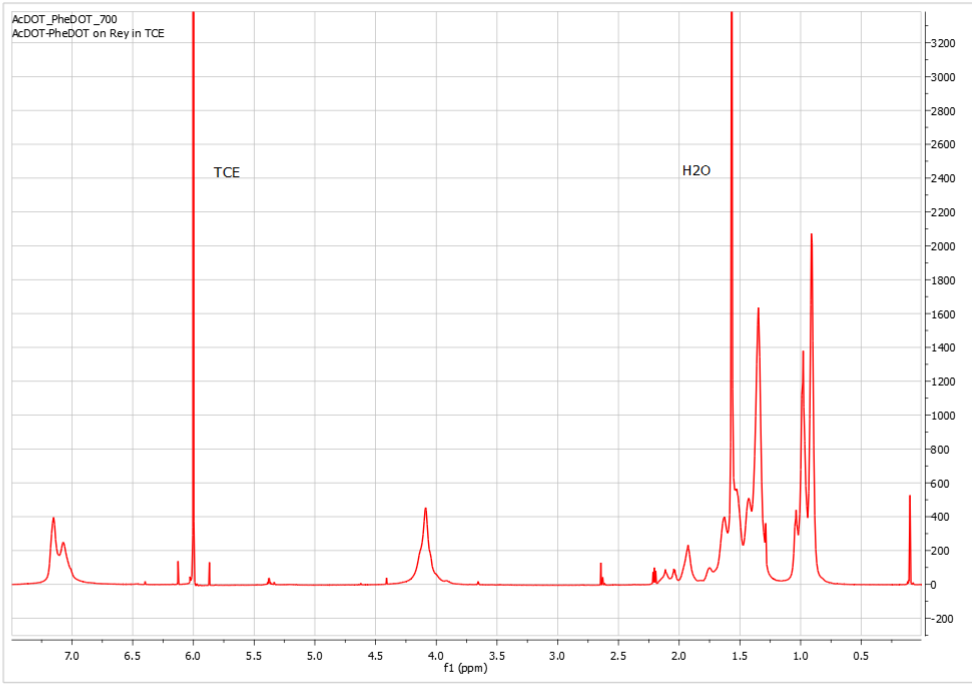

PheDOT-AcDOT$_2$

To a 38 mL Schlenk tube equipped with stir bar, biAcDOT-Br_2 (1.001 g, 1.0 eq.), PheDOT (0.2269 g, 1.0 eq.), palladium acetate (0.006 g, 2 mol%), pivalic acid (0.034 g, 0.3 eq.), and potassium carbonate (0.4181 g, 2.5 eq.) were added. 12 mL of DMAc was added to dissolve the contents and the tube was sealed under argon. The reaction mixture was premixed for 2 minutes. The tube was lowered into an oil bath and heated to 140 °C and allowed to stir vigorously overnight (~14 hours). After the flask was removed from the oil bath and allowed to cool to room temperature, the polymer was precipitated into methanol and stirred for one hour. The precipitate was filtered into a soxhlet extraction thimble and washed with methanol, acetone, and finally dissolved into hexanes. The washings were conducted until color was no longer observed during extraction. After dissolution from the thimble, the chloroform was removed using a rotary evaporator and then ~50 mL of chloroform was added followed by ~20 mg of a palladium scavenger (diethylammonium diethyldithiocarbamate) and ~20 mg of 18-crown-6 and then stirred for 2 hours at 50 °C then precipitated into 250 mL of methanol. The precipitate was vacuum filtered, using a Nylon pad (with a pore size of 20 μm) as the filter, and washed with a large volume of methanol and allowed to dry. The dried material was collected into a vial and dried under vacuum. The polymer was obtained as a fluffy, deep red solid in 94% yield (966 mg). ^{1}H-NMR (700 MHz, $C_2D_2Cl_4$, 50 ^{o}C) δ 7.08 (d, 4H), 4.07 (br, 8H), 1.98 (d, 4H), 1.73-1.2 (br, m), 1.07-0.82 (br). Anal. calcd. for $C_{50}H_{72}O_6S_3$ C 69.40, H 8.39, S 11.12, Found C 69.44, H 8.25, S 11.26. M_n = 51.8 kDa, Đ = 2.4, vs. PS in THF at 35°C.

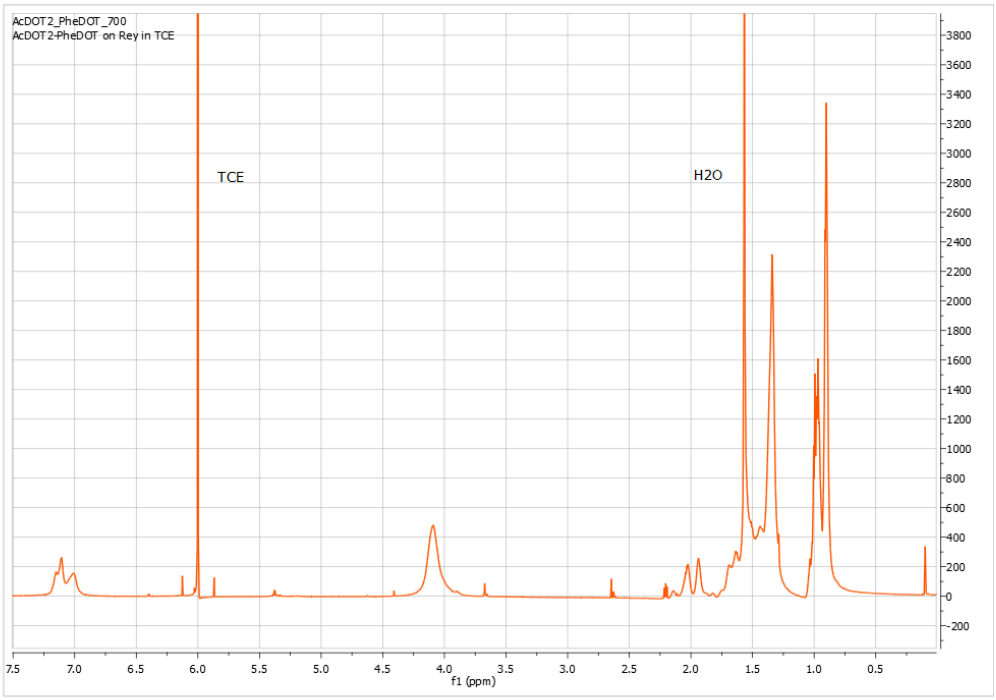
AcDOT2_PheDOT_700
AcDOT2-PheDOT on Rey in TCE
TCE
H2O
f1 (ppm)

CHAPTER 5. THE HETEROATOM ROLE IN POLYMERIC DIOXYSELENOPHENE/DIOXYTHIOPHENE SYSTEMS FOR COLOR AND REDOX CONTROL

Adapted from:

Ponder, J., F.; Pittelli, S., L.; Reynolds, J. R. Heteroatom Role in Polymeric Dioxyselenophene/Dioxythiophene Systems for Color and Redox Control. *ACS Macro Letters* **2016**, 5, 714−717

5.1 Polyselenophenes

Polyselenophenes have received attention in the field of organic electronics due to their similarities and differences to the more widely studied polythiophenes, where they possess reduced aromatic character, leading to increased quinoidal character and planarity between rings and yielding lower electronic band-gaps.[140,146-148] Of particular note is the computational and experimental work of the late Michael Bendikov on selenophene oligomers and polymers who developed extensive selenophene chemistry and made important comparisons with structurally similar thiophene-based polymers.[149-151] Recently, poly(3-alkylselenophenes) and copolymers containing 3-alkylselenophenes[152,153] along with other selenophene containing polymers have found use as both organic field-effect transistor (OFET)[154] and OPV[155] materials with enhanced

transport properties due to more extensive interchain interactions compared to their thiophene analogs.

5.2 Dioxyselenophenes (XDOSs)

In a similar comparison, electrochemically polymerized 3,4-alkylenedioxyselenophenes (XDOSs) have been investigated and compared to their analogous XDOTs as redox active and EC materials. This is illustrated in PProDOS, which exhibits a saturated blue hue due to a distinct red-shift[148,156] of the neutral polymer's $\pi \rightarrow \pi^*$ transition relative to the more purple color observed for the PProDOTs.[157,158] A red-shifted absorption of the PProDOS cation-radical (polaron state) relative to that observed for PProDOT moves the charged material's absorption of light more fully into the near-infrared.[158] These PXDOS materials have low onsets of oxidation (as low as −0.95 V vs Ag/AgCl),[150] which is of particular use in EC and electrochemical charge storage devices, such as SCs. For the PXDOS family of materials to become more attractive and useful for redox and organic electronic applications, it is necessary to move beyond electrochemical polymerizations with the preparation and processing of soluble polymers. The dehalogenative polymerization of dihalo XDOSs monomers were reported, yielding soluble oligomers with a low molecular weight (5 kDa), but no polymeric materials were presented.[159] To date, there is only one example, apart from this work, of a soluble XDOS polymer/copolymer. ProDOS functionalized with solubilizing side chains was electropolymerized to yield a low molecular weight product (7.2−9.3 kDa), which could subsequently be spray cast from a dichloromethane (DCM) solution.[157]

5.3 DHAP of EDOS and ProDOT-Classic-Br_2

While DHAP has emerged as a practical and versatile tool for the preparation of a wide range of small molecules and polymers, this method has not been well explored with selenophenes. There relatively few publications studying selenophene direct arylation or DHAP conditions and no reports of XDOSs prepared via these methods.[160- 163] As discussed in the rest of this thesis DHAP has been utilized to synthesize a large number of dioxythiophene-based polymers and copolymers for high contrast electrochromic and charge storage applications and here, for the first time, this chemistry has been extended to XDOS-based polymers. Specifically, the first synthesis of an alternating ProDOT-EDOS copolymer, applying standard DHAP conditions, is reported with EDOS serving as the dihydrogen species and a ProDOT derivative with 2-hexyldecyloxy solubilizing chains as the dihalide to yield ProDOT-EDOS, as illustrated in Scheme 5.1. The polymer was purified via Soxhlet extraction followed by reprecipitation and the repeat unit structure confirmed using elemental analysis and NMR (as shown in the experimental details). The molecular weight of the polymer (M_n = 12.5 kDa, Đ = 1.6) was determined via gel permeation chromatography (GPC) relative to polystyrene standards. The ProDOT-EDOS copolymer is highly soluble in common solvent including THF and toluene. The synthesis of this material was initially attempted using a ProDOT monomer bearing shorter 2-ethylhexyloxy side chains and resulted in a polymer that was only slightly soluble in hot chloroform and a GPC molecular weight estimation could not be made. A second attempt was made with the DHAP reaction being quenched by addition of methanol as soon as the polymer appeared to gel (after ~10 minutes). However, this did not improve the solubility of the resulting material. This lead

to the use of longer 2-hexyldecyloxy side chains as previously discussed in Chapter 3 to improve the solubility of ProDOT-EDOT.

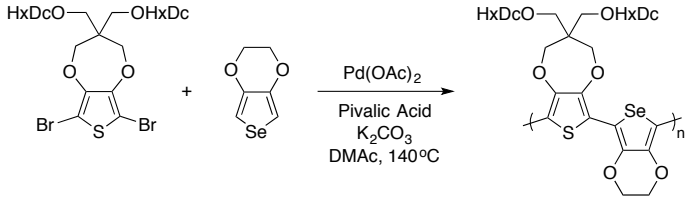

Scheme 5.1. Direct (hetero) arylation polymerization of a dibromo ProDOT derivative and EDOS to yield ProDOT-EDOS .

5.4 Electrochemistry of ProDOT-EDOS vs. ProDOT-EDOT and PProDOT

CV of a dropcast film of the polymer on a glassy carbon electrode exhibited a low onset of oxidation followed by a broad electrochemical response, as shown in Figure 5.1a. This onset of oxidation is lower than both the PProDOT homopolymer (ECP-M) and the ProDOT-EDOT alternating polymer bearing the same side chains. This is consistent with the low oxidation potential reported in the literature for electropolymerized XDOS polymers and is confirmed by DPV, as shown in Figure 5.1b, where ProDOT-EDOS shows a reduction in the onset of oxidation of 160 mV relative to ProDOT-EDOT simply by changing one of the heteroatoms in the repeat unit from sulfur to selenium. The higher current and corresponding increase in area of the CV trace correlates to a higher film capacitance, suggesting that XDOS-based materials could be

used in place of the XDOT materials currently under investigation as charge storage materials.

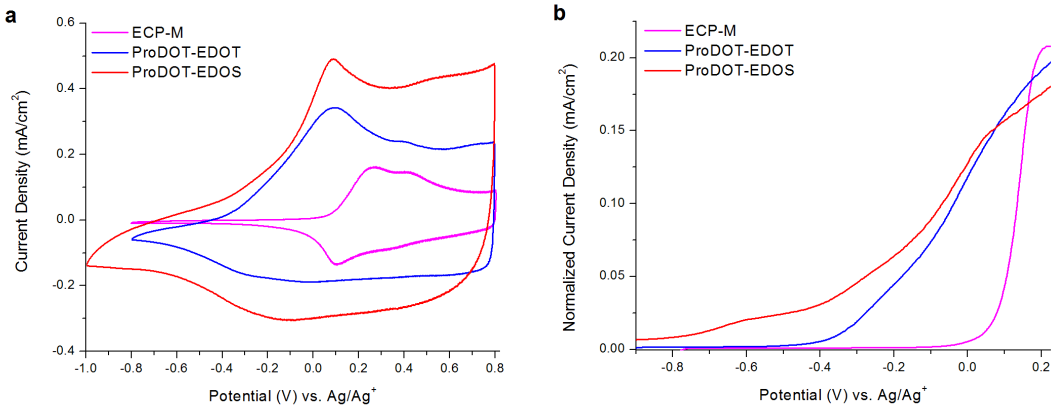

Figure 5.1. a) CVs and b) oxidative DPVs of ECP-M (magenta trace), ProDOT-EDOT (blue trace), and ProDOT-EDOS (red trace) drop cast to equal mass films (3 µL of 2 mg/mL solutions in $CHCl_3$) on glassy carbon electrodes, demonstrating the reduction in onset of oxidation and broad stable window of the polymer films as well as an increase in redox current.

5.5 Spectroelectrochemistry of ProDOT-EDOS

When spray cast from a chloroform solution (4 mg/mL) onto ITO glass, the resulting ProDOT-EDOS film appears as a slightly muted blue film (L*a*b* = 53, 1, −45). However, it can be seen in Figure 5.2a that following an electrochemical break-in with 5 CV cycles the neutral form of the film is converted to a deep blue color (L*a*b* = 53, −4, −47). Upon oxidation of the polymer the blue color disappears and a colorless and transmissive state (L*a*b* = 92, −3, −3) is formed, as seen in Figure 5.2a. The spectroelectrochemical series of the film in Figures 5.2b allows for the observation of the gradual oxidation of the polymer and the depletion of the charge neutral state as polarons

are formed, followed by bipolarons, and ultimately bipolaron band formation[30,31] with complete disappearance of the neutral state absorption by 0.8 V.

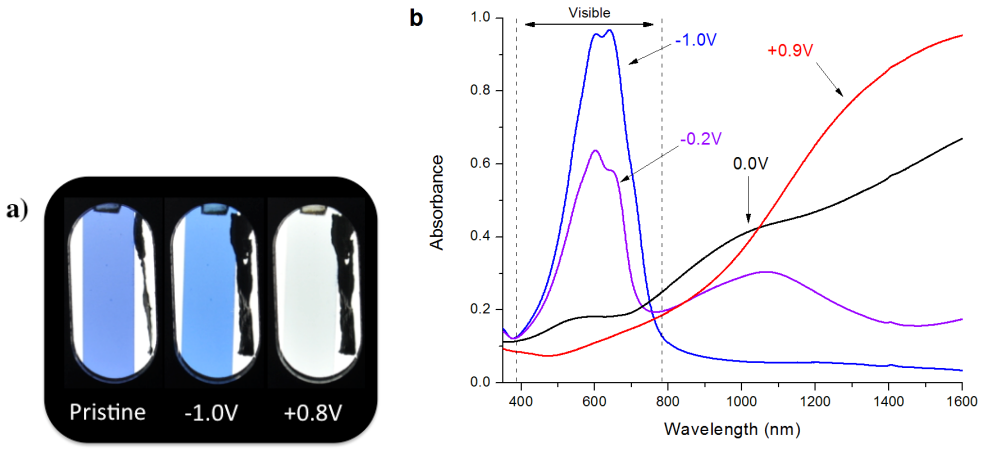

Figure 5.2. a) Photographs of a spray-cast film of ProDOT-EDOS on ITO in electrolyte solution in its pristine (as cast), charge neutral (-1.0V), and oxidized (+0.8V) forms and b) UV-vis absorption of ProDOT-EDOS on ITO at various applied potentials from the fully reduced, or charge neutral, form (blue trace) to the fully oxidized form (red trace).

5.6 Absorbance and Colorimetric Comparisons of ProDOT-EDOS, ProDOT-EDOT, PProDOT, and PEDOT

The UV−vis-NIR absorbance profiles of PProDOT, ProDOT-EDOT, and ProDOT-EDOS shown in Figure 5.3a demonstrate a red-shift in both peak and onset of absorbance for this family of polymers. Insertion of the less sterically encumbering EDOT in alternation with ProDOT leads to a relaxation of the torsional angles along the polymer backbone, as demonstrated previously in studies directed to color tuning in ECPs and discussed in Chapter 3. With the subsequent substitution of the sulfur atom for a selenium atom in the EDOS repeat unit, a further 41 nm red-shift in peak absorbance is

observed (Table 5.1). Using the energy for the onset of the π→π* transition in the polymer as an estimation of the optical bandgap ($E_{g,\,opt}$), we see a decrease from 1.97 to 1.77 eV and, finally, to 1.62 eV across this series. Tracking the hue and saturation of the films during oxidation, the colorimetry results in Figure 5.3b and Table 5.1 show how the materials transition from deeply colored states to highly transmissive, near neutral hued forms. The a* = −4 value for ProDOT-EDOS is unusual, as it does not contain a red component as we typically see in blue XDOT ECPs (specifically in PE_2 and PEDOT), which have small positive a* values.[144] As the polymer is oxidized, the colorimetry results track the b* axis relatively closely, minimizing secondary colors observed during electrochemical switching. From a plot of lightness value (L*) as a function of applied potential, shown in Figure 5.4a, it can be seen that the bleaching primarily occurs over a small potential window, from -0.4 to 0.1 V. This switch is relatively rapid with a 95% switch, calculated from the chronoabsorptiometry in Figure 5.5b, of 0.60 s.

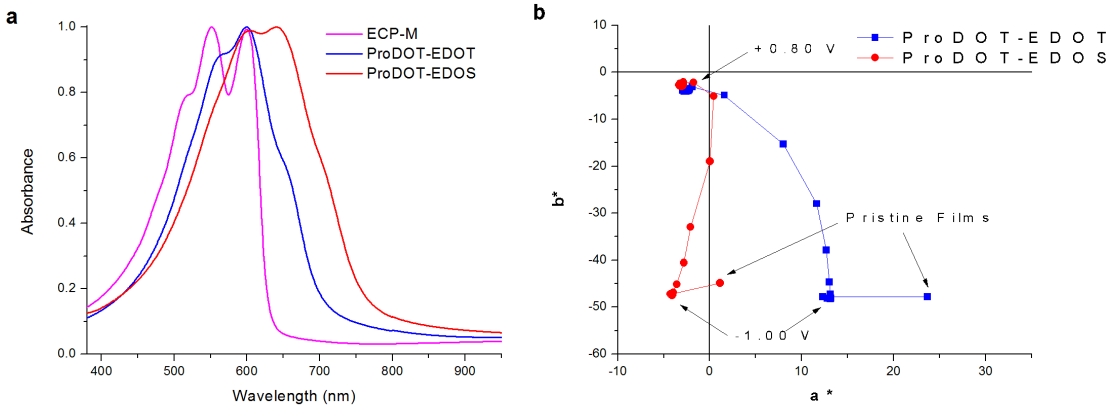

Figure 5.3. a) Normalized absorption spectra of PProDOT (magenta trace) at higher energy, ProDOT-EDOT (blue trace), and ProDOT-EDOS (red trace) at lower energy, and (b) a*b* diagram showing the change in color occurring during electrochemical doping (oxidation) of ProDOT-EDOT and ProDOT-EDOS.

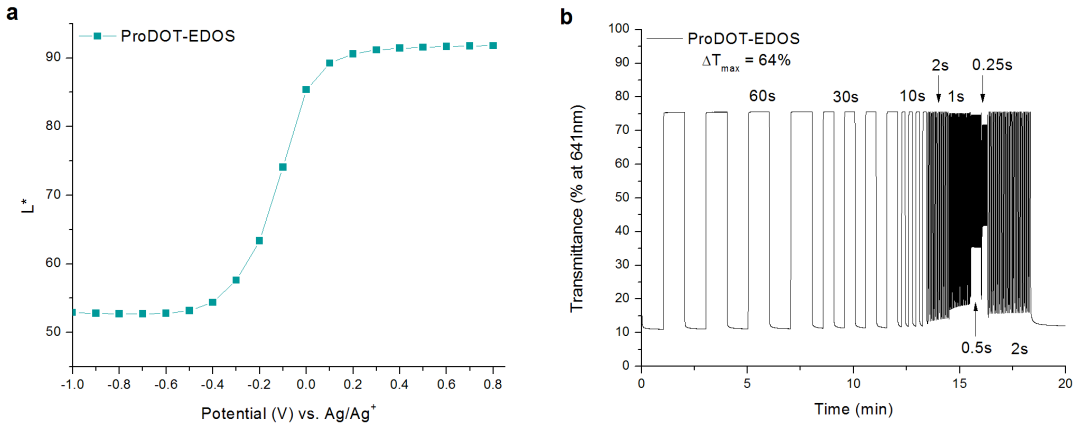

Figure 5.4. a) Lightness value (L*) of ProDOT-EDOS as a function of voltage and b) chronoabsorptiometry of ProDOT-EDOS on ITO switching between -1.0V and 0.8V in 0.5M $TBAPF_6$/PC.

Table 5.1. Optical, Colorimetric, and Electrochemical Comparisons of PProDOT, ProDOT-EDOT, ProDOT-EDOS, and PEDOT

Polymer	λ_{max} neutral (nm)	λ_{max} polaron (nm)	L*, a*, b* (neutral)	L*, a*, b* (oxidized)	$E_{g,\,opt}$ (eV)	Onset of Oxidation (V) by DPV
PProDOT	550	937	42, 58, -38	89, -3, -3	1.97	0.08
ProDOT-EDOT	600	970	52, 12, -48	93, -3, -3	1.77	-0.36
ProDOT-EDOS	641	1076	53, -4, -47	92, -3, -3	1.62	-0.52
PEDOT	629	923	35, 10, -54	81, -6, -10	1.66	-0.95

Interestingly, it can be see in Table 5.1 that the absorption maximum of ProDOT-EDOS and PEDOT are similar and the difference in $E_{g,\,opt}$ between the two is small (0.04 eV), suggesting that the materials will appear similar in perceived color. However, a quantitative comparison of the colorimetry values of the two polymers show that this is not true and the materials appear as distinct shades of blue. The color difference equation (ΔE^*_{ab}) presented in Chapter 2 (equation 2.1) was used to compare the colors, thereby determining if they are distinguishable to a standard observer.[94] Recall that if the value of ΔE^*_{ab} is greater than 2.2, two colors are distinguishable from each other. Despite the similarities in peak absorbance and $E_{g,\,opt}$, ProDOT-EDOS and PEDOT have a ΔE^*_{ab} value of 24, meaning that while they are both blue polymers they appear as distinctly different shades of blue. In contrast, PE_2 (λ_{max} = 613 nm, $E_{g,\,opt}$ = 1.71 eV) has a ΔE^*_{ab} value of 2.2 relative to PEDOT, making these two materials indistinguishable to a standard observer in spite of the larger difference in peak absorbance and $E_{g,\,opt}$. Comparing these polymers nicely demonstrates how perceived color is more complex than the bandgap and peak absorbance, but is dependent on the overall absorbance profile.

While altering the backbone structure in dioxythiophene polymers shifts the neutral absorbance, it generally does not have a significant effect on the polaronic absorption, which tends to be found between 780 and 980 nm, with some exceptions. This is exemplified in PProDOT and ProDOT-EDOT with a 50 nm difference in the neutral, and a 33 nm difference in the polaronic peak absorbance, corresponding to decreases in energy of 188 and 45 meV, respectively. Substitution of the sulfur for selenium on the 3,4-ethylenedioxyheterocyclic unit leads to a smaller energy reduction of

132 meV (a 41 nm red-shift) in the neutral absorbance and a larger energy reduction of 126 meV (a 106 nm red-shift) in the polaron absorption relative to ProDOT-EDOT. This tread is expected, base on the literature, to continue as the ratio of XDOS to XDOT is increased further. By moving the polaron further into the IR, it may be possible to reduce the extent of tailing of the charged state absorption into the visible, which may ultimately increase the EC contrast observed.

5.7 Conclusions on XDOSs

Given the large effect that substitution of a selenium atom in place of sulfur in these structures has on the redox behavior, neutral state absorbance, and polaron absorbance of the resulting copolymer, we envision that these dioxyselenophenes will be of practical use in color mixing of electrochromic polymers. The XDOS family of polymers can provide the long wavelength absorbance needed for brown and black blends without leading to the higher oxidation potential and lower EC contrast that donor−acceptor ECPs (e.g. ProDOT-alt-BTD) typically exhibit.[34] Additionally, the significant reduction in oxidation potential and broad electroactive response make this polymer, and others of its kind, of interest in charge storage research in both types I and II supercapacitors.

5.8 Experimental Details

5.8.1 Materials

Pivalic acid (99%) was purchased from Sigma and used as received. $Pd(OAc)_2$ (98%, Strem Chemicals), K_2CO_3 (anhydrous, Oakwood Products), 18-Crown-6 (99%, Acros), diethyldithiocarbamic acid diethylammonium salt (97%, TCI America) were all used as received. 6,8-dibromo-3,3-bis(((2-hexyldecyl)oxy)methyl)-3,4-dihydro-2H-thieno[3,4- b][1,4]dioxepine (ProDOT$(HxDcO)_2$-Br_2) was prepared as described in Chapter 3 and EDOS[140] was prepared using a published method and confirmed via mass spectrometry and NMR. ECP-M (M_n = 12.4 kDa, Đ = 1.8, THF at 35 °C vs. polystyrene standards), ProDOT-EDOT (M_n = 43.8 kDa, Đ = 1.4, THF at 35 °C vs. polystyrene standards), and PEDOT were prepared as described in Chapter 3. DMAc (HPLC grade, Alfa Aesar) was passed through a pad of basic alumina (Sigma Aldrich) and degassed via argon bubbling prior to use. Chloroform (BDH, 99.8 %) was used without further purification. 1,1,2,2-Tetrachloroethane-D_2 (TCE-D2) (99.6%, Cambridge Isotope Laboratory, Inc.) was used as received. Propylene carbonate (PC, Acros Organics, 99.5 %) was purified and dried using a solvent purification system from Vacuum Atmospheres. Tetrabutylammonium hexafluorophosphate ($TBAPF_6$, Alfa Aesar, 98 %) was purified by recrystallized from hot ethanol and dried under high vacuum.

5.8.2 Polymer Synthesis

`To a 38 mL Schlenk tube equipped with stir bar, ProDOT$(HxDcO)_2$-Br_2 (0.6876 g, 1.0 eq.), EDOS (0.1580 g, 1.0 eq.), palladium acetate (0.0039 g, 2 mol%), pivalic acid (0.033 g, 0.39 eq.), and potassium carbonate (0.2970 g, 2.57 eq.) were added. 8.5 mL (0.2 M) of DMAc was added to dissolve the contents and the tube was sealed under nitrogen.

The reaction mixture was premixed for 2 minutes at ambient temperature. The tube was lowered into a hot oil bath with a constant temperature of 140 °C and allowed to stir vigorously for 1 hour After the flask was removed from the oil bath and allowed to cool, a small amount of $CHCl_3$ was added the polymer dispersion was precipitated into methanol and stirred for two hour. The precipitate was filtered into a soxhlet extraction thimble and washed via soxhlet with methanol, acetone, and finally dissolved in the hexanes fraction. After dissolution from the thimble, the hexanes was removed via rotary evaporation and then 30 mL of chloroform was added to the polymer fraction followed by ~40 mg of a palladium scavenger (diethylammonium diethyldithiocarbamate) and ~40 mg of 18-crown-6 and then stirred for 2 hours at 40°C then precipitated into 250 mL of methanol. The precipitate was vacuum filtered, using a Nylon pad (with a pore size of 20 μm) as the filter, and washed with a large volume of methanol and allowed to dry. The dried material was collected into a vial and dried under vacuum. The polymer was obtained as a dark blue/black solid in 56.0% yield (398 mg) ^{1}H-NMR (500 MHz, TCE-D2, 100 ^{o}C) δ 4.6-4.1 (m, 4H), 3.66 (br, 4H), 3.41 (br, 4H), 1.58-1.10 (m, 58H), 1.02-0.85 (s, 12H). Anal. calcd. for $C_{47}H_{78}O_6SSe$ C 66.40, H 9.25, S 3.77, Found C 64.8, H 8.87, S 3.61. M_n = 12.5 kDa, Đ = 1.6, THF at 35 °C vs. polystyrene standards.

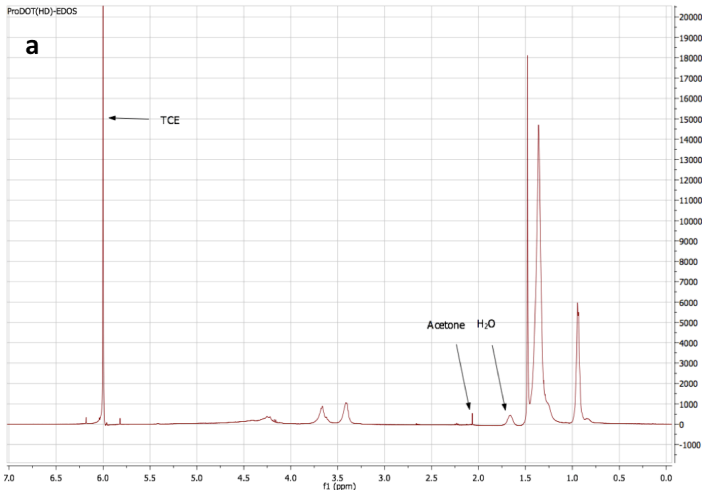
ProDOT(HD)-EDOS
a
TCE
Acetone
H_2O
f1 (ppm)

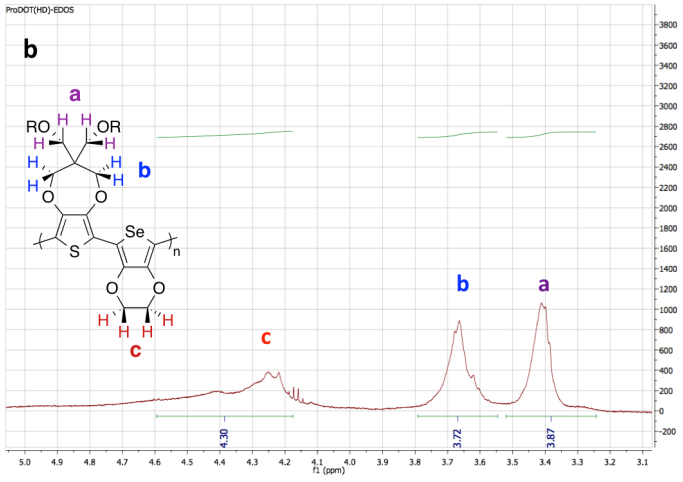
ProDOT(HD)-EDOS
b
a
b
c
RO
OR
Se
S
n
4.30
3.72
3.87
f1 (ppm)

CHAPTER 6. REPEAT UNIT STRUCTURE AND DOPING EFFECTS ON THE ELECTRICAL PROPERTIES OF DIOXYTHIOPHENE COPOLYMERS

6.6 Conductivity in Dioxythiophene Polymers

The broad electroactive response of the high EDOT content polymers in the previously reported ProDOT$_x$-EDOT$_y$ (P_xE_y) series has lead to these materials being effective as pseudocapacitive materials for charge storage applications. In Chapter 3 it was shown that increasing the EDOT content in the repeat unit of these copolymers lowers the onset of oxidation, increases the pseudocapacitance, and lowers the bandgap ($E_{g,\,opt}$) of the resulting material. Among these copolymers, ProDOT-EDOT$_2$ (PE_2) stands out as a soluble PEDOT analog with a vibrant blue charge neutral state that is optically indistinguishable from PEDOT and a similarly broad electroactive response.[144] As PEDOT is electrically conductive when doped,[14] it is worth investigating what conductivities can be obtained for the soluble P_xE_y series, as well as the potential of these materials, and other like them, for various applications. Two such applications are p-type organic thermoelectric (OTE) materials that require highly conductive polymers, and transparent polymer electrodes with minimal absorbance in the visible spectrum. For OTEs, the electrical conductivity (σ), Seebeck Coefficient (S), and the thermal conductivity (k) all determine the performance of a device and the dimensionless figure of merit zT.[34] Typically, only σ and S values are measured so the power factor (PF = $S^2\sigma$) can be reported while k is assumed to be low for polymers (0.1–1 W/m-K). These

thermoelectric properties are strongly correlated so a simultaneous enhancement of σ and S is challenging, thereby resulting in low PF and zT values. Nevertheless, significant advances have been made - Crispin and coworkers optimized the power factor of PEDOT:Tos by controlling its oxidation level with TDAE vapor (σ ~ 70 S/cm, S = 220 μV/K, resulting in a PF = 339),[164] while Pipe and coworkers reduced the dopant volume of DMSO-mixed PEDOT:PSS (σ ~ 900 S/cm, S = 70 μV/K, resulting in a PF = 441).[165] On the other hand, transparent electrode materials are simple assessed by their σ, transmissivity, and color neutrality.

To investigate the electrical properties of the P_xE_y copolymers, Nickel bis[1,2-bis(trifluoromethyl)-ethane-1,2-dithiolene] ($Ni(tfd)_2$) was chosen as the initial dopant for this study. This is primarily because of its planar structure and the fact that similar metal dithiolene complex based dopants, such as Molybdenum tris[1,2-bis(trifluoromethyl)-ethane-1,2-dithiolene] ($Mo(tfd)_3$), have been shown to be effective in organic electronic applications.[166,167] $Ni(tfd)_2$ has a reported reduction potential of 0.37 V vs. Fc/Fc^+ in CH_2Cl_2, making it a sufficiently strong dopant to remove an electron from all of the XDOT polymers in this study[168] To the best of my knowledge, $Ni(tfd)_2$ has not previously been reported as a dopant for conjugated polymers.

6.7 Experimental Setup

6.7.1 Polymer Synthesis

ECP-M was prepared via oxidative polymerization[127] while poly(ProDOT$_2$-*alt*-EDOT) (P_2E), poly(ProDOT-*alt*-EDOT) (PE), poly(ProDOT$_2$-*alt*-EDOT$_2$) (P_2E_2), and poly(ProDOT-*alt*-EDOT$_2$) (PE_2) were synthesized via direct (hetero)arylation polymerization (DHAP), as previously discussed in Chapter 3. Three additional polymers, namely poly(ProDOT-*alt*-dimethylProDOT), poly(ProDOT-*alt*-PheDOT), and poly(ProDOT-*alt*-EDTT) were prepared via DHAP in the same manner as the P_xE_y series; full synthetic details can be found in section 6.10.2 along with their ^{1}H-NMR spectra.

6.7.2 Film Preparation

All film preparation and doping procedures were performed in air. Films for σ measurements were prepared on glass substrates (500 μm thick) cleaned by sonication in toluene, acetone, and then isopropanol. Spray cast films were made from 4 mg/mL solutions of the polymer in chloroform using a hand-held airbrush (Iwata-Eclipse HP-BC, 15 psi). Spin coated films were cast from a 30 mg/mL solution at 650 rpm using a Laurell (Model WS-650MZ-23NPP) spin coater. Blade coated films were prepared using a Zehntner Testing Instruments blade coater (ZAA 2300) with an absolute blade height of 750 μm at variable speeds due to the different viscosity of the polymer solutions. For electrical measurements, four gold contact pads (1mm × 1mm, ~ 100 nm thick) were deposited on the prepared films using a shadow mask in an e-beam evaporator. The thickness of each polymer film (typically 300-600 nm) was determined after σ and S measurements via profilometry using a Bruker DektakXT profilometer.

6.7.3 Doping and Measurements Methods

$Ni(tfd)_2$[169] and $Mo(tfd)_3$[170] were prepared by Dr. Raghunath Dasarias previously described. All other dopants were obtained from commercial sources and used without further purification. The structures of the dopants/anions used are shown in Scheme 6.1. Silver (Ag^+) based dopants were kept in the dark and stored/weighed out in a glovebox to extend their shelf life. Initially, solution doping of the polymers dissolved in chlorobenzene prior to casting films was attempted. However, only ECP-M and P_2E remained in solution when the dopant was added, with the other polymers turning gray and crashing out of solution. The metal dithiolene dopants were dissolved in n-heptane at 10 mg/mL and films were immersed in these solutions (open to air) for either 10 seconds (for optical measurements) or 10 minutes (for electrical measurements) for dip doping. The films were then washed with clean n-pentane and allowed to air dry. The silver and iron based dopants were dissolved at 30 mg/mL in dry propylene carbonate (PC) and the films were immersed in these solutions (open to air) for 10 minutes unless otherwise noted. The films were then washed with clean PC and methanol and allowed to air dry.

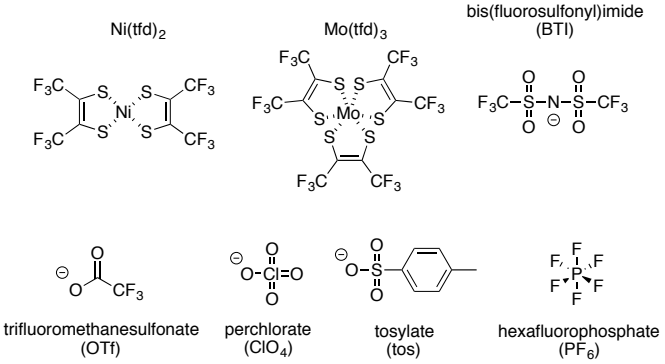

Scheme 6.1. Structures of the $Ni(tfd)_2$ and $Mo(tfd)_3$ dopants along with the anions discussed.

6.7.4 Electrical Conductivity and Seebeck Coefficient Measurements

Electrical conductivity measurements were performed as previously reported[16,17,18] using an in-house measurement setup. Micromanipulators with tungsten tips were used to make electrical contact to the gold contact pads, and sheet resistance was acquired based on the four-probe Van der Pauw technique. From this, the electrical conductivity was obtained using thickness values measured via profilometry. For Seebeck coefficient measurements, the film was suspended between two temperature-controlled Peltier stages (separated ~3 mm), and a series of temperature differences upto ΔT = 10 °C were applied between the stages. The thermoelectric voltage was measured between two contact pads on separate stages using the probe tips, while the temperature of each stage was measured with a K-type thermocouple in close proximity to the probe tips. Voltage and temperature data were acquired using a Keithley 2700 DMM with a 7708 Mux card via a LabVIEW interface. The Seebeck coefficient was extracted as the slope of the V - ΔT plot. In order to obtain temperature-dependent propeties, the Peltier stage temperature was changed from 20 – 100 °C using temperature controllers (Model LFI-3751). In all cases, thermal grease was applied on the backside of the substrate to ensure good thermal contact with the Peltier stage. Multiple films were measured to capture sample-to-sample variation; this is reported as the standard deviation and represented by error bars around the average value.

6.8 Solution Doping of the ProDOT$_x$-EDOT$_y$ Series

Films of the polymers were spray cast (~250-400 nm) to a transmittance of approximately 10% on glass and dipped into solutions (PC or n-heptane) of dopant for 10 minutes. Doping the XDOT polymers with $Ni(tfd)_2$ resulted in a dramatic and almost instantaneous color change from the vibrant as-cast states of the polymers to color neutral oxidized states that are highly transmissive in the visible region, as seen in Figure 6.1a and 6.1b. It should be noted that the copolymers are already slightly oxidized in the as-cast state, as seen by the polaronic absorbance around 900-1000 nm in Figure 6.1a, due to the low onset of oxidation of these polymers, as listed in Table 6.1. The films of these polymers can be can be converted to the undoped form by either electrochemical methods or treatment with hydrazine. However, we believe it is most useful to study how these materials doped from the as-cast form rather than adding other chemical treatment steps. In the oxidized spectra, the peaks that appears at ~820 nm are due to the $[Ni(tfd)_2]^-$ anions in the film and only bipolaron bands are observed for the polymers, indicating efficient doping.

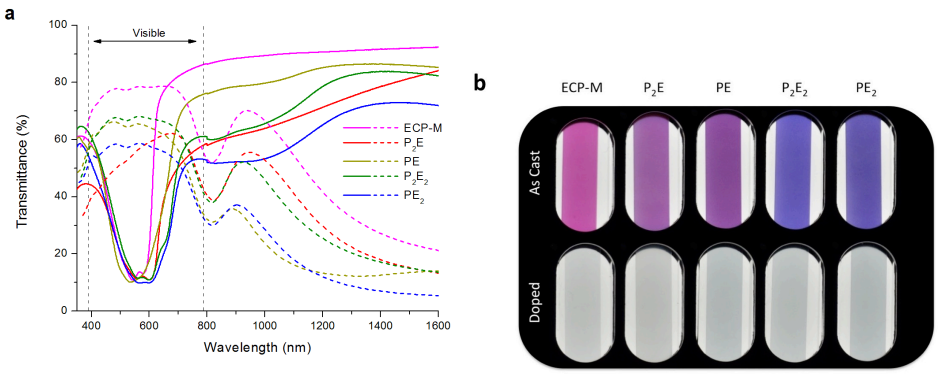

Figure 6.1. a) Transmittance spectrum of spray cast films of the polymer series in the as-cast and Ni(tfd)$_2$ doped state and b) the corresponding photographs of the films.

In the as-cast form (undoped or partially air doped) all of these polymers have σ values below 10^{-6} S/cm (the limit of detection for the experimental setup). Upon doping the polymers with Ni(tfd)$_2$ the conductivity increases to 10^{-3} S/cm for ECP-M and between 1-3 S/cm for the EDOT containing polymers; this is over a six orders-of-magnitude increase in conductivity by doping. As listed in Table 1, the electrical conductivity of the P_xE_y series show that, like the previously mentioned pseudocapacitance, there is a trend based on the EDOT content in the repeat unit.[1, 2] Incorporation of a biEDOT unit causes a larger increase in conductivity than a single EDOT unit even though the overall amount of EDOT in the repeat unit (50%) remains constant. This same observation was previously made for other properties (e.g. $E_{g,\,opt}$) of these polymers. There is not an apparent trend between the molecular weights and conductivity of the polymers, suggesting that the difference in conductivity is due to the repeat unit structure. This is understandable as soluble dioxythiophene based polymers are typically amorphous and other properties of these systems (e.g. λ_{max} or electrochromic

contrast) do not show molecular weight dependencies above a certain point, which is unique for each polymer (~ 8 kDa for ECP-M).[19-21] The Seebeck coefficients for all of these polymers are similar, with P_2E having the highest value of 35 μ V/K. We were unable to reliably measure the *S* value for doped ECP-M, potentially due the large resistances of these films.

Table 6.1. Molecular weight information and oxidation potentials of the P_xE_y polymer series and the electrical conductivities and Seebeck coefficients of the P_xE_y polymer series after doping with $Ni(tfd)_2$.

Polymer	M_n (kDa)	Đ (M_w/M_n)	Onset of Oxidation (V)[a]	σ of doped polymer films (S/cm)[b]	*S* of doped polymer films (μV/K) [b]
ECP-M	12	1.8	0.08	$1.2x10^{-3} \pm 0.1\ x10^{-3}$	Not measured
P_2E	15	2.0	-0.35	1.1 ± 0.1	35 ± 0.9
PE	NA	NA	-0.36	1.3 ± 0.2	18 ± 1
P_2E_2	14	4.5	-0.63	1.9 ± 0.2	20. ± 0.3
PE_2	56	1.8	-0.75	2.9 ± 0.3	27 ± 0. 2

a) by DPV vs. Ag/Ag^+ , b) spray cast films doped with $Ni(tfd)_2$

6.9 Understanding the Roles of Steric Interactions and Electron Density

The significant increase in σ when adding a small amount of EDOT (33%) to the repeat unit of ECP-M to make P_2E, is of particular interest as the further increase in σ with EDOT concentration to PE_2 (67%) is more gradual. To study this phenomenon, three new polymers were prepared that have clear structural similarities and differences to ProDOT and EDOT, as outlined in Scheme 6.2. First, the soluble ProDOT unit was copolymerized with dimethyl ProDOT (DMP) via DHAP, forming ProDOT-DMP. This is essentially ECP-M with half of the solublizing chains removed. When doped in the same manner, a two orders-of-magnitude increase in conductivity is seen, to 0.38 ± 0.04 S/cm. This indicates that the removal of some amount of side chains can significantly increase σ, which is as expected since alkyl chains add insulating material and may disrupt π- π stacking, thereby limiting hopping type transport. Next, reducing the steric interactions between the two ProDOT rings and slightly increasing the electron denisty on the thiophene by substitution of DMP with EDOT leads to a futher increase in conductivity to 1.3 S/cm. Then, maintaining the same steric interactions, the electron density on the thiophene ring can be greatly reduced by exchanging the EDOT for a 3,4-phenylenedioxythiophene (PheDOT) unit that we have previously studied. The reduction in electron density is due to the delocalization of the lone pairs in the dioxane ring into both the thiophene and the phenylene rings, as opposed to only the thiophene ring with EDOT.[22] This causes a nearly two orders-of-magnitude deacrease in conductivity to 0.054 ± 0.002 S/cm, indicating the importance of maintaining a high electron density on the thiophene rings. Futhermore, it can be speculated that monomers with even greater electron richness, such as dioxypyrroles and dioxyselenophene, may be useful for

achieving high σ. Finally, substitution of the oxygens for sulfurs in the dioxane ring of EDOT, making 3,4-ethylenedithiothiophene (EDTT), does not reduce the electron richness (as sulfur is a better π donor than oxygen) or change the steric interactions from the size of the ring, but replaces the energetically favorable and planarizing sulfur-oxygen interaction with repulsive sulfur-sulfur interactions.[23,24] This causes a large twisting between the ProDOT and EDTT rings and reduces the conductivity to 0.088 ± 0.006 S/cm, sugesting that, as expected, planarity between rings is important for electrically conductivity in conjugated polymer systems. Sumarizing these design criteria: side chains should be remove when possible, electron richness should be high, steric interactions should be minimized, and rings must be made coplanar (potentially through "conformational locking"). With these considerations in mind, the higher σ seen when using a biEDOT unit can be explained. BiEDOT is one of the most electron rich monomers used in organic electronics and is known to have a planar geometry (from x-ray crystal structures).[25] Additionally, the oxygens in biEDOT can interact with the sulfur atoms in the ajacent ProDOTs, and vice versa, leading to minimal twisting between rings and the low band-gap seen in this polymer.

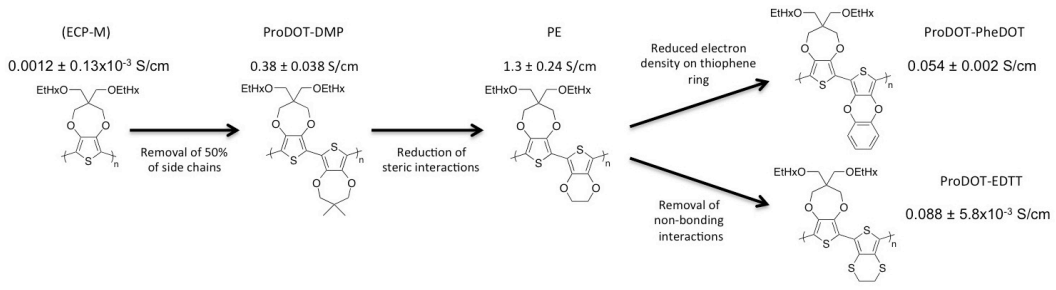

Scheme 6.2. Structures of new copolymers and their relationship to ECP-M and PE with corresponding conductivity values. (Ponder to change figure to look less like reactions).

6.10 Optimization of Film Casting Method

The film casting method was then investigated to determine its role in tuning conductivity. Of the many film casting methods available two roll-to-roll compatible methods, spray coating and blade coating, were compared along with spin coating. As previously discussed, spray cast films of PE_2 doped with $Ni(tfd)_2$ yield a σ of 2.9 ± 0.3 S/cm. Spin coated film yielded slightly higher σ values of 3.8 ± 0.8 S/cm. while blade coated films yielded the highest values with a σ of 4.7 ± 0.7 S/cm. This is largely due to the smoothness of the films prepared from each method. The smoother films produced from blade coating allows for more conductive pathways through the bulk of the film. Another manifestation of this was previously observed for ECP-M, with spin and blade coated films requiring a larger charge to switch and having a higher contrast compared to spray coated films due to less of the polymer being electronically isolated in the peaks of the relatively rough morphology.[12]

6.11 Dopant Optimization

Using this optimized casting method for PE_2, various dopants were tested and the thermoelectric properties were compared, as seen in Figures 2 a-c. $Mo(tfd)_3$ was selected as another metal dithiolene dopant due to its previously mentioned use in organic electronics. However, use of this dopant with PE_2 did not result in a high σ (0.43 ± 0.22 S/cm), potentially due to the large size of the dopant limiting penetration into the film. Iron(III) and Ag(I) based dopants were then investigated due to their relatively low cost, commercial availability, and previous usage in doping conjugated polymer films to

achieve high σ values.[26] Ferric triflate ($Fe(OTf)_3$), ferric perchlorate ($Fe(ClO_4)_3$), and ferric tosylate ($Fe(tos)_3$) all demonstrated significantly increased conductivity values of 49 ± 4, 76 ± 17, and 91 ± 14 S/cm, respectively. Similar to the iron dopants, silver bis(trifluoromethylsulfonyl)amide (AgBTI) and silver triflates (AgOTf) demonstrated increased σ values of 30 ± 9 and 98 ± 13 S/cm, respectively. This conductivity of PE_2 doped with BTI is slightly higher than regioregular P3HT doped with the same anion.[27]

$AgPF_6$ doped films yielded exceptionally high σ values of 255 ± 48 S/cm. This is not surprizing as PF_6 doped PEDOT has a reported conductivity of 300 S/cm.[28] The large difference in σ from doping with different silver dopants indicates that the anion size and shape plays a significant role in the resulting properties of the film. No obvious trend was observed in the Seebeck values and the large changes in σ controlled the PF (as seen in Figure 2c), with $AgPF_6$ doped films having a values of 7.2 μ W/m-K^2.

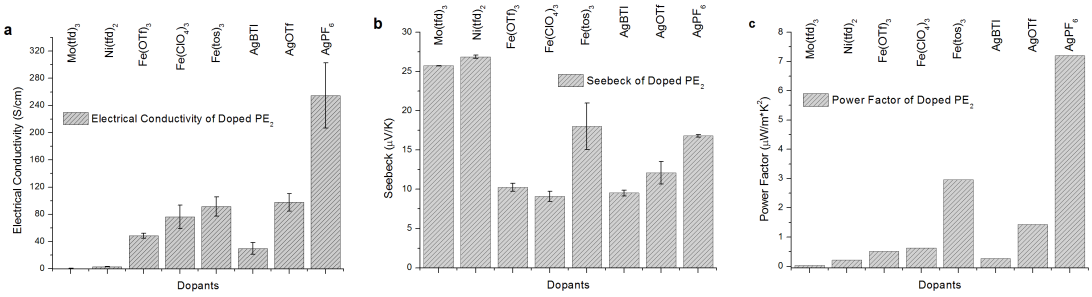

Figure 6.2. a) Electrical Conductivity, b) Seebeck, and c) Power Factor values of doped blade coated PE_2 films using various dopants.

Interestingly, this optimized set of conditions is specific to PE_2, with ProDOT-DMP having a σ of 0.11 ± 0.06 S/cm when cast and doped using the same conditions, a reduction of the initial the value of 2.9 ± 0.3 S/cm $Ni(tfd)_2$ dopant. This demonstrate that optimization must be performed for each new polymer and dopant in order to obtain the maximum conductivity for a given polymer and simply using a method described in the literature for another system will not necessarily result in meaningful/useful data.

6.12 Doping Level Optimization and Quantification of Doping

The final component for the conductivity optimization of PE_2 is tuning the doping level by changing the dopant concentration and/or doping time. Three solutions of $AgPF_6$/PC were prepared at various concentrations and the doping time was varied from 10 minutes to 2 hours, as listed in Table 2. The results were initially surprising as there is only a slight change in σ values as we vary dopant concentration. Moreover, given the error bars and rage of conductivity for all these samples, , as seen in Figure S2(except for the 10s doping experiment), there is not a statistical difference between these values. A somewhat larger change is seen in the *S* and PF values, but without a clear trend. X-ray photoelectron spectroscopy (XPS) measurements were performed on these films to elucidate the extent of doping. The sulfur to fluorine ratios, shown in Table 2, show 1 to 1 ratio for all doping conditions, indicating one PF_6^- anion per six rings (or two repeat units) in the polymer backbone. The sulfur to phosphorous ratio, seen in Table S1, has a larger variation, with values between 1:8 and 1:3. This difference is likely due to the relatively low amount of phosphorous in the film leading to less acurate ratios. It should be noted that there is silver metal (Ag^0) left on the surface of the film after doping, although this obviously does not contribute greatly to the large conductivity seen as both

AgOTf and AgBTI leave residual silver in the same manner but produce much lower conductivity films.

Table 6.2. Conductivity and Seebeck as functions of dopant concentration and doping time and the ratios of fluorine to sulfur in the films (from XPS).

Dopant Solution Concentration	Doping Time	σ of doped polymer films (S/cm)	S of doped polymer films (μV/K)	PF (μW/m-K^2)	S:F
1.2x10^{-3} M (0.30 mg/mL)	10 min	195 ± 24	19.8 ± 1.0	7.6	1:1
1.2x10^{-2} M (3.0 mg/mL)	10 min	233 ± 17	15.4 ± 3.4	5.6	1:1
1.2x10^{-1} M (30. mg/mL)	10 s	239 ± 11	17.1 ± 2.4	7.0	1:1
1.2x10^{-1} M (30. mg/mL)	10 min	255 ± 48	16.8 ± 0.2	7.2	1:1
1.2x10^{-1} M (30. mg/mL)	2 hrs	219 ± 15	11.9 ± 0.3	3.1	1:1

6.13 Testing of PE_2 as a Transparent Electrode for ECP Switching

Considering the other discussed application, PE_2 was tested as a transparent electrode material. A film of PE_2 was spray cast onto ITO glass and doped with $Fe(ClO_4)_3$ as previously described. As seen in Figure 6.4a and previously in Figure 6.1,

PE_2 is in the partially oxidized state upon casting and becomes transmissive and color neutral (shown in Figure 6.4b) when doped. This in itself is useful for solid state applications, but further study is need to determine the use of this material as an electrode in a redox active setup (e.g. electrochromic or supercapacitor devices. In a three-electrode cell the doped film can be electrochemically reduced to the charge neutral state (at -1.0 V vs, Ag/Ag^+), showing that the chemical doping process is reversible. Switching this polymer over the smaller electrochemical window of 0.0 to 1.0 V (as seen in Figure 6.4 and Figure 6.5) does not lead to a color change, with the electrochemical bleaching process occurring between -1.0 and -0.2 V. The spectra shown in Figure 6.4a and the colorimetry and photos in Figure 6.4b demonstrate the transmissive and colorless nature of this material over a broad electrochemical window. Combining this with the high electrical conductivity of the doped films makes this a promising material for redox active optical applications.

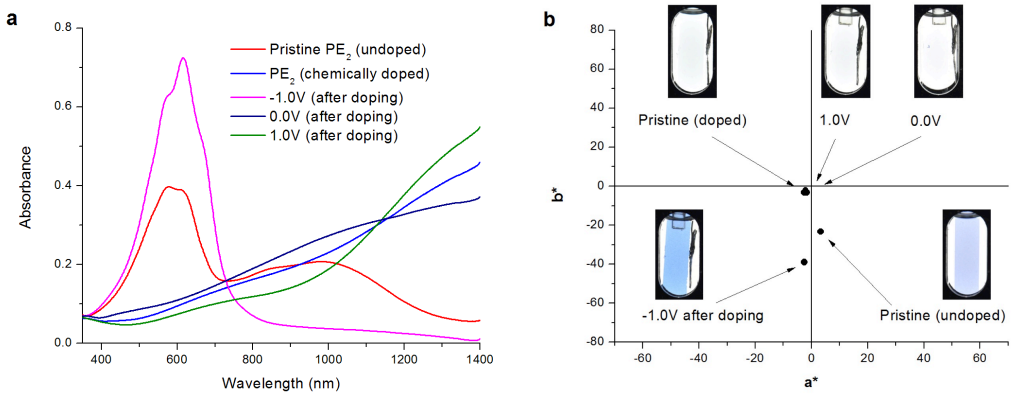

Figure 6.4. a) Spectra of PE_2 as cast, after solution doping, and at several potentials in an electrochemical cell (using 0.5M $TBAPF_6$/PC as the electrolyte) and b) a colorimetry plot with photos corresponding to the spectra.

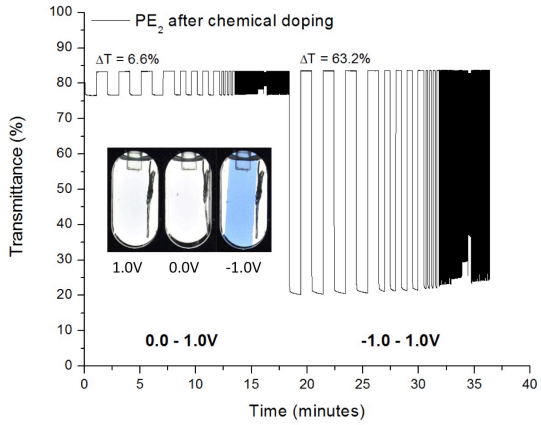

Fig. 6.5 Chronoabsorptiometry with photos of PE_2 switching between 0.0 and 1.0V followed by switching between -1.0 and 1.0V in 0.5M $TBAPF_6$/PC.

In order to test the actual use of this material in a redox active setup, a PE_2 was prepared and doped in the same manner as the previous experiment but on a non-conductive glass as the substrate. On top of the doped PE_2 a film of ECP-M was spray cast from THF. THF was used here, as this batch of PE_2 was only soluble in chlorinated solvents while ECP-M can be dissolved in THF or toluene. In the spectra of the as-cast ECP-M on PE_2, only the ECP-M absorption profile can be observed. After an initial electrochemical switching between -0.2 and 0.8 V, the charge neutral peak of ECP-M appears with the typical vibronic features and vibrant magenta/purple color seen in Figures 6.6a and 6.6b, respectively, when the potential is set at -0.2 V. When the potential is changed to 0.8 V the visible absorption of the ECP-M is bleached (ΔT = 48%) and the film becomes color neutral, as shown in Figure 6.6b. As seen in Figure 6.7, this switching is reversible, albeit somewhat slowly compared to using an ITO electrode

due to the lower conductivity of doped PE_2. Nevertheless, this is a proof-of-concept that doped PE_2 can be used as a transparent electrode.

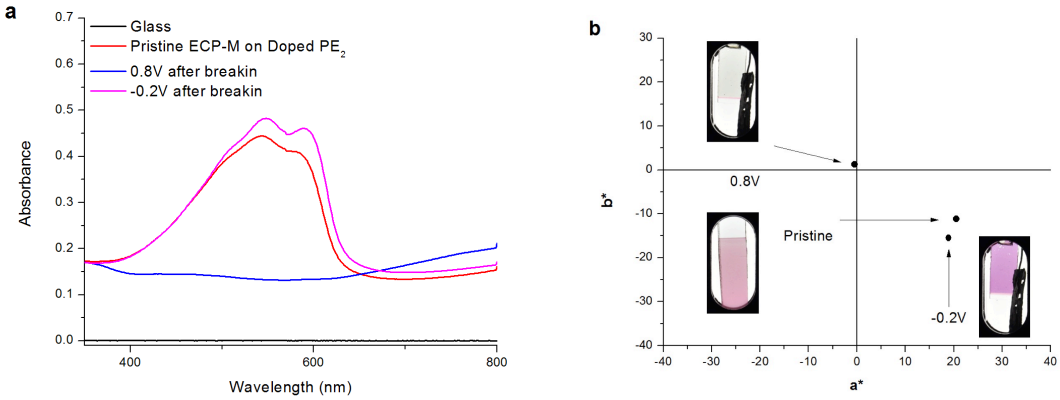

Figure 6.6. a) Spectra of ECP-M as cast and after electrochemical switching (using 0.5M $TBAPF_6$/PC as the electrolyte) on a doped PE_2 electrode and b) a colorimetry plot with photos corresponding to the spectra.

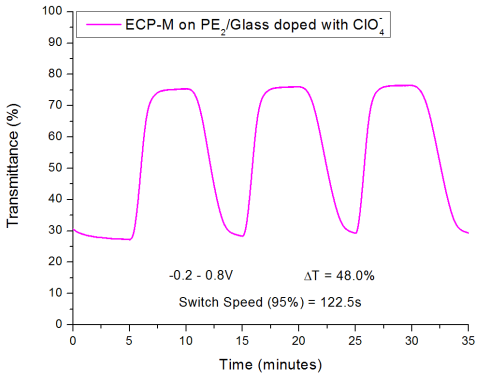

Figure 6.7. Chronoabsorptiometry of ECP-M on a doped PE_2/glass electrode switched in 0.5M $TBAPF_6$/PC.

6.14 Conclusion

In summary, through structural manipulation of the polymer repeat unit, the conductivity of dioxythiophene polymers was tuned from $1.2x10^{-3}$ S/cm to 2.9 S/cm. New XDOT copolymers were used to understand the structural requirement for high electrical conductivity in soluble XDOT copolymers and establish initial design rules. Optimization of the film casting method resulted in a doubling in the conductivity of PE_2 when using blade coating as opposed to spray casting. Screening of eight dopants resulted in PE_2 doped with PF_6 ions, approximate one per six rings, having an electrical conductivity of 255 S/cm; this indicates potential for these materials in various applications, including organic thermoelectrics. Spray cast films of PE_2 were doped using $Fe(ClO_4)_3$ and assessed as a transparent electrode material. A film of ECP-M was cast on one of these polymer electrodes and showed reversible electrochemical switching from a colored neutral state to a color neutral oxidized state. These results show that XDOT based polymers are a promising class of materials for thermoelectric and electrode applications. Further developments in the backbone structure along with side chain tuning and doping must be investigated in order to increase the conductivity even higher to obtain larger power factor values and for more effective transparent polymer electrodes.

6.15 Additional Experimental Details

6.15.1 Materials

EDTT-Br_2,[151] ProDOT-Br_2,[43] PheDOT,[22] and DMP [171] were prepared as described in the literature and confirmed using ^{1}H NMR and GC-MS (except for ProDOT-Br_2). The P_xE_y series was prepared as described in Chapter 3.

6.15.2 Polymer Synthesis

ProDOT-EDTT

To a 38 mL Schlenk tube equipped with stir bar, EDTT-Br_2 (0.5222 g, 1.0 eq.), ProDOT (0.6928 g, 1.0 eq.), palladium acetate (0.007 g, 2 mol%), pivalic acid (0.049 g, 0.3 eq.), and potassium carbonate (0.540 g, 2.5 eq.) were added. 16 mL of DMAc was added to dissolve the contents and the tube was sealed under argon. The reaction mixture was premixed for 2 minutes to ensure everything dissolved. The tube was lowered into an oil bath and heated to 140 °C and allowed to stir vigorously overnight (~14 hours). After the flask was removed from the oil bath and allowed to cool to room temperature, the polymer was precipitated into methanol and stirred for one hour. The precipitate was filtered into a soxhlet extraction thimble and washed with methanol, acetone, and finally dissolved into hexanes. The washings were conducted until color was no longer observed during extraction. After dissolution from the thimble, the chloroform was removed via rotary evaporation. Then ~50 mL of chloroform was added followed by ~20 mg of a palladium scavenger (diethylammonium diethyldithiocarbamate) and ~20 mg of 18-crown-6 and then stirred for 2 hours at 50 °C then precipitated into 250 mL of methanol. The precipitate was vacuum filtered, using a Nylon pad (with a pore size of 20 μm) as the filter, and washed with a large volume of methanol and allowed to dry. The dried material was collected into a vial and dried under vacuum. The polymer was obtained as

a red/orange solid in 17% yield (160 mg). ^{1}H-NMR (700 MHz, $C_2D_2Cl_4$, 50 ^{o}C) δ 4.24 (br, 4H), 3.59 (br, 4H), 3.34 (br, 5H), 1.44-1.25 (br), 1.93 (br). Anal. calcd. for $C_{31}H_{46}O_4S_4$ C 60.94, H 7.59, S 20.99, Found C 58.42, H 7.00, S 22.25. M_n = 9.4 kDa, Đ = 2.3, vs. PS in THF at 35 °C.

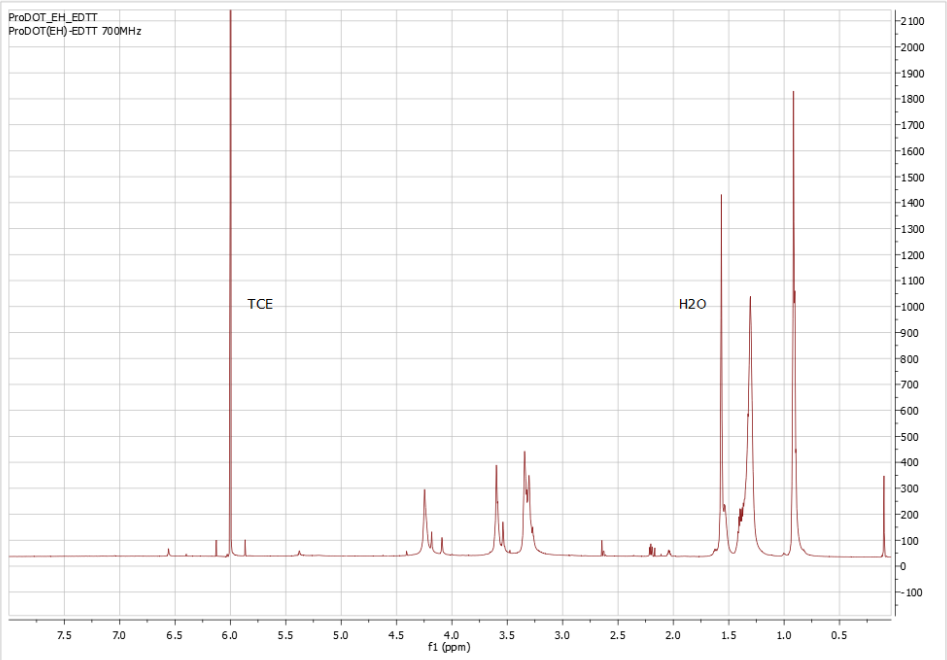

ProDOT-PheDOT

To a 38 mL Schlenk tube equipped with stir bar, ProDOT-Br_2 (0.867 g, 1.0 eq.), PheDOT (0.275 g, 1.0 eq.), palladium acetate (0.007 g, 2 mol%), pivalic acid (0.046 g, 0.3 eq.), and potassium carbonate (0.507 g, 2.5 eq.) were added. 14.5 mL of DMAc was added to dissolve the contents and the tube was sealed under argon. The reaction mixture was premixed for 2 minutes. The tube was lowered into an oil bath and heated to 140 °C and allowed to stir vigorously overnight (~14 hours). After the flask was removed from the

oil bath and allowed to cool to room temperature, the polymer was precipitated into methanol and stirred for one hour. The precipitate was filtered into a soxhlet extraction thimble and washed with methanol, acetone, and finally dissolved into hexanes. The washings were conducted until color was no longer observed during extraction. After dissolution from the thimble, the chloroform was removed via rotary evaporation. ~50 mL of chloroform was added followed by ~20 mg of a palladium scavenger (diethylammonium diethyldithiocarbamate) and ~20 mg of 18-crown-6 and then stirred for 2 hours at 50 °C then precipitated into 250 mL of methanol. The precipitate was vacuum filtered, using a Nylon pad (with a pore size of 20 μm) as the filter, and washed with a large volume of methanol and allowed to dry. The dried material was collected into a vial and dried under vacuum. The polymer was obtained as a dark red solid in 99% yield (902 mg). ^{1}H-NMR (700 MHz, $C_2D_2Cl_4$, 50 ^{o}C) δ 7.08 (br, 4H), 4.24 (br, 4H), 3.75 (m, 4H), 3.38 (br, 4H), 1.52-1.22 (br), 1.15-0.84 (br). Anal. calcd. for $C_{35}H_{46}O_6S_2$ C 67.06, H 7.40, S 10.23, Found C 66.76, H 7.24, S 10.33. Molecular weight to be determined.

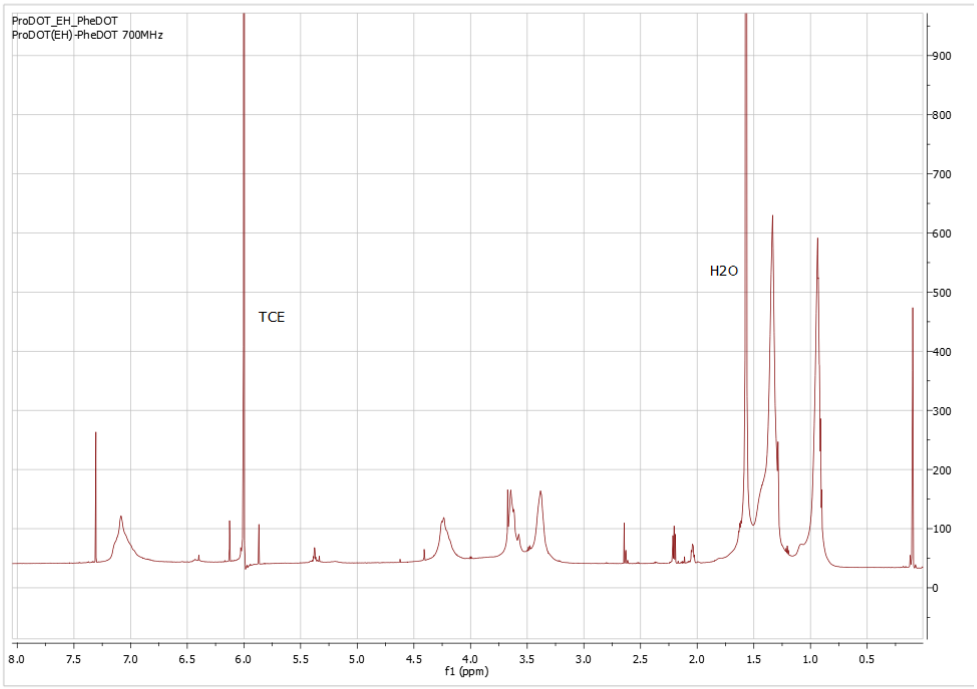

ProDOT-DMP

To a 38 mL Schlenk tube equipped with stir bar, ProDOT-Br_2 (0.8117 g, 1.0 eq.), ProDOT-Me_2 (0.2500 g, 1.0 eq.), palladium acetate (0.007 g, 2 mol%), pivalic acid (0.047 g, 0.3 eq.), and potassium carbonate (0.4707 g, 2.5 eq.) were added. 13.5 mL of DMAc was added to dissolve the contents and the tube was sealed under argon. The reaction mixture was premixed for 2 minutes. The tube was lowered into an oil bath and heated to 140 °C and allowed to stir vigorously from overnight (~14 hours). After the flask was removed from the oil bath and allowed to cool to room temperature, the polymer was precipitated into methanol and stirred for one hour. The precipitate was filtered into a soxhlet extraction thimble and washed with methanol, acetone, and finally dissolved into hexanes. The washings were conducted until color was no longer observed

during extraction. After dissolution from the thimble, the chloroform was removed via rotary evaporation and then ~50 mL of chloroform was added followed by ~20 mg of a palladium scavenger (diethylammonium diethyldithiocarbamate) and ~20 mg of 18-crown-6 and then stirred for 2 hours at 50 °C then precipitated into 250 mL of methanol. The precipitate was vacuum filtered, using a Nylon pad (with a pore size of 20 μm) as the filter, and washed with a large volume of methanol and allowed to dry. The dried material was collected into a vial and dried under vacuum. The polymer was obtained as a metallic looking purple solid in 88% yield (745 mg). ^{1}H-NMR (700 MHz, $C_2D_2Cl_4$, 50 ^{o}C) δ 4.19 (br, 4H), 3.88 (br, 4H), 3.64 (br, 4H), 3.36 (br, 4H), 1.48-1.23 (br), 1.17 (s, 4H), 0.98-0.85 (br). Anal. calcd. for $C_{34}H_{52}O_6S_2$ C 65.77, H 8.44, S 10.33, Found C 65.51, H 8.47, S 10.06. M_n = 17.1 kDa, Đ = 1.4, vs. PS in $CHCl_3$ at 40 °C.

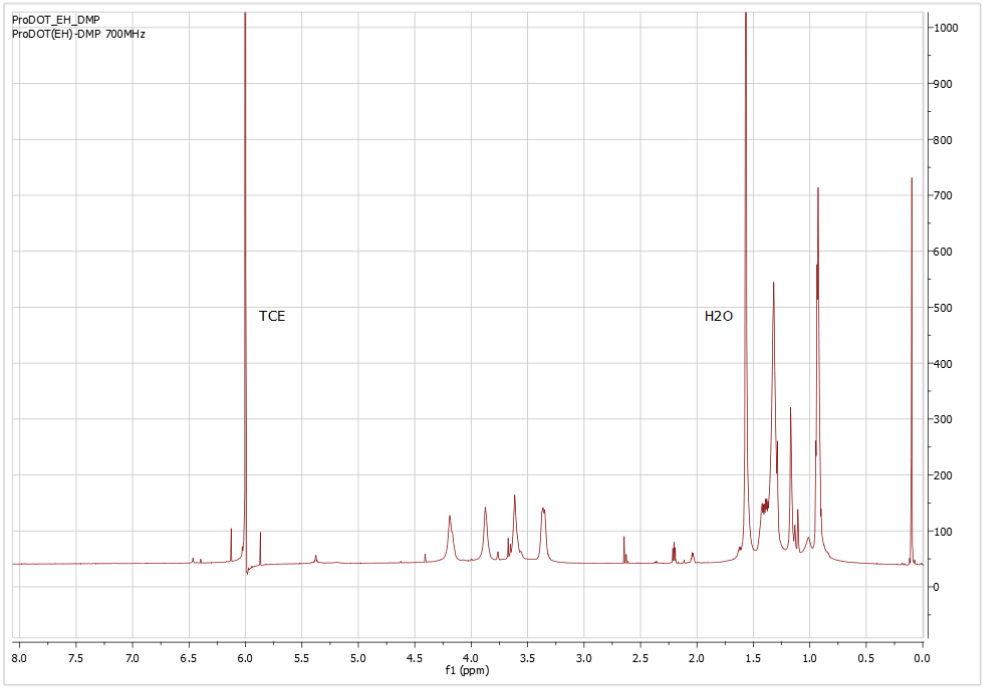

6.15.3 Instrumentation

The ^{1}H-NMR (64 scans) spectra were collected on a Bruker ASCEND 700 MHz instrument using $C_2D_2Cl_4$ as a solvent at a temperature of 323K. The molecular weight and dispersity of ProDOT-EDTT was obtained using a THF GPC at 35°C calibrated vs. polystyrene standards. The molecular weight and dispersities of ProDOT-DMP was obtained using a $CHCl_3$ GPC at 35°C calibrated vs. polystyrene standards. The electrochemical measurements on films were performed in a three-electrode cell setup using a Ag/Ag^+ reference electrode (10 mM $AgNO_3$ in 0.5 M $TBAPF_6$-ACN, $E_{1/2}$ for ferrocene: 68 mV) and the counter electrode was a platinum flag. The cyclic voltammetry was performed on an EG&G PAR (model 273A) potentiostat/galvanostatic under CorrWare control. Spectroelectrochemistry and chronoabsorptiometry were measured using an Agilent Technologies Cary 5000 UV-Vis-NIR Spectrophotometer under Cary WinUV control and a EG&G PAR (model 263A) potentiostat/galvanostatic under CorrWare control. X-ray photoelectron spectroscopy (XPS) was conducted using a Thermo Scientific instrument with a monochromatized Al K-α source (1486 eV). The base pressure of the measurement chambers was kept below 10-8 torr and all measurements were taken at room temperature. The elliptical spot used to irradiate the samples was 400 μ m (long axis).

CHAPTER 7. CONJUGATED POLYELECTROLYTES AS WATER PROCESSABLE PRECURSORS TO AQUEOUS COMPATIBLE REDOX ACTIVE POLYMERS FOR DIVERSE APPLICATIONS: ELECTROCHROMISM, CHARGE STORAGE, AND BIOCOMPATIBLE ORGANIC ELECTRONICS

Adapted from:

Ponder, J., F.; Österholm, A., M.; Reynolds, J. R. Conjugated Polyelectrolytes as Water Processable Precursors to Aqueous Compatible Redox Active Polymers for Diverse Applications: Electrochromism, Charge Storage, and Biocompatible Organic Electronics. *Chemistry of Materials* **2017**, 29, 4385−4392

7.1 The Importance of Aqueous Processing and Compatibility

Electroactive polymers have become increasingly important in the field of organic electronics, especially with the emergence of organic bioelectronics that makes use of the ability of these polymers to transport both electrons and ions.[172,173] While many applications, such as ECDs[174,175] and SCs[99,101], have advanced significantly over the past decade as a result of extensive material and device development, other applications, especially those that rely on aqueous compatible materials (i.e., a material that is redox active but not soluble in aqueous electrolytes) have seen slower progress. Two such areas

are biologically compatible organic electrochemical transistors (OECTs) for neural signaling and redox controlled drug release. Both of these applications require redox active polymers that can be reversibly doped and dedoped in aqueous media. Similarly, ECDs and SCs incorporating nonflammable and nontoxic aqueous electrolytes would be safer for research and development as well as disposable consumer products. These applications will also benefit from the increased ionic mobility and conductance of aqueous electrolytes (relative to organic electrolytes) as it relates directly to how fast these devices switch color and charge/ discharge. Additionally, processing the redox active films from water has considerable advantages, particularly the lack of toxic fumes.

7.2 Previous Methods to Achieve of Aqueous Solubility and/or Compatibility

Over the past decade the field of CPs has been moving away from electropolymerization as a deposition method to soluble polymers that can be characterized with a broader range of techniques (e.g., NMR, GPC, viscometry, etc.) and processed using a variety of roll-to-roll compatible methods. Solubility in CPs is typically achieved by functionalizing the polymer backbone with long, nonpolar hydrocarbon-based (alkyl) chains that provide high solubility in organic solvents due to increased conformational entropy and, as a result, ease their isolation and purification. To achieve aqueous compatibility, the surface polarity of the polymer film must be modified to reduce the hydrophobic nature imparted to the film by the alkyl side chains. One embodiment of this concept is the incorporation of glycol-based side chains onto a conjugated backbone that, while not typically providing aqueous solubility, are

sufficiently hydrophilic to allow for redox switching in aqueous media. This was recently demonstrated in a study by Nielsen et al., where organic soluble triethylene glycol functionalized polymers were found to be effective in OECTs, with accumulation mode devices (i.e., a device that is OFF at zero gate voltage) yielding higher transconductance values, the main figure of merit for OECTs, than PEDOT:PSS depletion mode devices (i.e., a device that is ON at zero gate voltage).[176] In spite of these excellent results, the above-mentioned polymer family demonstrates the poor organic and aqueous solubility often seen in CPs with glycol-based side chains, with only two of the five polymers prepared being sufficiently soluble for GPC molecular weight estimation. From this example we can see that glycol-functionalized polymers, while useful and worth continued investigation, are not a universal solution for obtaining aqueous compatibility and, furthermore, do not necessarily provide aqueous solubility. The limited solubility in organic solvents that is provided by these side chains also reduces the number of possible repeat unit structures that can be used, which in turn limits our ability to tune redox and color properties.

An approach to induce water solubility is to synthesize conjugated polyelectrolytes (CPEs) that have ionic functionalities (such as sulfonates) tethered to the backbone of, e.g., thiophene, EDOT, and pyrrole- based polymers.[177–180] However, the main issue with CPEs is that films of these polymers can redissolve in aqueous electrolytes, limiting their aqueous electrolyte compatibility. One way to circumvent dissolution is to immobilize the active polymer with a redox inactive cross-linker, such as 3-glycidyloxypropyl trimethoxysilane (GOPS), to render the film insoluble in water.[181] While it is an effective approach to stabilize PEDOT:PSS or other CPEs in aqueous

electrolytes, the addition of, e.g., GOPS does influence the redox properties of the CP,[181] most likely as a result of the lower ionic mobility in cross-linked films.

7.3 Outline of the Route to Water Soluble/Solvent Resistant Conjugated Polymers

In this chapter, a method1[44,182] is adapt for the preparation of a conjugated polymer with ester-based side chains that has high solubility in common organic solvents resulting in a material that is easily purified and fully characterized using standard methods (NMR, GPC, etc.) and then hydrolyzed to allow for aqueous processing. This is followed by a mild acid wash to render the polymer films solvent resistant (SR) and allow for redox switching in both organic and aqueous electrolyte solutions. While this method was previously used for aqueous processing and switching of nonoptimized ECPs, here we explore the scope and versatility of this method for a broader range of applications requiring redox activity.

As a key synthon, a ProDOT monomer was synthesized bearing multiple alkyl ester-based side chains having the carbonyl side of the ester closest to the propylene bridge. Using this design, upon hydrolysis, the carboxylate that is formed is covalently attached to the polymer backbone.[182] The ester-functionalized monomer is brominated and then polymerized with a heteroaryl dihydrogen species (specifically EDOT) using DHAP conditions to yield an organic soluble (OS) polymer that can be dissolved in common solvents including THF, toluene, and chloroform. Following purification of the OS-polymer, typical characterizations were performed to confirm the repeat unit structure and estimate molecular weight. As previously mentioned, the side chains that impart organic solubility and processablility are normally hydrocarbon-based and therefore

hydrophobic and do not provide aqueous solubility. This is illustrated in Scheme 7.1 (top left), where the OS-polymer selectively dissolves in chloroform and films of this polymer have relatively high contact angle (91.7 ± 1.0°) with water. The hydrophobic character prevents hydrated electrolyte ions from penetrating into the film upon redox cycling thereby inhibiting counterion insertion and electrochemical doping of the CP in aqueous media.[183] In order to overcome this hydrophobicity, the ester side chains were hydrolyzed to the corresponding CPE, and the polymeric carboxylate salt was found to dissolve in water (up to 10 mg/mL) due to the strong ion−dipole interactions between the carboxylates and water. As illustrated in Scheme 7.1 (top right), the water-soluble (WS) polymer can be cast using various methods to form films that can be further protonated via a dilute acid wash. The resulting film, now bearing carboxylic acid side chains, is insoluble in both organic and aqueous media and is termed solvent resistant (SR). The polar carboxylic acids on the surface, and in the bulk, of the film results in a hydrophilic surface with a low contact angle (29.2 ± 4.1°) that does not repel solvated ions and is capable of redox switching in both organic and aqueous media. However, if processing from organic solvents is required but aqueous compatibility is desired, the OS-polymer can be hydrolyzed in the solid state to produce the ionic polymer film and then acid treated to obtain the SR version.[44] Here, we demonstrate the versatility of this material and method by evaluating the SR-polymer in various aqueous-based electrolytes and electrochemical devices.

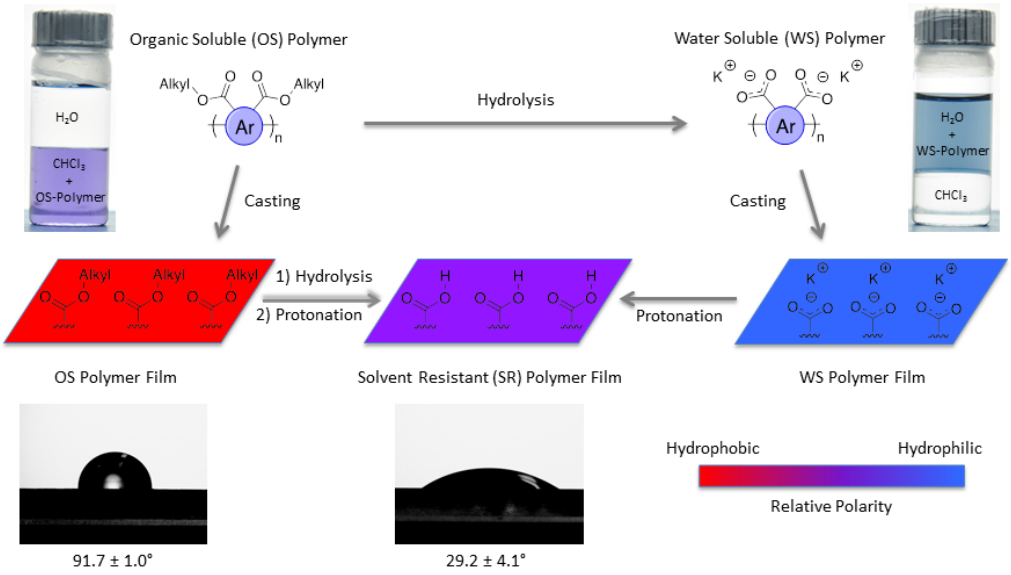

Scheme 7.1. General overview of the conversion of an organic soluble polymer (OS-Polymer) to the water-soluble CPE form, followed by acid treatment to a solvent resistant (SR-Polymer) and aqueous/organic compatible film along with images and contact angle measurements of the OS-Polymer and SR-Polymer discussed in this chapter.

7.4 Synthesis of the ProDOT-EDOT Model System

In this study, a poly(ProDOT-alt- EDOT) (PE) repeat unit structure was chosen as we have previously discussed in Chapter 3 how structures of this basic composition are suitable for both EC and charge storage applications.[144,184] The OS form of the polymer (OS-PE) was prepared via the DHAP (Figure 7.1) of EDOT and a functionalized dibromo-ProDOT monomer bearing ester side chains using standard conditions previously reported.[72] The polymer was purified using Soxhlet extraction, with the polymer dissolving in the chloroform fraction in excellent yield (94.4%) with a number-average molecular weight of 25 kDa (Đ = 2.8). The structure was confirmed via elemental analysis and high-resolution NMR (as shown in the synthetic details). A

portion of this polymer was hydrolyzed by refluxing the solid in a solution of KOH in methanol to convert it to the CPE form. As the methanol insoluble OS-PE is hydrolyzed, the solid polymer disperses into a fine powder as the side chains are removed. After filtering, washing, and drying, the polymer was found to selectively dissolve in water and to be insoluble in chloroform, as shown in Scheme 7.1.

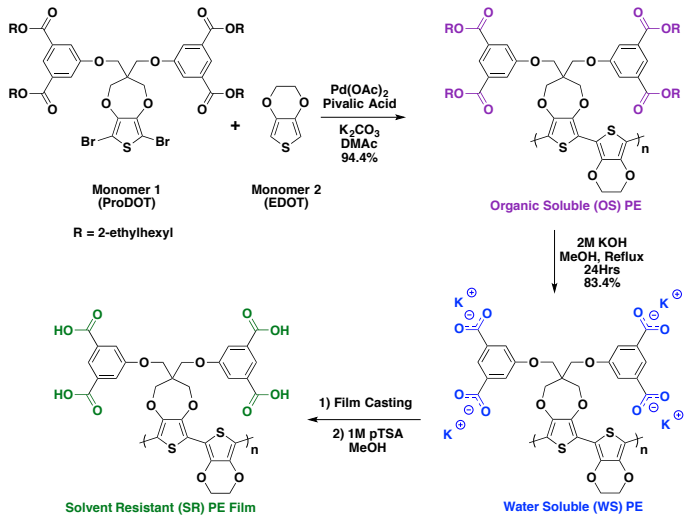

Figure 7.1. Synthetic route from monomers to the final solvent resistant polymer film.

7.5 Comparing Redox Behavior of Organic Soluble and Solvent Resistant Polymer Films in Organic Electrolytes

As shown in Figure 7.2, both the OS and the SR form of the polymer are electroactive in a PC-based electrolyte, but, more importantly, this figure also demonstrates that the redox behavior is not solely determined by the electroactive

backbone but also by the side chains as we observe large differences in the CVs that are directly related to the side chain cleavage. It is important to recall here that the backbone and degree of polymerization are identical for the two polymers as one is a precursor of the other. As expected from a polymer containing a substantial fraction of EDOT moieties in the repeat unit, the OS-PE has a low onset of oxidation determined by DPV to be −0.55 V relative to Fc/Fc^+ (shown in Figure 7.3a).[144] This is approximately the same onset of oxidation measured for the previously reported[73,144] polymers with the same conjugated backbone, but bearing 2-ethylhexyl (−0.54 V vs. Fc/Fc^+) or 2-hexyldecyl (−0.48 V vs. Fc/Fc^+) side chains (as shown in Figure 7.3b). The SR form, bearing the shortest side chains (film cast from water, then treated with 1 M pTSA/methanol), exhibits similar peak current but has an onset of oxidation that is 0.21 V lower (−0.76 V vs. Fc/Fc^+) than the OS form. This lower onset of oxidation results in the SR polymer having a broader electroactive window than not only the OS form but also the previously reported 2-ethylhexyl or 2-hexyldecyl functionalized analogues of the same polymer, indicating that the role of side chains on redox property tuning may be more intricate than generally thought. The lower oxidation potential of SR-PE is likely the result of a decrease in the steric bulk that occurs when we cleave the large ethylhexyl chains and replace them with protons. We do not observe a change in the oxidation potential of OS-PE that has been treated with pTSA/methanol, ruling out the possibility that the lower oxidation potential is purely due to solvent annealing or acid doping effects. The fact that the SR form can maintain a high current density throughout a larger electroactive window directly translates into a higher film capacitance, a property that is important not only for charge storage applications but also biosensors and OECTs.

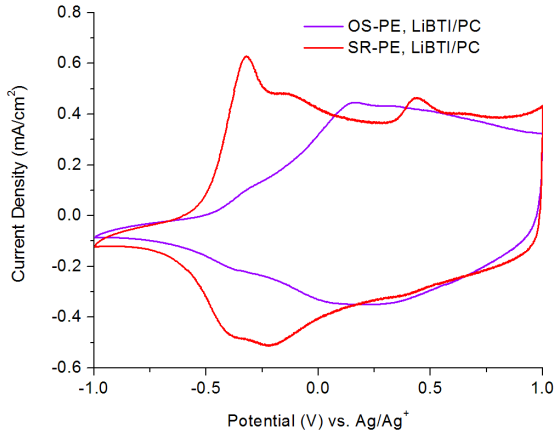

Figure 7.2. Cyclic voltammograms of drop cast films of the OS-polymer (purple line) and the SR-polymer (red line) on glassy carbon electrodes in 0.5 M LiBTI/PC at a scan rate of 50 mV/s.

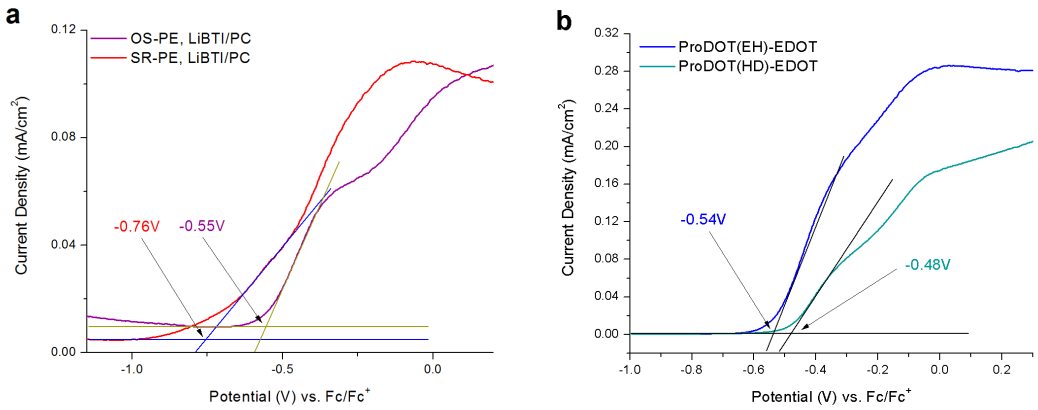

Figure 7.3. DPV curves of a) the OS-PE and SR-PE and b) the 2-ethylhexyl (ProDOT(EH)-EDOT) and 2-hexyldecyl (ProDOT(HD)-EDOT) functionalized polymers on glassy carbon electrodes in 0.5 M LiBTI/PC vs. Fc/Fc+.

7.6 Redox Behavior of the Solvent Resistant Polymer in Aqueous Electrolytes

As a result of the hydrophilic nature of the SR-PE, it is also highly electroactive in aqueous electrolytes of neutral or low pH, as shown in Figure 7.4a for both LiBTI/H_2O and salt water (NaCl/H_2O). Comparing the SR-PE in PC and water (Figure 7.2 and 7.4a)

with LiBTI serving as the electrolyte salt, we see minimal differences in the redox response of the films at low scan rates (≤250 mV/s), aside from the potential window being reduced to accommodate the stable window of water.[185] NaCl is an equally effective electrolyte salt for this polymer (Figure 7.4a), and no degradation is observed over repeated cycling. Monitoring the peak current as a function of scan rate allows us to assess the kinetic limitations of the redox cycling in both PC and aqueous electrolyte systems. SR-PE films in both aqueous electrolytes exhibit a linear scan rate dependence, as seen in Figure 7.4b, with peak current values within error of each other up to 10 V/s. This is important as most polymers, including the SR-PE and same backbone with branched alkyl side chains (ethylhexyl or hexyldecyl, see Figure 7.5), begin to show diffusion-controlled behavior at scan rates above 250 mV/s in PC-based electrolytes. Using a NaCl/H_2O electrolyte resulted in a smaller sample-to-sample deviation in peak current than the LiBTI/H_2O electrolyte despite all films being prepared identically. The film mass capacitance values (as determined by cyclic voltammetry at 50 mV/s) are comparable in both LiBTI/H_2O (42 ± 6 F/g) and NaCl/H_2O (33 ± 4 F/g) and approach the same values as higher scan rates, as seen in Figure 7.6. While it is difficult to make direct comparisons with literature as capacitance values are highly dependent on whether they are determined by cyclic voltammetry or electrochemical impedance spectroscopy (EIS) and on the scan rate, if determined by the former, the mass capacitance of SR-PE is comparable to PEDOT:PSS, which has a reported mass capacitance of 39 F/ g[186] (determined by EIS and assuming a density of 1 g/cm3). Electropolymerized PEDOT has a higher mass capacitance of 92 F/g,[187] not only due to the absence of solubilizing chains

or a matrix polymer, but also because it, unlike PEDOT:PSS, is able to completely depdope and achieve full depth of discharge.

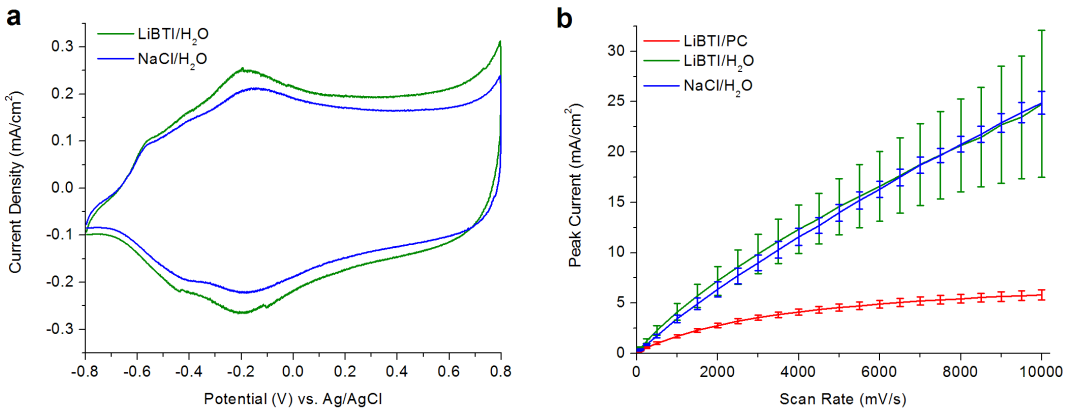

Figure 7.4. a) Cyclic voltammograms recorded at 50 mV/s and b) peak currents (with standard deviation) as a function of scan rate of films of SR-PE in various electrolytes (0.5 M).

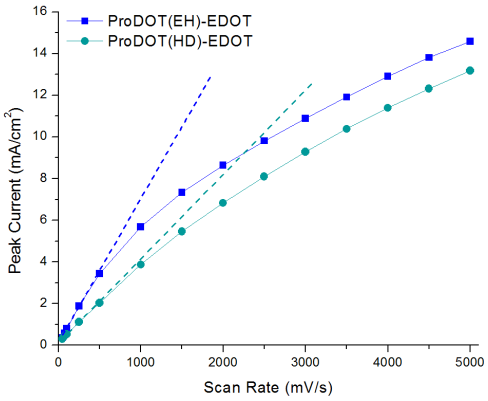

Figure 7.5. Scan rate dependences of drop-cast films of ProDOT(EH)-EDOT and ProDOT(HD)-EDOT on glassy carbon button electrodes in 0.5 M LiBTI/PC. Dashed lines illustrate the deviation from linearity at scan rates above 250 mV/s.

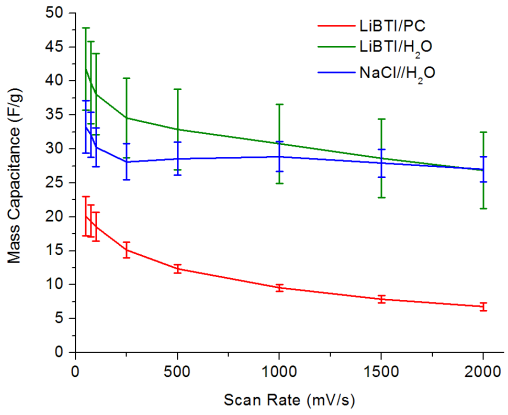

Figure 7.6. Mass capacitance (calculated from cyclic voltammograms) as a function of scan rate for films of SR-PE in various electrolytes.

It is important to note that the final protonation step that converts the CPE to a SR polymer does not require the use of pTSA but can be done using any acidic solution sufficiently strong to protonate the carboxylate groups. To demonstrate this, we performed the protonation step in a solution of 1 M HCl in methanol, which was found to be equally effective for rendering the films solvent resistant without changing the nature of the redox response.

7.7 Biologically Compatible and Novel Electrolytes

As a result of the effectiveness of $NaCl/H_2O$ as an electrolyte, the scope of the aqueous compatibility was further explored. First, Ringer's solution was tested, as it is compositionally similar to biological fluids, such as cerebral spinal fluid, and is often used in medical research. Second, human serum from blood was tested. From the CVs in Figure 7.7, it can be seen that both of these biologically relevant media are effective electrolytes for the SR-PE in their respective stable potential windows without

compromising the peak current, film capacitance (Figure 7.8a and 7.8b), or electrochemical reversibility. This is of particular importance as most OECT measurements are typically performed in NaCl/H_2O, which, while an excellent first test, is not comparable to actual biological electrolyte systems.[176,183,188] Because of this success, we decided to extend the family of electrolytes to commercial sports drinks to determine the versatility and robustness of SR-PE. Gatorade and Powerade were both found to be effective electrolytes for SR-PE in their stable potential windows (Figure 7.7). This is an important result as the question of long-term redox stability is a constant concern in the field of CPs. This redox activity and stability in biological electrolytes demonstrates the potential for this polymer, and others of the same kind, in bioelectronics and other applications requiring complex or "harsh" electrolytes. Specifically, the combination of high film capacitance and aqueous compatibility is necessary for OECT devices as the figure of merit, transconductance, is directly proportional to the capacitance of the redox active film.[176,186]

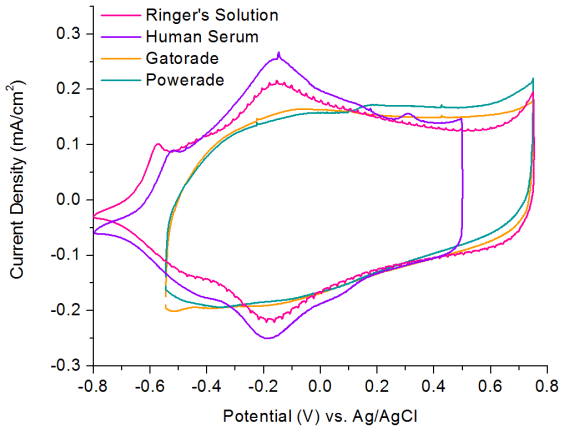

Figure 7.7. Cyclic voltammograms of the SR-PE in biologically relevant electrolytes (Ringer's solution and human serum) and sports drinks (Powerade and Gatorade) at a scan rate of 50 mV/s.

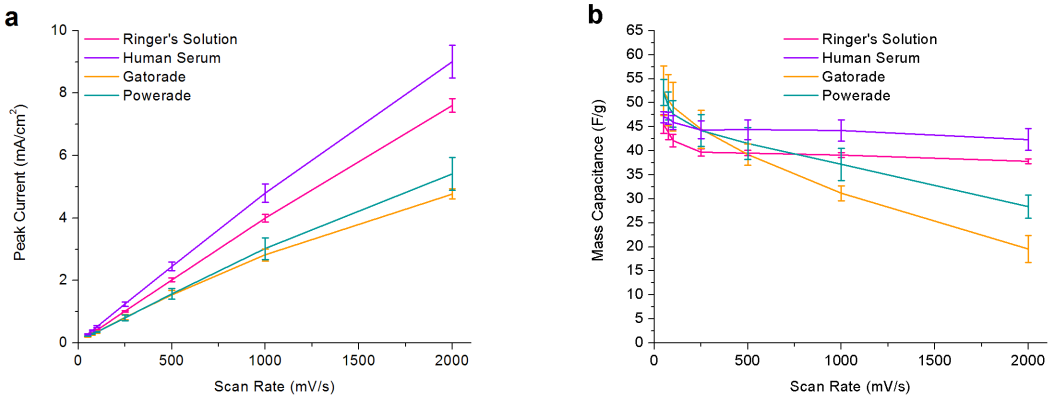

Figure 7.8. a) Peak current as a function of scan rate of SR-PE and b) mass capacitance as a function of scan rate of SR-PE films in various novel electrolytes.

7.8 Type I Supercapacitors incorporating solvent resistant polymers

To show the potential of these SR films in an electrochemical device, symmetrical Type I supercapacitors (schematic of the device architecture is shown in Chapter 2) were prepared that incorporated either the OS-PE or the SR-PE as the active material on both electrodes with LiBTI/PC (OS-PE and SR-PE), LiBTI/H_2O (SR-PE only), and NaCl/H_2O (SR-PE only) as the device electrolytes. Devices incorporating the OS-PE have linear scan rate dependence below 250 mV/s ($t_{discharge}$: 3.2 s). At higher scan rates, the mass capacitance drops rapidly and only ca. 10% of the initial capacitance is retained at 10 V/s, as seen in Figure 7.9. As we have shown for the films in a three-electrode cell in Figure 7.4b, the current becomes diffusion limited at scan rates above 250 mV/s, so this result was not unexpected. In contrast, devices incorporating the SR-PE maintain their current and mass capacitance up to a charge/discharge rate of 1 V/s ($t_{discharge}$: 0.8 s), suggesting that the reduced steric bulk and higher degree of polarity of the side chains enhance the

electrolyte−polymer interactions. Because of the lower electrolyte conductance (3 mS/cm) of LiBTI/PC compared to the aqueous analogues (LiBTI/H_2O = 21 mS/cm, NaCl/H_2O = 46 mS/cm), devices incorporating LiBTI/PC are not able to retain their capacitance above 1 V/s whereas the aqueous devices are able to retain ~80% of their original capacitance even at 10 V/s ($t_{discharge}$: 0.08 s), as seen in Figure 7.10a and b. As shown in Figure 7.10c, the fill factor (recall that this is a measure of deviation from ideal behavior[88,184]) of devices incorporating NaCl/H_2O remains unchanged from 50 mV/s up to 10 V/s. Devices incorporating LiBTI/H_2O only exhibit a decrease of ~15% of their fill factor at 10 V/s, while LiBTI/PC devices decreased to approximately half their initial values. The energy densities for these devices calculated form CVs at 10 V/s are 0.65 ± 0.40 Wh/kg, 3.14 ± 1.0 Wh/kg, and 4.47 ± 0.35 Wh/kg, for LiBTI/PC, LiBTI/H_2O, and NaCl/H_2O, respectively. Correspondingly, the power densities for these devices calculated from CVs at 10 V/s are 6.52 ± 4.0 kW/kg ($t_{discharge}$ = 0.1s), 39.4 ± 13 kW/kg ($t_{discharge}$ = 0.08s), and 55.9 ± 4.4 kW/kg ($t_{discharge}$ = 0.08s), for LiBTI/PC, LiBTI/H_2O, and NaCl/H_2O, respectively. To put this into context; commercially available supercapacitors have energy and power densities of 4-9 Wh/kg and 3-10 kW/kg, respectively.

Previous literature has demonstrated that hydrated ions are more mobile in polar environments, such as CPEs or in polymer films with polar side chains, e.g., glycols, alcohols, or acids rather than alkyl based side chains.[183,189−192] The results presented here clearly support these conclusions, as a large difference in performance between the OS and SR-PE films are observed, and suggest that the alkyl side chains are limiting ion movement into/ out of the film.

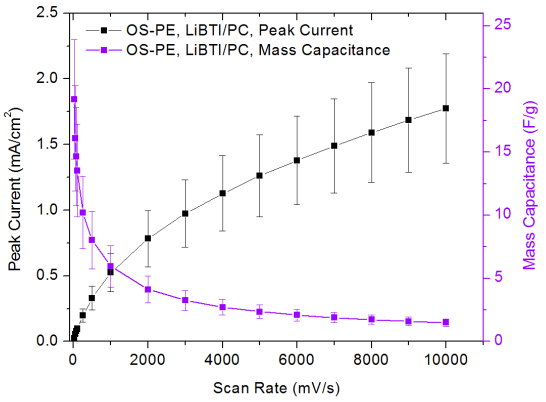

Figure 7.9. Peak current and mass capacitance as functions of scan rate for OS-PE devices with LiBTI/PC as the electrolyte.

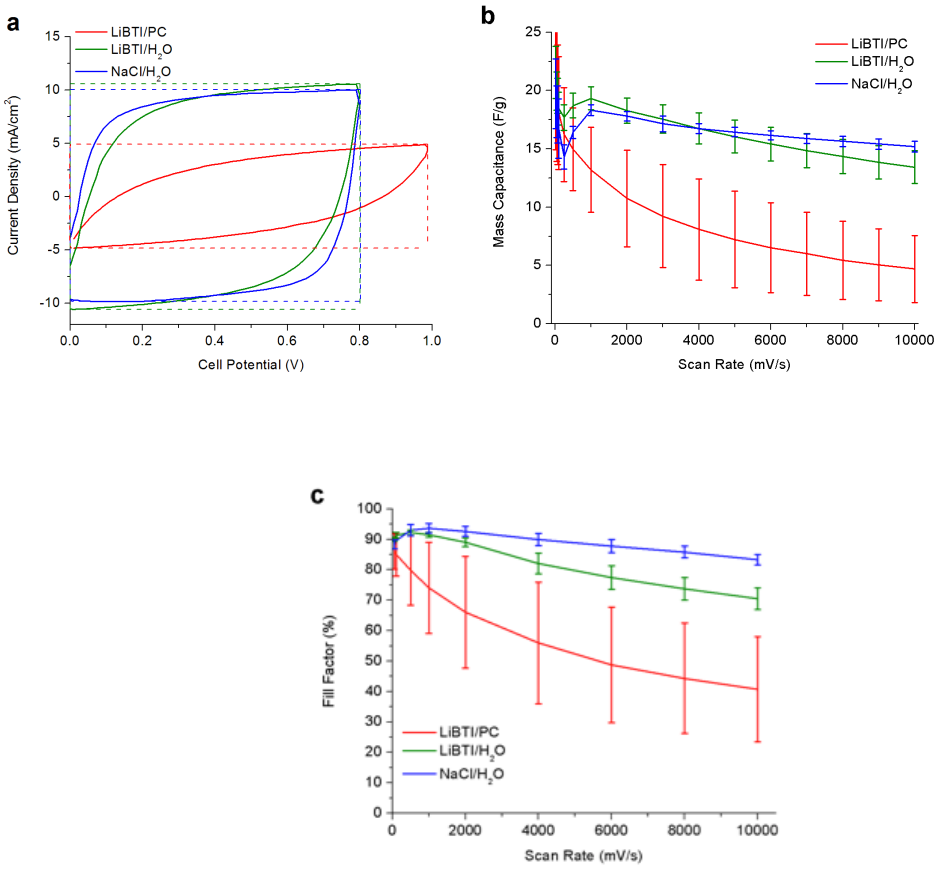

Figure 7.10. a) Representative CVs of Type I supercapacitors incorporating SR films and various electrolytes (with dashed lines indicating ideal performance), b) the mass capacitance, and c) the fill factor of these devices as a functions of scan rate.

To more closely mimic actual device operation, the devices were evaluated by galvanic cycling where the charge/discharge behavior is monitored as a function of current density. As shown in Figure 7.11a for devices incorporating $NaCl/H_2O$ as device electrolyte, the charge/discharge behavior is highly symmetrical, as expected in an ideal supercapacitor, up to exceptionally high current densities of 20 A/g, corresponding to a ~1.1 s discharge time. This demonstrates that these devices have low internal resistance, fast ion diffusion, and fast charge transfer kinetics. The cycling stability of devices incorporating salt water and assembled under ambient conditions, was monitored over 175 000 charge/ discharge cycles at 1 V/S (Figure 7.11b), and these devices are able to maintain >75% of their initial capacitance during these tests. This clearly demonstrates that water does not degrade these dioxythiophene-based CP over time, and it is expected that the observed drop in current could be reduced by device preparation under inert atmosphere to remove oxygen from the device. The next step for this research is to extend this method to other materials with repeat units optimized for charge storage and electrodes appropriate for a commercial device. In the end, you cannot achieve a much more cost-effective or environmentally benign solution than salt water.

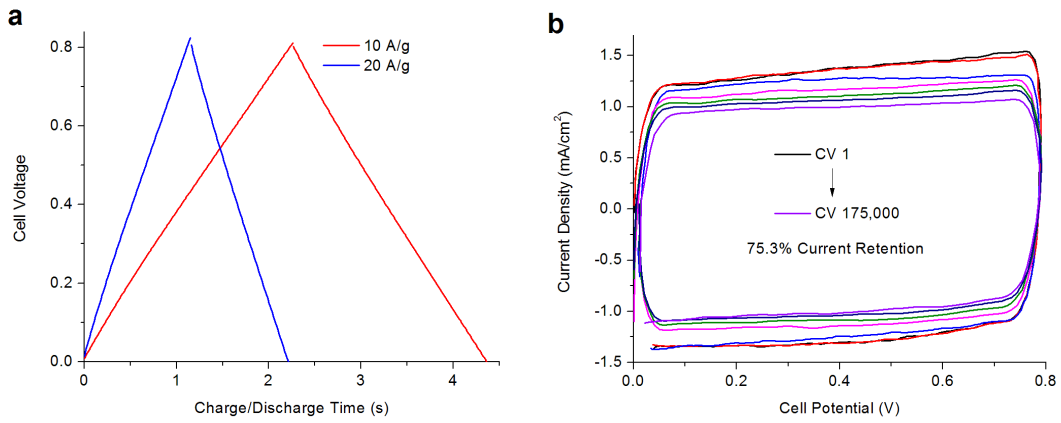

Figure 7.11. a) Galvanic cycling of a Type I SR-PE supercapacitor using a 0.5 M NaCl/H_2O electrolyte and b) select CVs of an identical device over 175,000 charge/discharge cycles at 1 V/s.

7.9 Towards High Contrast and Rapidly Switching Salt Water-based Electrochromic Materials

To demonstrate yet another application for this water processable/solvent resistant polymer system, films were spray cast onto ITO-coated glass from water and evaluated as electrochromic materials. As shown in Figure 7.12a, this material is effective as a high contrast EC material with a vibrant blue neutral state (λ_{max} = 613 nm) and a highly transmissive oxidized state. Similarly to other ProDOT$_x$-EDOT$_y$ copolymers discussed in Chapter 3,[144] the polaronic/radical cation absorbance is found at ~1000 nm, and the bipolaron/dication band >1500 nm exhibits minimal tailing into the visible, resulting in the highly color neutral oxidized state. Films coated to a transmittance of only 2% at λ_{max} in the colored state can maintain a high contrast (ΔT @ λmax = 68.0%) and switch to an oxidized state with a transmittance of ~70%. The rapid redox switching seen in the

supercapacitors incorporating this polymer translates to a rapid change in color as shown in the chronoabsorptiometry in Figure 7.12b where 95% of a full contrast switch is achieved in just 0.17 s for a SR-PE film deposited to a transmittance of ~7% in the neutral state. This is significantly faster than what is typically seen for EC polymers (including the same backbone structure with branched alkyl side chains in organic electrolytes) that require 0.5 to >2s to complete a full switch between the two states. This is not only due to the high ionic conductance of the salt water as this specific polymer is switching faster than previously reported aqueous compatible electrochromic polymers[44,193,194] but is also due to the incorporation of EDOT units into the backbone, which was previously shown[73,144] results in rapidly switchable EC polymers.

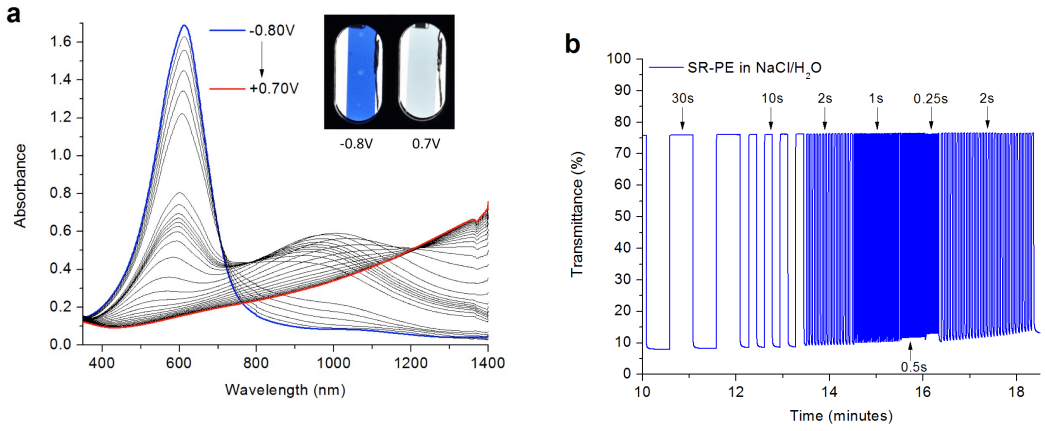

Figure 7.12. a) Spectra recorded in 50 mV increments from -0.80 V to 0.70 V (vs. Ag/AgCl) and photos taken at -0.80 V and 0.70 V. b) Transmittance at λ_{max} as a function of switching time of a spray-cast film of the SR-PE on ITO glass in 0.5 M NaCl/H_2O switching from the charge neutral state (-0.80 V vs. Ag/AgCl) to the oxidized state (0.70 V vs. Ag/AgCl).

7.10 Conclusions and Perspective on WS/SR Polymers for Various Applications

In summary, this reported methodology of forming solvent resistant films from water-soluble polymers that are processed as aqueous-based inks has allowed for redox switching in a large variety of organic, inorganic, and biologically compatible electrolytes. Supercapacitor using the solvent resistant side chain have a higher mass capacitance and are able to maintain this capacitance at significantly higher scan/discharge rates than the corresponding polymer with hydrophobic side chains. NaCl in water was found to offer the best device performance with highly reversible behavior at scan rates of up to 10 V/s and charge/ discharge currents of 20 A/g. The use of salt water did not compromise stability, as the devices continued to operate effectively even after 175,000 charge/discharge cycles. The significance of this cannot be overstated, as the long-term stability of conjugated polymer-based redox active devices (such charge storing supercapacitors and ECDs) is vital for commercial use.

With this information in mind we should again consider bioelectronics. The combination of aqueous compatibility, high capacitance, excellent EC properties, and stability in aqueous media over extended cycling suggest that this material, and others like it, would be useful for bioelectronic applications, specifically OECTs. The high electrochromic contrast is potentially useful is this area as well, as monitoring color changes facilitates the determination of the extent of doping throughout the bulk of a film and, correspondingly, ion uptake and swelling of the polymer in various electrolyte systems.[176,190,195,196]

7.11 Experimental Details

7.11.1 Materials

ProDOT(EH)-EDOT and ProDOT(HD)-EDOT were prepared as previously reported.[73,144] The dibromo-tetraester ProDOT monomer was prepared via a previously published method.[182] EDOT (97 %) was obtained from Alfa Aesar and vacuum distilled prior to use. $Pd(OAc)_2$ (98 %, Strem Chemicals), pivalic acid (99 %, Sigma), K_2CO_3 (anhydrous, Oakwood Products), 18-Crown-6 (99 %, Acros), diethyldithiocarbamic acid diethylammonium salt (97 %, TCI America), KOH (Technical Grade, Fisher Scientific), and pTSA (monohydrate, 98 %, Alfa Aesar) were used as received. DMAc (HPLC grade, Alfa Aesar) was filtered through a pad of alumina (basic, Sigma Aldrich) and degassed by argon bubbling prior to use. Sodium chloride (NaCl, biotechnology grade, Amresco) and lithium bis(trifluoromethanesulfonimide) (LiBTI, 99 %, Acros Organics) were used as received. Gatorade™ (Glacier Cherry) and Powerade™ (White Cherry) were purchased from a local grocery store and were degassed with argon. Propylene carbonate (PC, Acros Organics, 99.5 %) was purified using a solvent purification system built by Vacuum Atmospheres. Deionized (DI) water was collected by purification of tap water using a EMD Millipore Milli-Q Ultrapure Water system. Ringer's Solution (Amphibian, Lab Grade) and Human Serum (Normal) were purchased from Ward's Science and Atlanta Biologicals, respectively. Other solvents used (such as methanol, hexanes, and diethyl ether) were obtained from VWR and used as received except for chloroform, which was obtained from BDH. The cellulose separator was a cut piece of filter paper (Qualitative, Fine, Fisher Scientific).

7.11.2 Instrumentation

The ^{1}H-NMR (64 scans) spectra were collected on a Bruker ASCEND 800 MHz instrument using $C_2D_2Cl_4$ as a solvent at a temperature of 323K. The molecular weight and dispersity of the polymer were obtained using a THF GPC at 35°C calibrated vs. polystyrene standards. The electrochemical measurements on films were performed in a three-electrode cell setup using either a Ag/Ag^{+} reference electrode (10 mM $AgNO_3$ in 0.5 M $TBAPF_6$/ACN, $E_{1/2}$ for ferrocene: 68 mV) for organic electrolytes or a Ag/AgCl reference electrode (1M KCl, purchased from CH Instruments, Inc.) for aqueous electrolytes, the counter electrode was a platinum flag. The cyclic voltammetry was performed on an EG&G PAR (model 273A) potentiostat/galvanostatic under CorrWare control. The long-term charge/discharge experiments on the Types I supercapacitor devices were performed on a Pine bipotentiostat (model AFCBP1) and monitored using AfterMath software. Galvanic cycling experiments were performed on a Metrohm Autolab Potentiostat/Galvanostat (Type PGSTAT101) and were monitored using NOVA 2.0 software. Spectroelectrochemistry and chronoabsorptiometry were measured using an Agilent Technologies Cary 5000 UV-Vis-NIR Spectrophotometer under Cary WinUV control and a EG&G PAR (model 263A) potentiostat/galvanostatic under CorrWare control.

7.11.3 Polymer Synthesis, Hydrolysis, and Acid Treatment

Organic Soluble Poly(ProDOT-alt-EDOT) (OS-PE) Synthesis: The dibromo-tetraester ProDOT monomer (monomer 1) (1.00 g, 0.869 mmol, 1.00 equiv) and freshly distilled EDOT (monomer 2) (0.123 g, 0.869 mmol, 1.00 equiv) were added to a 38 mL pressure vessel equipped with a stir bar. $Pd(OAc)_2$ (4 mg, 0.02 equiv), pivalic acid (26 mg, 0.3 equiv), K_2CO_3 (0.299 g, 2.5 equiv), and DMAc (8.7 mL, 0.2 M, degassed with argon) were added, and the vessel was sealed under argon and placed in an oil bath at 140 °C and stirred overnight (~14 h). The reaction was cooled to ambient temperature, the reaction mixture was precipitated into methanol, and the resulting solution/precipitate was filtered into a Soxhlet thimble. The polymer was purified via Soxhlet extraction using methanol, acetone, and hexanes and then dissolved in chloroform. Approximately 40 mg of a palladium scavenger (diethylammonium diethyldithiocarbamate) and ~40 mg of 18-crown-6 were added to the polymer/chloroform solution which was concentrated under vacuum and then stirred for 2 h at 40 °C and subsequently precipitated into methanol. After filtering, washing with methanol, and drying the precipitate under vacuum, 0.928 g (94.4%) of a dark purple solid was obtained. ^{1}H-NMR (800 MHz, $C_2D_2Cl_4$, 50 °C) δ8.24 (t, 2H), 7.8 (d, 4H), 4.4 (d, 4H), 4.3−3.8 (br, 8H), 1.7 (s, 4H), 1.45−1.0 (br, 36H), 1.0−0.6 (br, 29H). Anal. Calcd for $C_{63}H_{86}O_{14}S_2$ C 66.88, H 7.66, S 5.67, Found C 66.85, H 7.62, S 5.73. M_n = 25.4 kDa, Đ = 2.8 (THF GPC at 35 °C vs polystyrene standards)

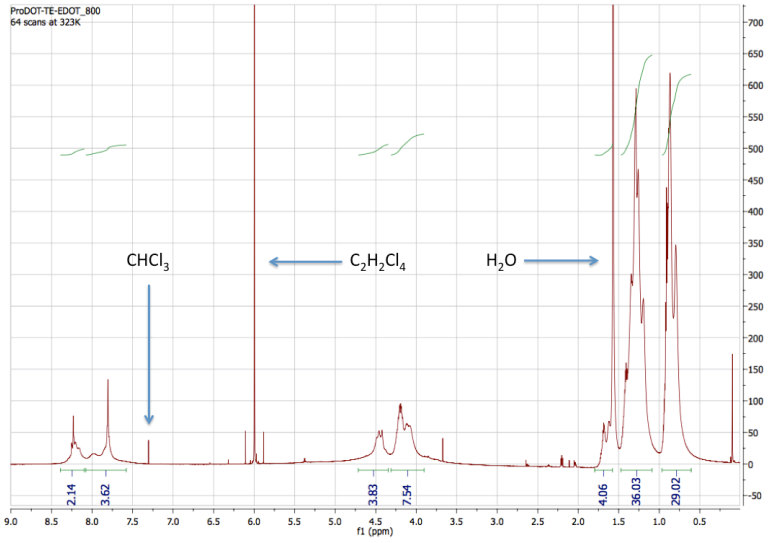

Post-Polymerization Hydrolysis To Form Water-Soluble PE (WS-PE): The OS-PE (400 mg) and a stir bar were added to a 100 mL round-bottom flask with 50 mL of 2.0 M KOH/methanol solution. The solution was degassed by bubbling argon through it for 30 min. The round-bottom flask was equipped with a reflux condenser and covered in argon and heated to reflux (65 °C) for 24 h while vigorously stirring. After cooling to room temperature, the suspension was filtered over a 0.45 µm filter and washed with methanol, chloroform, and diethyl ether. The solid polymer cake was dried under high vacuum overnight to yield 246 mg (83.4% recovery) of a water-soluble CPE, WS-PE.

Film Preparation/Post-Processing Functionalization: The WS-PE was dissolved in deionized water and either spray cast (4 mg/mL) onto ITO-glass substrates on a hot plate (~60 °C) or drop cast (2 mg/ mL, 2 µL, 4 µg of polymer) onto glassy carbon button electrodes and air- dried for 30 min. The films were then dipped into a 1 M solution of p-toluenesulfonic acid (pTSA)/methanol (or 1 M hydrochloric acid

(HCl)/methanol) for 10 min (open to air). The resulting solvent resistant films were washed with methanol and allowed to air-dry. All film measurements (except for EC characterizations) were made in triplicate to ensure reproducibility.

7.11.4 Type I Supercapacitor Device Fabrication

To evaluate this polymer for supercapacitor applications, electrodes were prepared by drop casting films onto glassy carbon electrodes (area: 0.07 cm2). Both of the electrodes were electrochemically conditioned by cycling them in the respective electrolytes (25 cycles for aqueous electrolytes and up to 100 cycles for lithium bis(trifluoromethanesulfonyl)imide (LiBTI)/ propylene carbonate (PC)). One of the polymer-coated electrodes was then electrochemically reduced to convert the polymer film to the charge neutral form (−1.0 V vs Ag/Ag+ for LiBTI/PC and −0.8 V vs Ag/ AgCl for aqueous electrolytes) for 30 s, and the other polymer films were converted to the fully oxidized form (1.0 V vs Ag/Ag+ for LiBTI/PC and 0.8 V vs Ag/AgCl for aqueous electrolytes) for 30 s. The two polymer- coated electrodes were assembled into a Swagelok-type setup and separated by a cellulose-based separator soaked in electrolyte. Before device assembly, the electrolyte solutions were degassed via argon bubbling, but no additional measures were taken to remove oxygen and moisture from the device as they were built on the bench in an ambient environment. All device measurements (except galvanic cycling and lifetime tests) were made on at least three devices to ensure reproducibility.

CHAPTER 8. INCREASED MASS CAPACITANCE THROUGH SIDE CHAIN DEFUNCTIONALIZATION OF CONJUGATED POLYMERS

8.1 The High Side Chain to Backbone Ratio in Soluble Polymers and its Effect on Redox Switching and Mass Capacitance

The use of solubilizing side chains has allowed for solution processablility and a broad range of possible characterizations on conjugated polymers. Additionally, side chains can impart (or remove) order in a film and can be used to finely tune the morphology of polymer films and polymer/discrete molecule blends.[197,198] However, in order to solubilize a polymer the side chains used must be relatively large, reducing the active material in the film. As shown in Scheme 8.1, many common polymers have more than 50% of their mass coming from side chains, compared to electropolymerized materials that can have no side chain at all. These side chains are redox inactive and electrically insulating. Moreover, it has been shown that the typical alkyl side chains, compared to more polar ones, can inhibit ion flow through a film.[199] This was previously demonstrated in Chapter 7, with carboxylic acid side chains allowing for more rapid redox switching than using alkyl chains.[200] Along with the slower redox switching and limited electrolyte compatibility, the significant mass of alkyl side chains, and side chains

in general, in charge storage materials, such as PE_2, reduce the mass capacitance of films and devices.

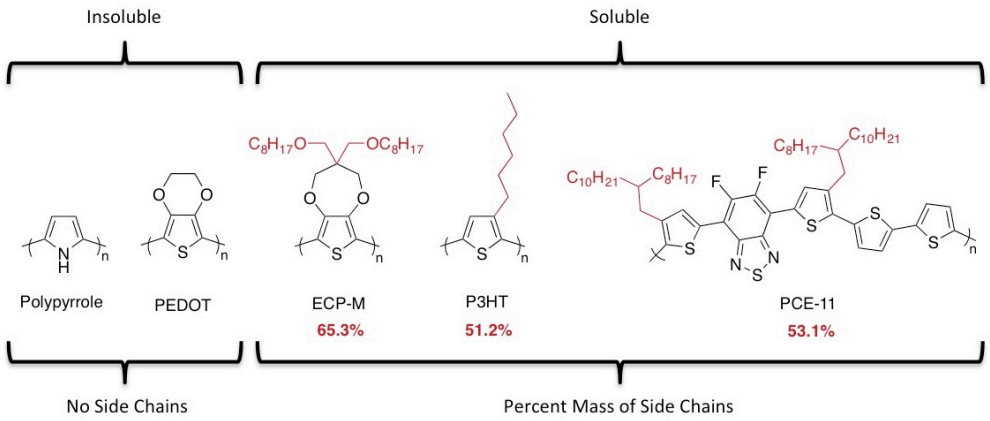

Scheme 8.1. Structures of a few common soluble and insoluble conjugated polymers with the percent mass of side chains shown.

8.2 Methods for Side Chain Defunctionalization

Side chains have been cleaved from polymer backbones following processing using several different methods. The group of Fréchet has used thermally cleavable groups to tune the interface properties of polythiophene for hybrid solar cells and to tune the band-gap of BTD copolymers.[201,202] The Krebs group has explored acid cleavable silyl-based side chains for the preparation of polythiophene.[203] As previously discussed in Chapter 7, the Reynolds group has used polymers with ester-based side chains that can be cleaved via hydrolysis to impart redox switching in aqueous electrolytes and tune the properties of the polymer film.[182,193,194,200] The ester groups are more commonly oriented so that the carbonyl group is closest to the backbone, resulting in water soluble carboxylates upon hydrolysis. Alternatively, the ester can be oriented so that only an

alcohol remains on the polymer backbone after hydrolysis and the cleaved side chain bearing the carbonyl group in the form of a carboxylate. This was demonstrated with polyProDOT derivatives that, following film casting, were hydrolyzed via dipping in a KOH solution.[179] IR spectra of the polymers show no indications of residual carbonyl groups after hydrolysis. The polarity of the alcohol groups on the polymer results in aqueous compatibility in a manner similar to the solvent resistant (SR) method discussed in Chapter 7. However, the materials previously prepared via this route were only examined as electrochromic materials and the overall redox behavior was not explored.

PE_2 has been found to be a useful material and basic structure for redox active applications including electrochromism and charge storage.[144] As shown in Scheme 8.2, the majority of PE_2 by mass (54%) is side chains. As discussed in Chapter 3, if the side chains were not taken into account this material would have a mass capacitance higher than electropolymerized PEDOT. The SR carboxylic acid-based side chains described in Chapter 7, hereafter referred to as SR-COOH, also consist of a large amount (47%) of side chains (or side groups to be more accurate) that do not directly contribute to charge storage. Using the method developed by Reeves and described above, a PE_2 polymer has been prepared so that upon hydrolysis only alcohol groups remain. This results in only ~12% of the polymers mass consisting of side chains. This not only increases the mass capacitance of the film but also allows for aqueous compatibility.

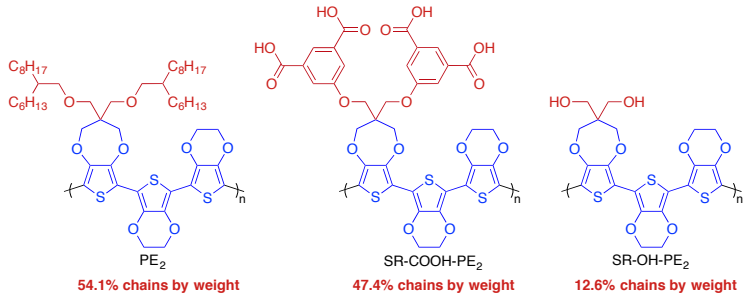

Scheme 8.2. The structures of several ProDOT-EDOT$_2$ copolymers bearing hydrocarbon of solvent resistant side chains.

8.3 Development of SR-OH-PE$_2$

The carboxylic acid side chain was prepared via oxidation of 2-hexyldecanol using Jones Reagent, as shown in Figure 8.1. The side chain was then attached via a S_N2 reaction with ProDOT(CH_2Br)$_2$ to yield the new ProDOT monomer using a previously described route.[193] This material was then brominated with NBS using THF as the solvent. It should be noted that the bromination was initially attempted in DMF, although this did not result in the desired product because of the low solubility of the long non-polar side chains in the highly polar DMF.

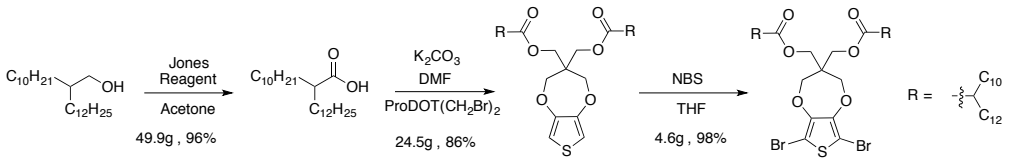

Figure 8.1. Synthesis of the dibromo ProDOT monomer bearing ester side chains.

As outlined in Figure 8.2, DHAP was performed using typical conditions to yield the poly(ProDOT(2-decyltetradecyl ester)$_2$-EDOT$_2$) materials, DTe-PE$_2$. This material is then converted post-processing to the solvent resistant alcohol (SR-OH) form via

immersion in hot KOH/methanol for 30 minutes. Full synthetic details can be found in section 8.6.

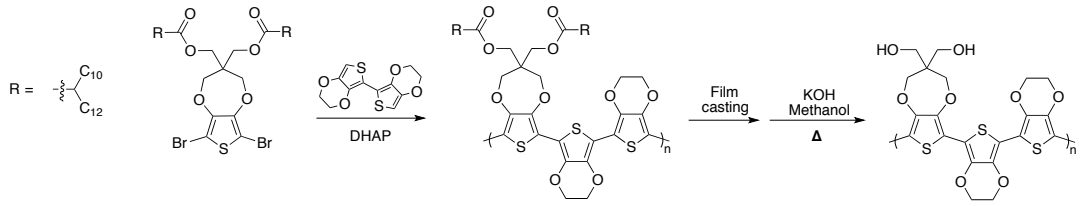

Figure 8.2. DHAP of the ProDOT monomer with biEDOT to yield DTe-PE_2 and the following film casting and hydrolysis to generate SR-OH-PE_2.

8.4 Redox Behavior Analysis of PE_2 Polymers

8.4.1 Onset of Oxidation and Cyclic Voltammetry

From the onset of oxidation for the polymers it can be seen that changing the nature of the side chains has a significant affect on the material properties. As seen in Figure 8.3a and numerically in Table 8.1, there is little difference between the original PE_2 and the SR-COOH precursor polymer, Te- PE_2. This result is consistent with the PE polymers discussed in Chapter 7. However, unlike the previous result, SRCOOH-PE_2 also shows approximately the same onset in both organic and aqueous electrolytes. The new DTe-PE_2 has a 90 mV lower oxidation potential than PE_2 bearing only alkyl side chains. Upon hydrolysis the onset lowers by an additional 10 mV in LiBTI/PC and by 100 mV in LiBTI/H_2O, as shown in Figure 8.3b. This significant reduction in the onset can be attributed to a reduction in steric bulk around the ProDOT unit.

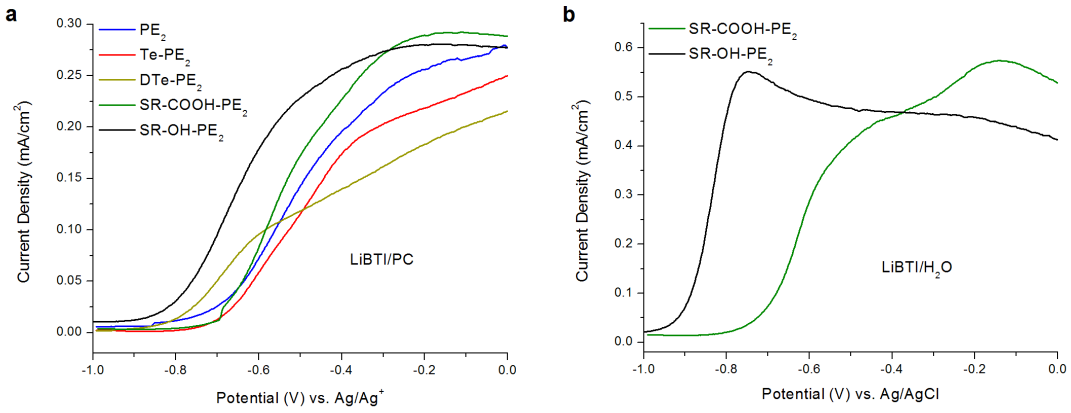

Figure 8.3. DPV traces of films of the PE_2 polymers on glassy carbon button electrodes in a) 0.5 M LiBTI/PC or b) LiBTI/H_2O.

Table 8.1. Onset of oxidation (by DPV) and mass capacitance at a scan rate of 50 mV/s of films of the PE_2 polymers on glassy carbon button electrodes in 0.5 M LiBTI/PC.

	PE_2[a]	Te-PE_2[a]	DTe-PE_2[a]	SR-COOH-PE_2 (PC)[a]	SR-COOH-PE_2 (H_2O)[b]	SR-OH-PE_2 (PC)[a]	SR-OH-PE_2 (H_2O)[b]
Onset of Oxidation (V)	-0.70	-0.70	-0.79	-0.69	-0.70	-0.80	-0.89
Mass Capacitance (F/g)	66 ± 10	56 ± 7	53 ± 3	39 ± 5	50. ± 2	156 ± 21	144 ± 46

a) Measured in LiBTI/PC using a Ag/Ag^+ reference. b) Measured in LiBTI/H_2O using a Ag/AgCl reference

CV traces of the PE_2 and Te-PE_2 polymers (Figure 8.4 a) are similar, as with the DPV onsets. The SR-COOH-PE_2 has more pseudocapacitive behavior because of the

relative independence of the current from approximately -0.5 to 0.8 V. Both the DTe-PE_2 and SR-OH-PE_2 have exceptionally broad redox responses, with the SR-OH polymer storing slightly more charge.

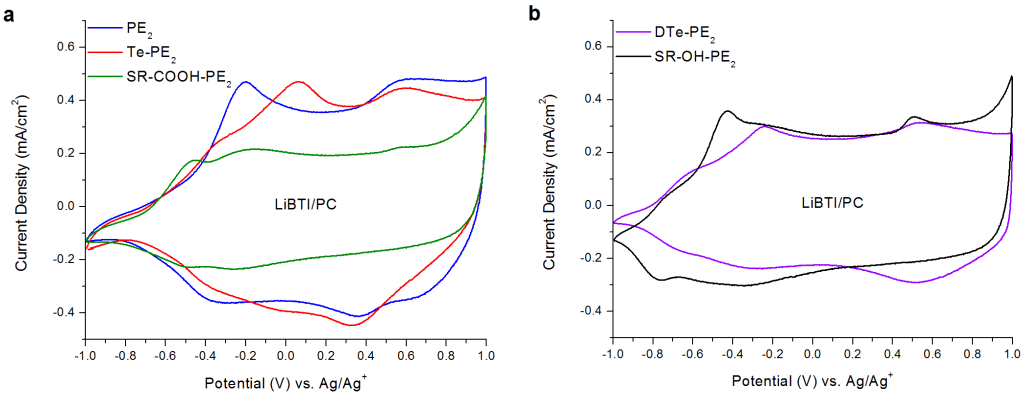

Figure 8.4. CV traces of films of the PE_2 polymers on glassy carbon button electrodes in 0.5 M LiBTI/PC.

From the charge required to switch the films the mass capacitance can be calculated, as listed in Table 8.1. The variation in mass capacitance (in F/g) is larger than initially expected based on the CVs. The mass of the SR-OH polymer was calculated by assuming full cleavage of the side chains upon hydrolysis based on the IR data previously discussed. The removal of the side chain not only broadens the electroactive response, thereby increasing capacitance directly, but results in a significantly reduction in mass. The calculated capacitance of SR-OH-PE_2 (156 F/g) in LiBTI/PC is higher than what has been obtained for electropolymerized PEDOT (92 F/g)[187] and is close to the theoretical maximum for PEDOT of 210 F/g (assuming a doping level of 0.33, as discussed in Chapter 1). Comparing the SR-COOH-PE_2 and SR-OH-PE_2 in LiBTI/H_2O, as shown in Figure 8.5, depicts the difference in electroactivity from the reduced steric bulk. The

increase in CV area (the charge) along with the reduced polymer mass results in a capacitance 144 F/g in an aqueous electrolyte. Additionally, the current independence from approximately -0.7 to 0.8 V makes this polymer an ideal material for SC devices.

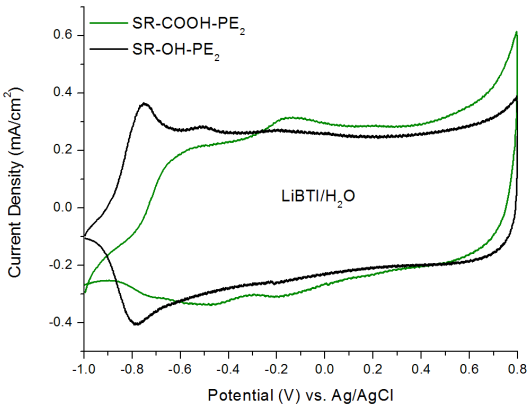

Figure 8.5. CV traces of films of two SR PE_2 polymers on glassy carbon button electrodes in 0.5 M LiBTI/H_2O.

8.4.2 Mass Capacitance and Switching Speed

Plotting the mass capacitance as a function of scan rate allows for an assessment of the relative switching speeds of the polymers. All of the polymers switching in an organic electrolyte show significant drops in capacitance at higher scan rates, as shown in Figures 8.6a and 8.6b. SR-COOH-PE_2, while having a lower initial capacitance, has the least decrease at higher scan rates, possibly because of the acid groups allowing efficient ion transport. The capacitance of SR-OH-PE_2 at 10 V/s is comparable to the SR-COOH at 50 mV/s because of the initially high values. In an aqueous electrolyte, the SR-OH-PE_2 has a ~3x high capacitance than the SR-COOH-PE_2. This does come at the cost of a high deviation between samples, as seen in Figure 8.7.

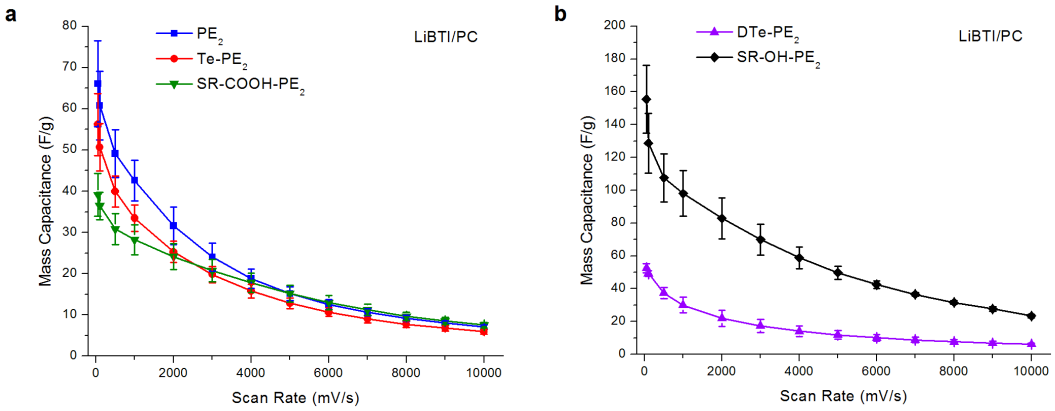

Figure 8.6. Mass capacitance as a function of scan rate of films of the PE_2 polymers on glassy carbon button electrodes in 0.5 M LiBTI/PC.

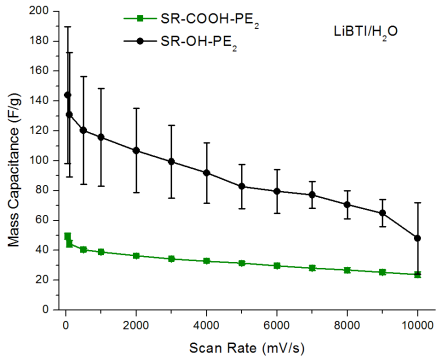

Figure 8.7. Mass capacitance as a function of scan rate of films of the two SR PE_2 polymers on glassy carbon button electrodes in 0.5 M LiBTI/H_2O.

8.5 Conclusions

The use of the cleavable side chains presented here increases the mass capacitance and the broadness of the redox response. The SR-OH-PE_2 can be switched in either organic or aqueous electrolytes and has the lowest onset of oxidation of any of the materials presented in this thesis and is approximately the same electropolymerized PEDOT. The mass capacitance of SR-OH-PE_2 is higher than electropolymerized PEDOT with the benefit of processablility. The SR-OH-PE_2 films have larger deviations between films, although the exact cause is currently unknown and requires further study.

8.6 Experimental Details

8.6.1 Materials

$Pd(OAc)_2$ (98 %, Strem Chemicals), pivalic acid (99 %, Sigma), K_2CO_3 (anhydrous, Oakwood Products), 18-Crown-6 (99 %, Acros), diethyldithiocarbamic acid diethylammonium salt (97 %, TCI America), KOH (Technical Grade, Fisher Scientific), and pTSA (monohydrate, 98 %, Alfa Aesar) were used as received. 2-Decyltetradecyl alcohol (97) was purchased from Sigma and was used as received. Chromium(VI) oxide was purchased from Alfa Aesar and used as received. Anhydrous DMF was obtained from AMD. Lithium bis-(trifluoromethanesulfonyl)imide (LiBTI, 0.5 M, Acros Organics,

99%) in either propylene carbonate (PC, Acros Organics, 99.5%, purified using a solvent purification system from Vacuum Atmospheres) or deionized H_2O (from a EMD Millipore Milli-Q Ultrapure Water system) was used as the electrolyte. DMAc (HPLC grade, Alfa Aesar) was filtered through a pad of alumina (basic, Sigma Aldrich) and degassed by argon bubbling prior to use. The electrochemical measurements on films were performed in a three-electrode cell setup using either a Ag/Ag^+ reference electrode (10 mM $AgNO_3$ in 0.5 M LiBTI/ACN, $E_{1/2}$ for ferrocene: 70 mV) for organic electrolytes or a Ag/AgCl reference electrode (1M KCl, purchased from CH Instruments, Inc.), the counter electrode was a platinum flag

8.6.2 Instrumentation

The cyclic voltammetry was performed on an EG&G PAR (model 273A) potentiostat/galvanostatic under CorrWare control. The ^{1}H-NMR (64 scans) spectra were collected on a Bruker 700 MHz instrument using $C_2D_2Cl_4$ as a solvent at a temperature of 323K. The molecular weight and dispersity of the polymer were obtained using a THF GPC at 35°C calibrated vs. polystyrene standards.

8.6.3 Monomer Synthesis

2-Decyltetradecyl acid

56.38 grams of CrO_3 was dissolved in 56 mL of concentrated sulfuric acid and 170 mL of DI water to make a chromic acid solution. Separately, 50.002 grams of 2-decyltetradecanol was dissolved in ~280 mL of acetone in a 1 L RB flask. The RB was

cooled in an ice bath and an addition funnel was added to the setup. Using the addition funnel, chromic acid solution was added over several hours. The initially clear acetone solution turned red and then gradually tuned green during this addition. The reaction was allowed to stir overnight at ambient temperature. The reaction was then quenched by the slow addition of isopropanol. The solution was extracted using 1:1 diethyl ether:ethyl acetate and washed with several litters of DI water. The organic layer was filtered through celite and the solvent removed under vacuum. This resulted in a pale green oil that solidified under vacuum overnight. The product was obtained as 49.9 grams (96%) of a wax like solid. ^{1}H-NMR (700 MHz, $CDCl_3$, 25 ^{o}C) δ 2.38 (m, 2H), 1.67-1.45 (m, 12H), 1.38-1.23 (br, 34H), 0.91 (t, 6H, J = 7.1 Hz). ^{13}C-NMR (176 MHz, $CDCl_3$, 25 ^{o}C) δ 44.99, 32.25, 31.93, 31.92, 29.75, 29.66, 29.60, 29.56, 29.48, 29.37, 29.35, 27.39, 22.70, 14.13. HRMS (EI) m/z calcd for $C_{24}H_{48}O_2$ 368.3654, found 368.3664.

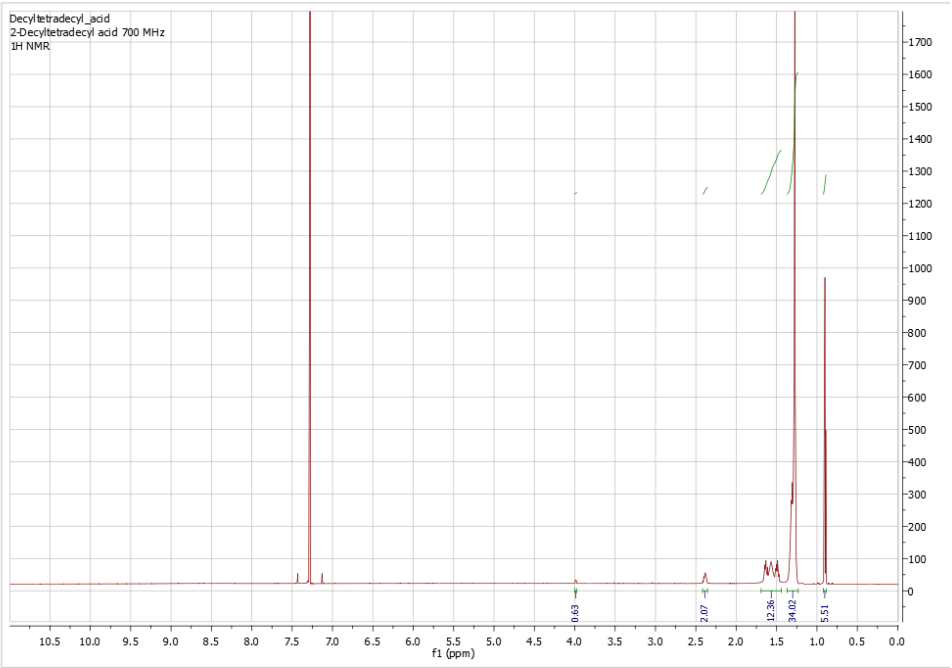

ProDOT(DcTd)$_2$

10.0 grams (1 eq.) of ProDOT($CH_2Br)_2$ was placed in a 500 mL RB flask along with 27.22 grams (2.5 eq.) 2-decyltetradecyl acid and 16.165 grams (4 eq.) of K_2CO_3. This setup was placed under argon with a reflux condenser and 194 mL of anhydrous DMF was added. The reaction was heated to 100 ^oC overnight. The mixture was cooled to ambient temperature and extracted using diethyl ether and DI water followed by brine. The organic layer was filtered through a pad of neutral silica (washing with diethyl ether) and the solvent was removed under vacuum. The resulting oil was purified by column chromatography using 10% ethyl acetate in hexanes. The product was obtained as 24.5 grams (86%) of a viscous oil. ^{1}H-NMR (700 MHz, $CDCl_3$, 25 ^oC) δ 6.49 (s, 2H), 4.21 (s, 4H), 4.06 (s, 4H), 2.35 (m, 2H), 1.59 (br, m, 5H), 1.47 (br, m, 5H), 1.35-1.20 (br, 88H), 0.90 (t, 14H, J = 7.1 Hz). ^{13}C-NMR (176 MHz, $CDCl_3$, 25 ^oC) δ 175.95, 149.05, 105.43, 72.55, 62.53, 46.01, 45.70, 32.30, 31.95, 29.71, 29.68, 29.66, 29.64, 29.59, 29.50, 29.39, 29.36, 22.71, 14.14. MS (MALDI) m/z calcd for $C_{57}H_{104}O_6S$ 916.76, found 939.83 (M + Na).

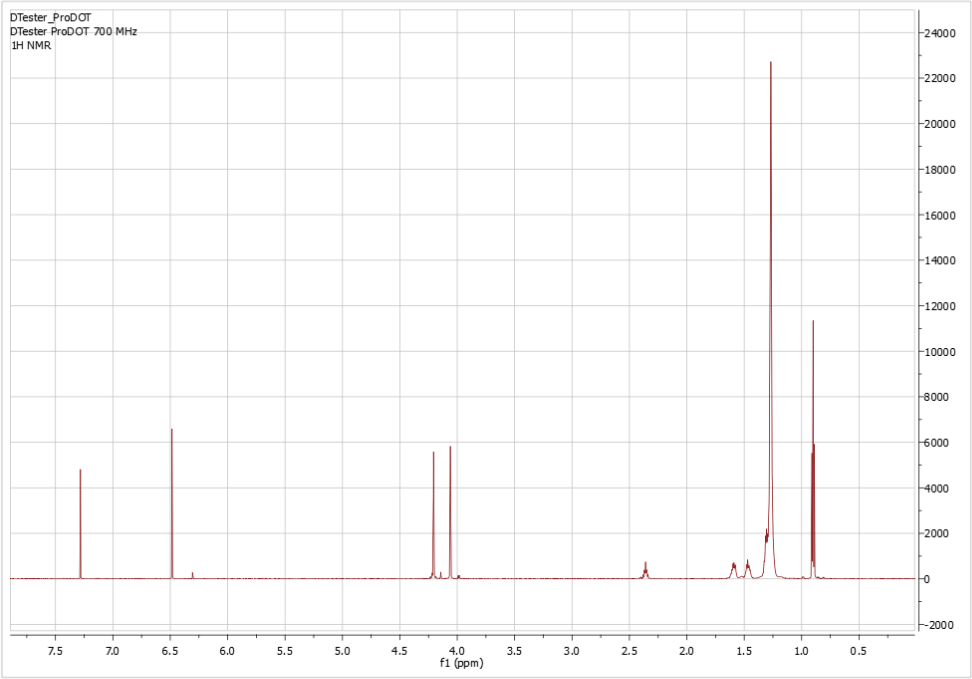

ProDOT(DcTd)$_2$-Br$_2$

4.008 grams (1 eq.) of ProDOT(DcTd)$_2$ was placed in a 250 mL RB flask and 44 mL of anhydrous THF was added. Under argon, 1.939 grams (2.5 eq.) of NBS was slowly added. The reaction mixture was cover with aluminum foil and allowed to stir overnight. The reaction mixture was filtered through a pad of neutral silica (washing with diethyl ether) and the solvent was removed under vacuum. The resulting oil was purified via column chromatography using hexanes. The product was obtained as 4.6 grams (98 %) of a viscous oil. ^{1}H-NMR (700 MHz, $CDCl_3$, 25 ^{o}C) δ 4.22 (s, 4H), 4.14 (s, 4H), 2.36 (m, 3H), 1.67-1.53 (br, m, 7H), 1.52-1.42 (br, m, 5H), 1.35-1.20 (br, 96H), 0.90 (t, 14H, J = 7.1 Hz). ^{13}C-NMR (176 MHz, $CDCl_3$, 25 ^{o}C) δ 175.85, 146.40, 91.48, 73.06, 62.40, 46.20, 45.67, 32.26, 31.94, 29.72, 29.69, 29.67, 29.64, 29.59, 29.51, 29.39, 29.37, 27.49,

22.71, 14.14. MS (MALDI) m/z calcd for $C_{57}H_{102}O_6SBr_2$ 1074.58, found 1097.64 (M + Na).

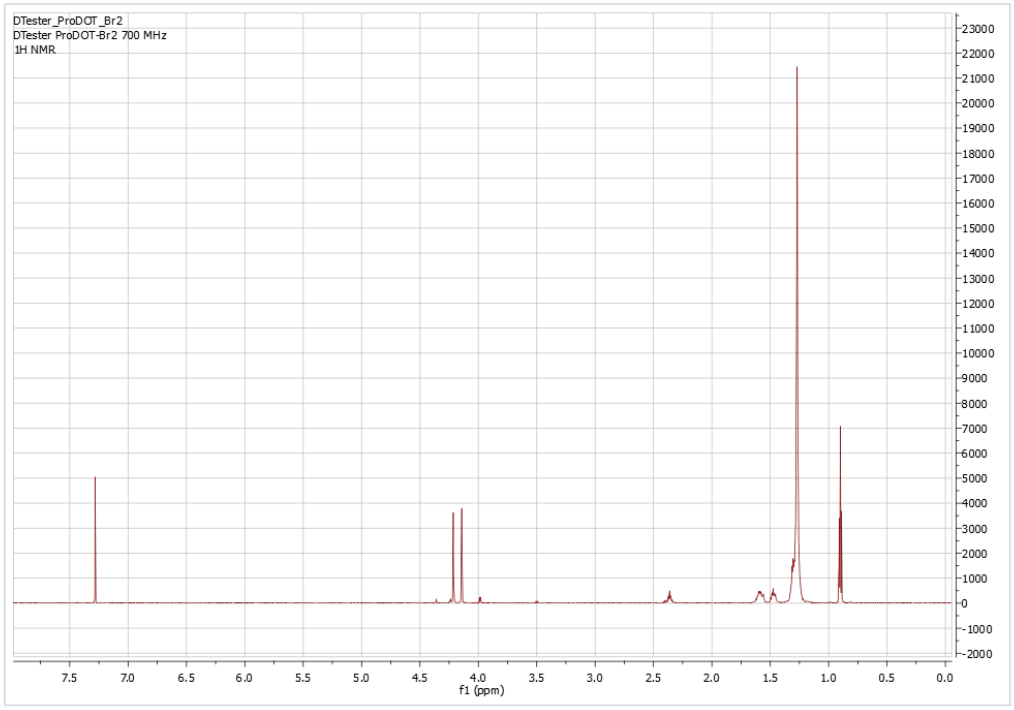

8.6.4 Polymer Synthesis

Te-PE_2

The dibromo-tetraester ProDOT and biEDOT monomers were prepared via previously published methods[33,37] The dibromo-tetraester ProDOT monomer (1.0002 g, 0.869 mmol, 1 eq.), biEDOT (0.2453 g, 0.869 mmol, 1 eq.) and a stir bar were added to a 38 mL pressure vessel. $Pd(OAc)_2$ (4.1 mg, 2 mol %), pivalic acid (26.7 mg, 0.3 eq.), K_2CO_3 (0.3004g, 2.5 eq.), and *N,N*-dimethylacetamide (8.7 mL, 0.2 M, degassed by argon bubbling) were added to the reaction vessel which was then sealed under argon and

placed in a preheated oil bath (140 °C) and stirred overnight (~14 hours). The reaction was then cooled to ambient temperature and 5 mL of chloroform was added. The solution was precipitated into methanol and the resulting mixture was filtered into a Soxhlet thimble. The polymer was purified via Soxhlet extraction using methanol, acetone, hexanes, and then dissolving into chloroform. Approximately 20 mg of a palladium scavenger (diethylammonium diethyldithiocarbamate) and of 18-crown-6 were added to the polymer/chloroform solution, which was concentrated under vacuum using a rotary evaporator and then stirred for 2 hours at 40°C, and subsequently precipitated into methanol. After filtering, washing with methanol, and drying the precipitate under vacuum, 0.7193 g (yield: 65.1%) of organic soluble PE_2 (OS-PE_2) was obtained as a blue/black solid. It should be noted that upon drying the polymer becomes partially oxidized from air. This is reversible using hydrazine or electrochemical reduction. ^{1}H-NMR (800 MHz, $C_2D_2Cl_4$, 50 °C) δ8.28 (t, 2H), 7.89 (d, 4H), 4.46 (t, 4H), 4.27 (m, 8H), 3.95 (d, 2H), 1.74 (s, 4H), 1.50-1.03 (m, 45H), 1.00-0.53 (br, 31H). Anal. calcd. for $C_{69}H_{90}O_{16}S_3$ C:65.17, H:7.13, S:7.56, Found C:63.53, H:6.74, S:8.20. M_n = 16.0 kDa, Đ = 1.33 (THF GPC at 35˚C vs. polystyrene standards).

WS-PE_2

75 mL of methanol, 8.4 g KOH (to make a 2 M solution) and a stir bar were added to a 100 mL round bottom flask. The solution was degassed via argon bubbling for 30 minutes. Te-PE_2 (304.5 mg) was then added and the round bottom flask was equipped with a reflux condenser. The flask was covered in argon and heated to reflux (65 °C) for 24 hours while vigorously stirring. After cooling to room temperature, the suspension was poured into a break apart funnel with a 0.45-micron filter and washed with methanol,

chloroform, and diethyl ether. The resulting solid polymer was dried under vacuum overnight to yield 176.5 mg (75.7% recovery) of the water-soluble version of the copolymer (WS-PE_2) as a dark purple powder.

SR-PE_2

Films of the WS-PE_2 were converted to the SR form by dipping into 1 M pTSA/methanol for 10 minutes, as previously described in Chapter 7.

DTe-PE_2

The ProDOT$(DcTd)_2$-Br_2 monomer (0.7848 g, 1.00 equiv) and biEDOT (0.2060 g, 1.00 equiv) were added to a 38 mL pressure vessel equipped with a stir bar. $Pd(OAc)_2$ (6 mg, 0.02 equiv), pivalic acid (28 mg, 0.3 equiv), K_2CO_3 (0.2811 g, 2.5 equiv), and DMAc (7.3 mL, 0.2 M, degassed with argon) were added, and the vessel was sealed under argon and placed in an oil bath at 140 °C and stirred overnight (~14 h). The reaction was cooled to ambient temperature, the reaction mixture was precipitated into methanol, and the resulting solution/precipitate was filtered into a Soxhlet thimble. The polymer was purified via Soxhlet extraction using methanol, and acetone and then dissolved in hexanes. Approximately 40 mg of a palladium scavenger (diethylammonium diethyldithiocarbamate) and ~40 mg of 18-crown-6 were added to the polymer/chloroform solution which was concentrated under vacuum and then stirred for 2 h at 40 °C and subsequently precipitated into methanol. After filtering, washing with methanol, and drying the precipitate under vacuum, 0.328 g (38%) of a dark blue solid was obtained. ^{1}H-NMR (700 MHz, $C_2D_2Cl_4$, 50 °C) δ 4.55-4.18 (m, 12H), 1.9-1.55 (br), -1.55-1.09 (be), 1.03-0.84 (br). Anal. Calcd for $C_{69}H_{110}O_{10}S_3$ C 69.31, H 9.27, S 8.04,

Found C 66.75, H 8.81, S 8.89 M_n = 16.8 kDa, Đ = 1.1 (THF GPC at 35 °C vs polystyrene standards)

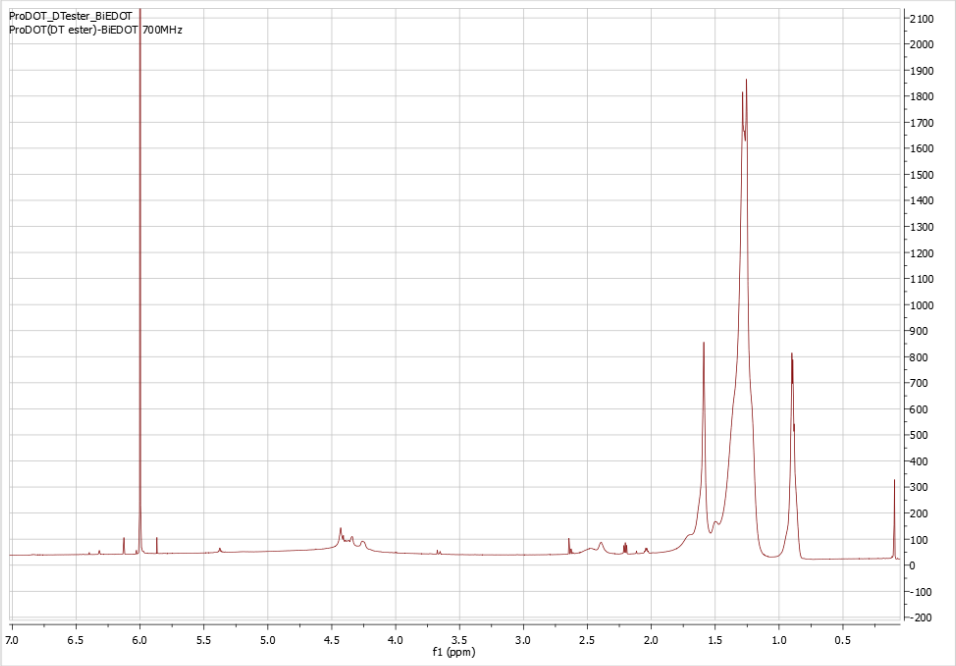

SR-OH-PE_2

Following drop casting of DTe-PE_2 films on glassy carbon button electrodes, the electrodes were suspended in a solution of 2 M KOH in methanol at 55 °C for 30 minutes. The electrodes were then washed with methanol and allowed to air dry.

CHAPTER 9. CONCLUSIONS, PERSPECTIVE, PATH FORWARD, AND FURTHER QUESTIONS

"It's the questions we can't answer that teach us the most. They teach us how to think. If you give a man an answer, all he gains is a little fact. But give him a question and he'll look for his own answers."

- Patrick Rothfuss, The Wise Man's Fear

9.1 Conclusions and Perspective

The research presented in this thesis has created state of the art electrochromic and capacitive polymer that possess superior properties, processablility, and versatility than previously explored materials. Systematic repeat unit manipulation has lead to design rule for new charge storage materials. Analysis of interring interactions and electronic characteristics has resulted in an understanding of electrical conductivity in soluble XDOT copolymers. Chemical functionalization/defunctionalization of XDOT copolymers tunes the bulk polarity of polymer films as results in exceptionally rapid redox switching in environmentally benign, aqueous electrolytes.

While the primarily applications discussed are charge storage and electrochromism, it is clear that the exceptional properties of the polymers discussed will be of impact to other areas in organic electronics research. The use of the WS/SR polymers in organic

bioelectronic devices is of particular interest due to the rapid and stable aqueous redox switching along with the tunable capacitance of ProDOT/EDOT copolymers. The work presented can be considered in four aspects: charge storage, electrochromism, electrical conductivity, and water solubility/compatibility.

9.1.1 Charge Storage

The development of a soluble PEDOT analogue, in the form of a PE_2 repeat unit, has set a new standard for polymer charge storage and lead to an overall change in how this research is performed. It has moved us from electropolymerized films to solution processable materials and further developments have brought about aqueous processing and compatibility. Tuning of the polymer side chains resulted in redox active films using benign aqueous electrolytes including human serum and NaCl/water with superior switching speed ion transport compared to typical soluble or electropolymerized polymers. These materials have now been used successfully in flexible SC devices and work is underway in using them in interdigitated micro SCs and bioelectronic applications. The results and materials in Chapters 3, 7, and 8 can be used to make better SC devices, however, it is unclear how to improve upon these structures for p-type materials. The next step for SC research must lie in, either n-type polymers so that Type IV SCs can be built, or in device engineering to demonstrate the true potential of these materials. While Type III devices are fundamentally interesting, I do not believe that a single material can be designed for p and n-type charge storage without compromising various figures of merit, such as fill factor.

9.1.2 Electrochromism

In terms of EC properties, the materials presented here are on par with state of the art electrochromic materials. The fact that organic soluble PE_2, in the neutral state, is optically indistinguishable from PEDOT to a standard observer makes it an ideal candidate for color mixing and other applications requiring a blue to color neutral ECP. The addition of XDOSs and PheDOTs to the list of usable monomers for EC research is expected to allow for finer color tuning and control of redox properties. Moreover, these units provide specific properties that can be used in designing new materials. The inherently lower band-gap of XDOS containing polymers can be used as a simple way to red-shift the absorbance of materials without additional structural modifications. The exceptional stability of PheDOT with or without bromides allows for larger, more complex monomers to be prepared without degradation due to excessive electron density. The higher onset of oxidation of PheDOT containing polymers compared to the corresponding EDOT polymer, while not useful for SCs, is also convenient for polymer blending as, ideally, all of the polymers in the blend should oxidize at approximately the same potential to minimize intermediate colors being observed.

9.1.3 Electrical Conductivity of Polymers

The results of Chapter 6 show that a high electrical conductivity (~250 S/cm for PE_2) can be obtained from p-doped soluble dioxythiophene based polymers that are relatively amorphous. This conductivity, combined with the low onset of oxidation, allows PE_2 to act as a color neutral electrode materials for other ECPs. Further studies will be needed to determine if the Seebeck coefficient and/or the electrical conductivity

can be raised to a level that would allow them to compete with PEDOT:PSS. These results have lead to increased interest in the conductivity of soluble XDOT-based polymers when doped.

9.1.4 Water Solubility/Compatibility

The WS/SR and SR-OH polymers discussed in Chapters 7 and 8, respectively, are of interest not only as SC and EC materials, but also in applications ranging from ion sensing to controlled drug release to transparent electrode materials. The higher solution conductance and lower toxicity of aqueous compared to organic electrolytes is useful for almost any redox active application. Currently, the WS/SR polymers are being evaluated for plasmonic resonance tuning of metal nano-structures in collaboration with the Tsukruk group.

9.2 Path Forward

9.2.1 PheDOTs

The PheDOT unit can now be used as a standard monomer for designing electrochromic materials. Soluble PheDOTs are a possible next step as it could act as a planar solubilizing unit for ordered conjugated polymers. However, these alkylated PheDOTs are tedious to make using the present synthetic method. Alkylated 3,4-vinylenedioxythiophenes (VDOTs) are another possible next step. This could yield highly ordered and planar materials, like the soluble PheDOT, that are of interest for EC,

SC, and conductivity research. The structures of soluble PheDOT and VDOT homopolymers are shown in Figure 9.1.

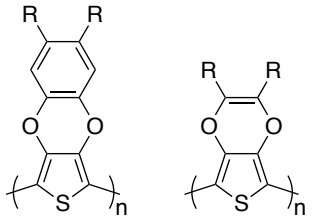

Figure 9.1. Structures of polyPheDOT (left) and polyVDOT (right) functionalized with solubilizing side chains.

9.2.2 XDOSs

The results of Chapter 5 show that copolymers containing XDOSs behave as expected based on the literature and that these polymers can be prepared using our typical methods. New XDOS homopolymers would be useful as electropolymerized XDOSs can have peak absorbances between 700 and 800 nm, removing the need to have a donor-acceptor polymer in black or brown ECP blends and thereby increasing the integrated contrast across the visible. The problem with using these materials is the low yield (around 30%) and toxic chemicals required to form 3,4-dimethoxyselenophene. One route to avoid this is to start from sodium selenide (from the reaction of sodium metal with elemental selenium) and ethyl bromoacetate followed by a Hinsberg Condensation to form the 2,5-diester selenophene-3,4-diol. This compound has been reported in the literature and could be used as a convenient starting point to many different XDOS monomers. While this route consists of more steps than the typical procedure, I believe it will result in an easier synthesis overall.

9.2.3 Conductivity in Soluble XDOT Polymers

The high electrical conductivity of PF_6^- doped PE_2 is promising for soluble XDOT materials for transparent electrodes and OTE materials. The WS/SR polymers are an obvious next set of materials to be studied as the side chains can be manipulated without altering the degree of polymerization, thereby removing a variable. New polymers with more rigid structures, from either non-bonding interactions or fused ring, and improved packing could also be a route to high conductivity materials. Finally, the dopant (both cation and anion) clearly plays a significant role in the resulting conductivity. However, finding the optimal dopant for a given system is not a trivial task and one should not assume that the conditions and dopants that are best for one system would give the highest conductivity for another. Two dopants of great interest are ferric hexafluorophosphate ($Fe(PF_6)_3$) and thianthrinium perchlorate. Unfortunately, $Fe(PF_6)_3$ has not been reported (in the absence of ligands) and thianthrinium perchlorate is shock sensitive and can explode. Perhaps the solution lies in the development of new dopants.

9.2.4 WS/SR Polymers

The WS/SR method presented in Chapter 7 shows great promise for many applications. SR-PE_2 is currently being investigated as a pseudocapacitive materials in flexible Type I supercapacitor devices using a non-woven carbon nanotube textile as the electrodes. Additionally, another one of these polymers (SR-ProDOT-DMP) is being evaluated as an active material for OECTs because of the combination of aqueous compatibility, efficient ionic mobility, and relatively high capacitance. The treatment of these films with different metal ions (such as Ca^{2+}) could be useful for tuning the

thermoelectric properties of the films, however, no experiments in this area have been performed.

9.2.5 Cleavable Side Chains

Investigation of these materials in SC devices is needed to compare them to electropolymerized devices. Spectroelectrochemistry and chronoabsorptiometry could be used to compare the ion mobility of the SR-OH films to the SR-COOH. Possibly the most interesting use of SR-OH-PE_2 is as a transparent electrode material. It is expected that the electrical conductivity of this material upon doping will be higher than the ~250 S/cm of PF_6^- doped PE_2 bearing alkyl side chains as most of the insulating side chains are removed. Moreover, once polymer is cast and the side chains are cleaved other materials can be coated over it using a variety of methods without disrupting the SR-OH-PE_2 electrode.

9.3 Further Questions

9.3.1 Why is the CPE used in Chapter 7 redox inactive?

Interestingly, the CPE forms of PE and PE_2 are redox inactive in typical organic electrolytes ($TBAPF_6$ or LiBTI in PC or ACN) and ionic liquids (neat or in PC). This is unexpected as other CPEs not only switch but also can self-dope. While I am unsure how to probe this phenomenon, impedance spectroscopy is a logical first step. Additionally, comparable CPEs with carboxylate side chains that are not attached to a phenyl may

provide incite. Another question is weather the CPE form will be inactive if it is formed via hydrolysis of the film after casting rather than in the bulk followed by isolation.

9.3.2 How do we make Near-IR absorbing ECPs without acceptors?

ECPs that absorb long wavelength visible or IR light are important for applications ranging from display to sensors to IR antennas, Currently, acceptor units (such as benzothiadiazole or isoindigo) must be used to make long wavelength absorbing EC polymers. These units reduce the contrast of the resulting film and tends to cause trailing of the bipolaron band into the visible region, resulting in blue/gray oxidized states. While it should be noted that electropolymerized PEDOS-C_6 absorbs out to ~800 nm (λ_{max} = 763 nm), a soluble analog of this compound has not been produced and a route to further lowering of the bandgap in an all donor system is not known. Perhaps a poly(3,6-dioxyselenoselenophene) such as the structure proposed in Figure 9.2.

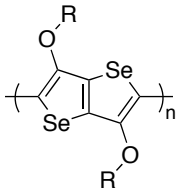

Figure 9.2. Proposed structure of a poly(3,6-dioxyselenoselenophene).

9.3.3 How can decarboxylative coupling be used as a polymerization method?

In 2010 Frank Arroyave reported a Pd catalyzed decarboxylative coupling between Aryl bromides and dioxypyrrole carboxylates to prepare trimers and expanded

on this work the following year with the synthesis of additional trimers and pentimers in moderate to high yield.[204,205] One can imagine that this reaction could be performed using a dibromide and a dicarboxylate to form dioxypyrrole copolymers, as shown in Figure 9.3. However, both Frank and I have failed to achieve this. The reactions conditions reported by Frank do not result in high weight polymers and my few attempts to modify the procedure have yielded inconsistent results. If this method were optimized for polymerizations it would allow for a simple route to high-gap ECPs and could solve several long-term problems in the EC field. How do we tune the reaction so that coupling occurs fast enough and at a low enough temperature that the XDOP does not decarboxylate, either through palladium catalysis of thermally, without a corresponding coupling event?

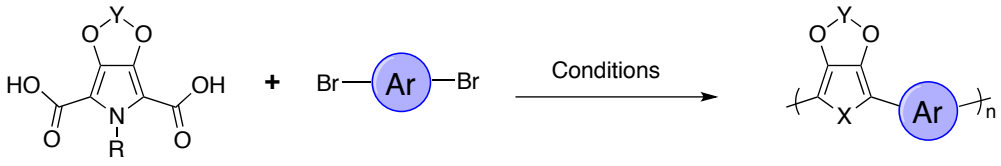

Figure 9.3. A proposed decarboxylative polymerization of an aryl dibromide and a dicarboxylic acid XDOP.

9.3.4 Why does DHAP not proceed efficiently with highly electron rich compounds?

DHAP is known to require different conditions (primarily different solvent polarity) based on the electron richness of the monomers used and, as discussed in chapter 2, a universal set of reaction conditions have yet to be developed. While some electron rich molecules, such as XDOTs and XDOSs, undergo C-H activation readily,

others do not. For example, 3,4-Propylenedioxypyrrole (ProDOP) and 3,4-ethylenedithiothiophene (EDTT), both of which are more electron rich than EDOT, do not undergo Pd catalyzed C-H activation efficiently. Why? As XDOPs undergo decarboxylative and Suzuki cross-coupling reactions, we can conclude that the problem lies in the C-H activation step and not in the reductive elimination step. One possibility is a lack of coordination of between the electron rich unit and the Pd(II) catalyst. Another is a decrease in the acidity of the C-H bond because of the increased electron richness of the ring, thereby halting the catalytic cycle at the concerted Metalation deprotonation step. I do not expect increasing the polarity of the solvent will provide the needed push for the reaction although addition of a stronger based (such as KO*t*Bu) could be a route to explore. Could additives that promote C-H activation be used the reaction media to drive the reaction? Maybe a bimetallic catalyst system, with one metal for the C-H activation followed by transmetalation to the Pd(II)?

"'I checked it very thoroughly,' said the computer, 'and that quite definitely is the answer. I think the problem, to be quite honest with you, is that you've never actually known what the question is.'"

- Douglas Adams, The Hitchhiker's Guide to the Galaxy

"Look at me still talking when there's science to do."

- Jonathan Coulton, Still Alive

REFERENCES

1. Ito, T.; Shirakawa, H.; Ikeda, S., Simultaneous polymerization and formation of polyacetylene film on the surface of concentrated soluble Ziegler-type catalyst solution. *J. Polym. Sci. Polym. Chem. Ed.* **1974,** *12* (1), 11-20.

2. Chiang, C. K.; Druy, M. A.; Gau, S. C.; Heeger, A. J.; Louis, E. J.; MacDiarmid, A. G.; Park, Y. W.; Shirakawa, H., Synthesis of highly conducting films of derivatives of polyacetylene, (CH)x. *J. Am. Chem. Soc.* **1978,** *100* (3), 1013-1015.

3. Chien, J. C. W., *Polyacetylene: Chemistry, Physics, and Material Science*. 1st ed. ed.; Academic Press Inc., Orlando, FL: 1984.

4. Heeger, A. J., Semiconducting and Metallic Polymers: The Fourth Generation of Polymeric Materials (Nobel Lecture). *Angew. Chem., Int. Ed.* **2001,** *40* (14), 2591-2611.

5. Rasmussen, S. C., Electrically Conducting Plastics: Revising the History of Conjugated Organic Polymers. In *100+ Years of Plastics. Leo Baekeland and Beyond*, American Chemical Society: 2011; Vol. 1080, pp 147-163.

6. Rasmussen, S. C., On the origin of 'synthetic metals'. *Mater. Today* **2016,** *19*, 244-245.

7. Runge, F., F., *Poggendorfs Ann. Phys. u. Chem.* **1834,** *31*, 513-524.

8. McNeill, R.; Siudak, R.; Wardlaw, J.; Weiss, D., Electronic conduction in polymers. I. The chemical structure of polypyrrole. *Aust. J. Chem.* **1963,** *16* (6), 1056-1075.

9. Bolto, B. A.; McNeill, R.; Weiss, D., Electronic conduction in polymers. III. Electronic properties of polypyrrole. *Aust. J. Chem.* **1963,** *16* (6), 1090-1103.

10. Armour, M.; Davies, A. G.; Upadhyay, J.; Wassermann, A., Colored electrically conducting polymers from furan, pyrrole, and thiophene. *Journal of Polymer Science Part A-1: Polymer Chemistry* **1967,** *5* (7), 1527-1538.

11. Shirakawa, H., The Discovery of Polyacetylene Film: The Dawning of an Era of Conducting Polymers (Nobel Lecture). *Angew. Chem., Int. Ed.* **2001,** *40* (14), 2574-2580.

12. Heeger, A. J., Semiconducting polymers: the Third Generation. *Chem. Soc. Rev.* **2010,** *39* (7), 2354-2371.

13. Müller, H. K.; Hocker, J.; Menke, K.; Ehinger, K.; Roth, S., Long-term conductivity decrease in polyacetylene samples. *Synth. Met.* **1985,** *10* (4), 273-280.

14. Elschner, A., Kirchmeyer, S., W. Lövenich, W., Merker, U., Reuter K., *PEDOT: Principles and Applications of an Intrinsically Conducting Polymer*. CRC Press: Boca Raton, FL, USA, **2011**.

15. Jonas, F., W. Schmidtberg, W., Bayer AG patent, **1988**.

16. Heywang, G.; Jonas, F., Poly(alkylenedioxythiophene)s—new, very stable conducting polymers. *Adv. Mater.* **1992,** *4* (2), 116-118.

17. Dietrich, M.; Heinze, J.; Heywang, G.; Jonas, F., Electrochemical and spectroscopic characterization of polyalkylenedioxythiophenes. *J. Electroanal. Chem.* **1994,** *369* (1), 87-92.

18. Kumar, A.; Welsh, D. M.; Morvant, M. C.; Piroux, F.; Abboud, K. A.; Reynolds, J. R., Conducting poly (3, 4-alkylenedioxythiophene) derivatives as fast electrochromics with high-contrast ratios. *Chem. Mater.* **1998,** *10* (3), 896-902.

19. Gaupp, C. L.; Welsh, D. M.; Reynolds, J. R., Poly (ProDOT-Et_2): A High-Contrast, High-Coloration Efficiency Electrochromic Polymer. *Macromol. Rapid Commun.* **2002,** *23* (15), 885-889.

20. Reeves, B. D.; Grenier, C. R. G.; Argun, A. A.; Cirpan, A.; McCarley, T. D.; Reynolds, J. R., Spray Coatable Electrochromic Dioxythiophene Polymers with High Coloration Efficiencies. *Macromolecules* **2004,** *37* (20), 7559-7569.

21. Roquet, S.; Leriche, P.; Perepichka, I.; Jousselme, B.; Levillain, E.; Frere, P.; Roncali, J., 3,4-Phenylenedioxythiophene (PheDOT): a novel platform for the synthesis of planar substituted [small pi]-donor conjugated systems. *J. Mater. Chem.* **2004,** *14* (9), 1396-1400.

22. Perepichka, I. F.; Roquet, S.; Leriche, P.; Raimundo, J.-M.; Frère, P.; Roncali, J., Electronic Properties and Reactivity of Short-Chain Oligomers of 3,4-Phenylenedioxythiophene (PheDOT). *Chemistry – A European Journal* **2006,** *12* (11), 2960-2966.

23. Leriche, P.; Blanchard, P.; Frere, P.; Levillain, E.; Mabon, G.; Roncali, J., 3,4-Vinylenedioxythiophene (VDOT): a new building block for thiophene-based pi-conjugated systems. *Chem Commun* **2006,** (3), 275-7.

24. Pettersson, L. A. A.; Carlsson, F.; Inganäs, O.; Arwin, H., Spectroscopic ellipsometry studies of the optical properties of doped poly(3,4-ethylenedioxythiophene): an anisotropic metal. *Thin Solid Films* **1998,** *313–314* (0), 356-361.

25. Groenendaal, L.; Jonas, F.; Freitag, D.; Pielartzik, H.; Reynolds, J. R., Poly(3,4-ethylenedioxythiophene) and Its Derivatives: Past, Present, and Future. *Adv. Mater.* **2000,** *12* (7), 481-494.

26. Roncali, J.; Blanchard, P.; Frere, P., 3,4-Ethylenedioxythiophene (EDOT) as a versatile building block for advanced functional π-conjugated systems. *J. Mater. Chem.* **2005,** *15* (16), 1589-1610.

27. Spencer, H. J.; Skabara, P. J.; Giles, M.; McCulloch, I.; Coles, S. J.; Hursthouse, M. B., The first direct experimental comparison between the hugely contrasting properties of PEDOT and the all-sulfur analogue PEDTT by analogy with well-defined EDTT-EDOT copolymers. *J. Mater. Chem.* **2005,** *15* (45), 4783-4792.

28. Chance, R. R.; Brédas, J. L.; Silbey, R., Bipolaron transport in doped conjugated polymers. *Phys. Rev. B* **1984,** *29* (8), 4491-4495.

29. Aleshin, A.; Kiebooms, R.; Menon, R.; Heeger, A. J., Electronic transport in doped poly (3,4-ethylenedioxythiophene) near the metal-insulator transition. *Synth. Met.* **1997,** *90* (1), 61-68.

30. Bubnova, O.; Khan, Z. U.; Wang, H.; Braun, S.; Evans, D. R.; Fabretto, M.; Hojati-Talemi, P.; Dagnelund, D.; Arlin, J.-B.; Geerts, Y. H.; Desbief, S.; Breiby, D. W.; Andreasen, J. W.; Lazzaroni, R.; Chen, W. M.; Zozoulenko, I.; Fahlman, M.; Murphy, P. J.; Berggren, M.; Crispin, X., Semi-metallic polymers. *Nat. Mater.* **2014,** *13* (2), 190-194.

31. Brédas, J.; Thémans, B.; Fripiat, J.; André, J.; Chance, R., Highly conducting polyparaphenylene, polypyrrole, and polythiophene chains: An ab initio study of the geometry and electronic-structure modifications upon doping. *Phys. Rev. B* **1984,** *29* (12), 6761.

32. Heinze, J.; Frontana-Uribe, B. A.; Ludwigs, S., Electrochemistry of Conducting Polymers—Persistent Models and New Concepts. *Chemical Reviews* **2010,** *110* (8), 4724-4771.

33. Bredas, J.; Marder, S., The WSPC Reference on Organic electronics: Organic semiconductors, vol. 1 Basic concepts, vol. 2 Fundamental aspects of materials and applications. World Scientific, Singapore: 2015.

34. Bubnova, O.; Crispin, X., Towards polymer-based organic thermoelectric generators. *Energy & Environmental Science* **2012,** *5* (11), 9345-9362.

35. Beljonne, D.; Cornil, J.; Sirringhaus, H.; Brown, P.; Shkunov, M.; Friend, R.; Bredas, J., Optical signature of delocalized polarons in conjugated polymers. *Adv. Funct. Mater.* **2001,** *11* (3), 229-234.

36. Lee, K.; Cho, S.; Park, S. H.; Heeger, A.; Lee, C.-W.; Lee, S.-H., Metallic transport in polyaniline. *Nature* **2006,** *441* (7089), 65-68.

37. Thomas, C., A. Donor-Acceptor Methods for Band Gap Reduction in Conjugated Polymers: The Role of Electron Rich Donor Heterocycles. University of Florida, **2002**.

38. Furukawa, Y., Electronic Absorption and Vibrational Spectroscopies of Conjugated Conducting Polymers. *The Journal of Physical Chemistry* **1996,** *100* (39), 15644-15653.

39. Bredas, J. L.; Street, G. B., Polarons, bipolarons, and solitons in conducting polymers. *Acc. Chem. Res.* **1985,** *18* (10), 309-315.

40. Dyer, A. L.; Thompson, E. J.; Reynolds, J. R., Completing the Color Palette with Spray-Processable Polymer Electrochromics. *ACS Appl. Mater. Interfaces* **2011,** *3* (6), 1787-1795.

41. Dyer, A. L.; Craig, M. R.; Babiarz, J. E.; Kiyak, K.; Reynolds, J. R., Orange and Red to Transmissive Electrochromic Polymers Based on Electron-Rich Dioxythiophenes. *Macromolecules* **2010,** *43* (10), 4460-4467.

42. Amb, C. M.; Kerszulis, J. A.; Thompson, E. J.; Dyer, A. L.; Reynolds, J. R., Propylenedioxythiophene (ProDOT)-phenylene copolymers allow a yellow-to-transmissive electrochrome. *Polymer Chemistry* **2011,** *2* (4), 812-814.

43. Kerszulis, J. A.; Amb, C. M.; Dyer, A. L.; Reynolds, J. R., Follow the Yellow Brick Road: Structural Optimization of Vibrant Yellow-to-Transmissive Electrochromic Conjugated Polymers. *Macromolecules* **2014,** *47* (16), 5462-5469.

44. Amb, C. M.; Beaujuge, P. M.; Reynolds, J. R., Spray-Processable Blue-to-Highly Transmissive Switching Polymer Electrochromes via the Donor–Acceptor Approach. *Adv. Mater.* **2010,** *22* (6), 724-728.

45. Diaz, A.; Kanazawa, K. K.; Gardini, G. P., Electrochemical polymerization of pyrrole. *J. Chem. Soc., Chem. Commun.* **1979,** (14), 635-636.

46. Poverenov, E.; Li, M.; Bitler, A.; Bendikov, M., Major Effect of Electropolymerization Solvent on Morphology and Electrochromic Properties of PEDOT Films. *Chem. Mater.* **2010,** *22* (13), 4019-4025.

47. Winther-Jensen, B.; West, K., Vapor-Phase Polymerization of 3,4-Ethylenedioxythiophene: A Route to Highly Conducting Polymer Surface Layers. *Macromolecules* **2004,** *37* (12), 4538-4543.

48. Meng, H.; Perepichka, D. F.; Wudl, F., Facile Solid-State Synthesis of Highly Conducting Poly(ethylenedioxythiophene). *Angew. Chem., Int. Ed.* **2003,** *42* (6), 658-661.

49. Azarian, D.; Dua, S. S.; Eaborn, C.; Walton, D. R., Reactions of organic halides with R3 MMR3 compounds (M= Si, Ge, Sn) in the presence of tetrakis (triarylphosphine) palladium. *J. Organomet. Chem.* **1976,** *117* (3), C55-C57.

50. Kosugi, M.; Sasazawa, K.; Shimizu, Y.; Migita, T., Reactions of allyltin compounds Iii. Allylation of aromatic halides With allyltributyltin in the presence of tetrakis (triphenylphosphine) palladium (0). *Chem. Lett.* **1977,** *6* (3), 301-302.

51. Milstein, D.; Stille, J., A general, selective, and facile method for ketone synthesis from acid chlorides and organotin compounds catalyzed by palladium. *J. Am. Chem. Soc.* **1978,** *100* (11), 3636-3638.

52. Miyaura, N.; Yanagi, T.; Suzuki, A., The palladium-catalyzed cross-coupling reaction of phenylboronic acid with haloarenes in the presence of bases. *Synth. Commun.* **1981,** *11* (7), 513-519.

53. King, A. O.; Okukado, N.; Negishi, E.-i., Highly general stereo-, regio-, and chemo-selective synthesis of terminal and internal conjugated enynes by the Pd-catalysed reaction of alkynylzinc reagents with alkenyl halides. *J. Chem. Soc., Chem. Commun.* **1977,** (19), 683-684.

54. Braga, A. A.; Morgon, N. H.; Ujaque, G.; Maseras, F., Computational characterization of the role of the base in the Suzuki− Miyaura cross-coupling reaction. *J. Am. Chem. Soc.* **2005,** *127* (25), 9298-9307.

55. Akira, K.; Taeko, I.; Minoru, Y.; Ryu-ichi, S.; Toru, T.; Toshiaki, S., Arylation and Vinylation Reactions of Benzo[b]furan via Organopalladium Intermediates. *Bull. Chem. Soc. Jpn.* **1973,** *46* (4), 1220-1225.

56. Alberico, D.; Scott, M. E.; Lautens, M., Aryl−Aryl Bond Formation by Transition-Metal-Catalyzed Direct Arylation. *Chemical Reviews* **2007,** *107* (1), 174-238.

57. Tetsuya, S.; Masahiro, M., Catalytic Direct Arylation of Heteroaromatic Compounds. *Chem. Lett.* **2007,** *36* (2), 200-205.

58. Ishiyama, T.; Takagi, J.; Yonekawa, Y.; Hartwig, J. F.; Miyaura, N., Iridium-Catalyzed Direct Borylation of Five-Membered Heteroarenes by Bis (pinacolato) diboron: Regioselective, Stoichiometric, and Room Temperature Reactions. *Adv. Synth. Catal.* **2003,** *345* (9-10), 1103-1106.

59. Ackermann, L.; Lygin, A. V., Ruthenium-catalyzed direct C–H bond arylations of heteroarenes. *Org. Lett.* **2011,** *13* (13), 3332-3335.

60. Ueda, K.; Amaike, K.; Maceiczyk, R. M.; Itami, K.; Yamaguchi, J., β-Selective C–H Arylation of Pyrroles Leading to Concise Syntheses of Lamellarins C and I. *J. Am. Chem. Soc.* **2014,** *136* (38), 13226-13232.

61. Jafarpour, F.; Rahiminejadan, S.; Hazrati, H., Triethanolamine-Mediated Palladium-Catalyzed Regioselective C-2 Direct Arylation of Free NH-Pyrroles. *The Journal of Organic Chemistry* **2010,** *75* (9), 3109-3112.

62. Okamoto, K.; Zhang, J.; Housekeeper, J. B.; Marder, S. R.; Luscombe, C. K., C–H Arylation Reaction: Atom Efficient and Greener Syntheses of π-Conjugated Small Molecules and Macromolecules for Organic Electronic Materials. *Macromolecules* **2013,** *46* (20), 8059-8078.

63. Wang, Q.; Takita, R.; Kikuzaki, Y.; Ozawa, F., Palladium-Catalyzed Dehydrohalogenative Polycondensation of 2-Bromo-3-hexylthiophene: An Efficient Approach to Head-to-Tail Poly(3-hexylthiophene). *J. Am. Chem. Soc.* **2010,** *132* (33), 11420-11421.

64. Morin, P.-O.; Bura, T.; Sun, B.; Gorelsky, S. I.; Li, Y.; Leclerc, M., Conjugated Polymers à la Carte from Time-Controlled Direct (Hetero)Arylation Polymerization. *ACS Macro Letters* **2015,** *4* (1), 21-24.

65. Pouliot, J.-R.; Grenier, F.; Blaskovits, J. T.; Beaupré, S.; Leclerc, M., Direct (Hetero)arylation Polymerization: Simplicity for Conjugated Polymer Synthesis. *Chemical Reviews* **2016,** *116* (22), 14225-14274.

66. Rudenko, A. E.; Thompson, B. C., Optimization of direct arylation polymerization (DArP) through the identification and control of defects in polymer structure. *Journal of Polymer Science Part A: Polymer Chemistry* **2015,** *53* (2), 135-147.

67. Rudenko, A. E.; Thompson, B. C., Influence of the Carboxylic Acid Additive Structure on the Properties of Poly(3-hexylthiophene) Prepared via Direct Arylation Polymerization (DArP). *Macromolecules* **2015,** *48* (3), 569-575.

68. Kuwabara, J.; Yasuda, T.; Choi, S. J.; Lu, W.; Yamazaki, K.; Kagaya, S.; Han, L.; Kanbara, T., Direct Arylation Polycondensation: A Promising Method for the Synthesis of Highly Pure, High-Molecular-Weight Conjugated Polymers Needed for Improving the Performance of Organic Photovoltaics. *Adv. Funct. Mater.* **2014,** *24* (21), 3226-3233.

69. Kuwabara, J.; Yamazaki, K.; Yamagata, T.; Tsuchida, W.; Kanbara, T., The effect of a solvent on direct arylation polycondensation of substituted thiophenes. *Polymer Chemistry* **2015,** *6* (6), 891-895.

70. Broll, S.; Nübling, F.; Luzio, A.; Lentzas, D.; Komber, H.; Caironi, M.; Sommer, M., Defect Analysis of High Electron Mobility Diketopyrrolopyrrole Copolymers Made by Direct Arylation Polycondensation. *Macromolecules* **2015,** *48* (20), 7481-7488.

71. Matsidik, R.; Komber, H.; Sommer, M., Rational Use of Aromatic Solvents for Direct Arylation Polycondensation: C–H Reactivity versus Solvent Quality. *ACS Macro Letters* **2015,** *4* (12), 1346-1350.

72. Estrada, L. A.; Deininger, J. J.; Kamenov, G. D.; Reynolds, J. R., Direct (Hetero)arylation Polymerization: An Effective Route to 3,4-Propylenedioxythiophene-Based Polymers with Low Residual Metal Content. *ACS Macro Letters* **2013,** *2* (10), 869-873.

73. Kerszulis, J. A.; Johnson, K. E.; Kuepfert, M.; Khoshabo, D.; Dyer, A. L.; Reynolds, J. R., Tuning the painter's palette: subtle steric effects on spectra and colour in conjugated electrochromic polymers. *Journal of Materials Chemistry C* **2015,** *3* (13), 3211-3218.

74. Fujinami, Y.; Kuwabara, J.; Lu, W.; Hayashi, H.; Kanbara, T., Synthesis of Thiophene- and Bithiophene-Based Alternating Copolymers via Pd-Catalyzed Direct C–H Arylation. *ACS Macro Letters* **2012,** *1* (1), 67-70.

75. Grenier, F.; Aïch, B. R.; Lai, Y.-Y.; Guérette, M.; Holmes, A. B.; Tao, Y.; Wong, W. W. H.; Leclerc, M., Electroactive and Photoactive Poly[Isoindigo-alt-EDOT] Synthesized Using Direct (Hetero)Arylation Polymerization in Batch and in Continuous Flow. *Chem. Mater.* **2015,** *27* (6), 2137-2143.

76. Bura, T.; Blaskovits, J. T.; Leclerc, M., Direct (Hetero)arylation Polymerization: Trends and Perspectives. *J. Am. Chem. Soc.* **2016,** *138* (32), 10056-10071.

77. Hayashi, S.; Koizumi, T., Chloride-promoted Pd-catalyzed direct C–H arylation for highly efficient phosphine-free synthesis of π-conjugated polymers. *Polymer Chemistry* **2015,** *6* (28), 5036-5039.

78. Bura, T.; Morin, P.-O.; Leclerc, M., En Route to Defect-Free Polythiophene Derivatives by Direct Heteroarylation Polymerization. *Macromolecules* **2015,** *48* (16), 5614-5620.

79. Wakioka, M.; Takahashi, R.; Ichihara, N.; Ozawa, F., Mixed-Ligand Approach to Palladium-Catalyzed Direct Arylation Polymerization: Highly Selective Synthesis of π-Conjugated Polymers with Diketopyrrolopyrrole Units. *Macromolecules* **2017,** *50* (3), 927-934.

80. Odian, G., *Principles of Polymerization*. Wiley: **2004**.

81. Dudnik, A. S.; Aldrich, T. J.; Eastham, N. D.; Chang, R. P. H.; Facchetti, A.; Marks, T. J., Tin-Free Direct C–H Arylation Polymerization for High Photovoltaic Efficiency Conjugated Copolymers. *J. Am. Chem. Soc.* **2016,** *138* (48), 15699-15709.

82. Gobalasingham, N. S.; Noh, S.; Thompson, B. C., Palladium-catalyzed oxidative direct arylation polymerization (Oxi-DArP) of an ester-functionalized thiophene. *Polymer Chemistry* **2016,** *7* (8), 1623-1631.

83. Guo, Q.; Jiang, R.; Wu, D.; You, J., Rapid Access to 2,2′-Bithiazole-Based Copolymers via Sequential Palladium-Catalyzed C–H/C–X and C–H/C–H Coupling Reactions. *Macromol. Rapid Commun.* **2016,** *37* (9), 794-798.

84. Guo, Q.; Wu, D.; You, J., Oxidative Direct Arylation Polymerization Using Oxygen as the Sole Oxidant: Facile, Green Access to Bithiazole-Based Polymers. *ChemSusChem* **2016,** *9* (19), 2765-2768.

85. Gobalasingham, N. S.; Pankow, R. M.; Thompson, B. C., Synthesis of random poly(hexyl thiophene-3-carboxylate) copolymers via oxidative direct arylation polymerization (oxi-DArP). *Polymer Chemistry* **2017,** *8* (12), 1963-1971.

86. Grenier, F.; Goudreau, K.; Leclerc, M., Robust Direct (Hetero)arylation Polymerization in Biphasic Conditions. *J. Am. Chem. Soc.* **2017,** *139* (7), 2816-2824.

87. Brousse, T., Bélanger, D.,; Long, J., W., To Be or Not To Be Pseudocapacitive? *J. Electrochem. Soc.* **2015,** *162* (5), A5185-A5189.

88. Österholm, A. M.; Shen, D. E.; Dyer, A. L.; Reynolds, J. R., Optimization of PEDOT Films in Ionic Liquid Supercapacitors: Demonstration As a Power Source for Polymer Electrochromic Devices. *ACS Appl. Mater. Interfaces* **2013,** *5* (24), 13432-13440.

89. Bredas, J.-L., Mind the gap! *Materials Horizons* **2014,** *1* (1), 17-19.

90. Stalder, R.; Mei, J.; Subbiah, J.; Grand, C.; Estrada, L. A.; So, F.; Reynolds, J. R., n-Type conjugated polyisoindigos. *Macromolecules* **2011,** *44* (16), 6303-6310.

91. Kerszulis, J. A. Reading the Rainbow: Tailoring the Properties of Electrochromic Polymers. Georgia Institute of Technology, **2014**.

92. Bulloch, R. H., Redox-Active Conjugated Polymers for Electrochromic and Supercapacitor Applications. Georgia Institute of Technology, **2015**.

93. Schanda, J., CIE Colorimetry. In *Colorimetry*, John Wiley & Sons, Inc.: **2007**.

94. Wyszecki, G., Stiles, W., S., *Color Science: Concepts and Methods, Quantitative Data and Formulae*. 2nd ed. ed.; Wiley: Hoboken, NJ, USA, **2000**.

95. Sharma, G., Bala, R., *Digital Color Imaging Handbook*. 1.7.2 ed.; CRC Press: **2002**.

96. Mahy, M.; Van Eycken, L.; Oosterlinck, A., Evaluation of Uniform Color Spaces Developed after the Adoption of CIELAB and CIELUV. *Color Research & Application* **1994,** *19* (2), 105-121.

97. Bulloch, R. H.; Kerszulis, J. A.; Dyer, A. L.; Reynolds, J. R., An Electrochromic Painter's Palette: Color Mixing via Solution Co-Processing. *ACS Appl. Mater. Interfaces* **2015,** *7* (3), 1406-1412.

98. Lübbe, E., *Colours in the Mind - Colour Systems in Reality: A formula for colour saturation*. Books on Demand: **2010**.

99. Schon, T. B.; McAllister, B. T.; Li, P.-F.; Seferos, D. S., The rise of organic electrode materials for energy storage. *Chem. Soc. Rev.* **2016,** *45* (22), 6345-6404.

100. Conway, B. E., *Electrochemical Supercapacitors: Scientific Fundamentals and Technological Applications*. Springer US: **1999**.

101. Bryan, A. M.; Santino, L. M.; Lu, Y.; Acharya, S.; D'Arcy, J. M., Conducting Polymers for Pseudocapacitive Energy Storage. *Chem. Mater.* **2016,** *28* (17), 5989-5998.

102. Winter, M.; Brodd, R. J., What Are Batteries, Fuel Cells, and Supercapacitors? *Chemical Reviews* **2004,** *104* (10), 4245-4270.

103. Skotheim, T. A.; Reynolds, J., *Handbook of Conducting Polymers.* 3rd ed., Vol 2, CRC Press: **2007**.

104. Huang, Q.; Wang, D.; Zheng, Z., Textile-Based Electrochemical Energy Storage Devices. *Adv. Energy Mater.* **2016,** *6* (22).

105. Ertas, M.; Walczak, R. M.; Das, R. K.; Rinzler, A. G.; Reynolds, J. R., Supercapacitors Based on Polymeric Dioxypyrroles and Single Walled Carbon Nanotubes. *Chem. Mater.* **2012,** *24* (3), 433-443.

106. Estrada, L. A.; Liu, D. Y.; Salazar, D. H.; Dyer, A. L.; Reynolds, J. R., Poly[Bis-EDOT-Isoindigo]: An Electroactive Polymer Applied to Electrochemical Supercapacitors. *Macromolecules* **2012,** *45* (20), 8211-8220.

107. Chiang, C. K.; Fincher, C. R.; Park, Y. W.; Heeger, A. J.; Shirakawa, H.; Louis, E. J.; Gau, S. C.; MacDiarmid, A. G., Electrical Conductivity in Doped Polyacetylene. *Phys. Rev. Lett.* **1977,** *39* (17), 1098-1101.

108. Kim, Y. H.; Sachse, C.; Machala, M. L.; May, C.; Müller-Meskamp, L.; Leo, K., Highly Conductive PEDOT:PSS Electrode with Optimized Solvent and Thermal Post-Treatment for ITO-Free Organic Solar Cells. *Adv. Funct. Mater.* **2011,** *21* (6), 1076-1081.

109. Cho, B.; Park, K. S.; Baek, J.; Oh, H. S.; Koo Lee, Y.-E.; Sung, M. M., Single-crystal poly (3, 4-ethylenedioxythiophene) nanowires with ultrahigh conductivity. *Nano Lett.* **2014,** *14* (6), 3321-3327.

110. Patel, S. N.; Glaudell, A. M.; Kiefer, D.; Chabinyc, M. L., Increasing the thermoelectric power factor of a semiconducting polymer by doping from the vapor phase. *ACS Macro Letters* **2016,** *5* (3), 268-272.

111. Lu, J.; Pinto, N. J.; MacDiarmid, A. G., Apparent dependence of conductivity of a conducting polymer on an electric field in a field effect transistor configuration. *J. Appl. Phys.* **2002,** *92* (10), 6033-6038.

112. Jonas, F.; Heywang, G., Technical applications for conductive polymers. *Electrochim. Acta* **1994,** *39* (8–9), 1345-1347.

113. Sun, K.; Zhang, S.; Li, P.; Xia, Y.; Zhang, X.; Du, D.; Isikgor, F.; Ouyang, J., Review on application of PEDOTs and PEDOT:PSS in energy conversion and storage devices. *J. Mater. Sci.: Mater. Electron.* **2015,** *26* (7), 4438-4462.

114. Krafft, W.; Jonas, F.; Muys, B.; Qintens, D. Antistatic plastic materials. DE4211461A1, **1993**.

115. Pei, Q.; Zuccarello, G.; Ahlskog, M.; Inganäs, O., Electrochromic and highly stable poly(3,4-ethylenedioxythiophene) switches between opaque blue-black and transparent sky blue. *Polymer* **1994,** *35* (7), 1347-1351.

116. Gustafsson, J. C.; Liedberg, B.; Inganäs, O., In situ spectroscopic investigations of electrochromism and ion transport in a poly (3,4-ethylenedioxythiophene) electrode in a solid state electrochemical cell. *Solid State Ionics* **1994,** *69* (2), 145-152.

117. Chen, X.; Xing, K.-Z.; Inganäs, O., Electrochemically Induced Volume Changes in Poly(3,4-ethylenedioxythiophene). *Chem. Mater.* **1996,** *8* (10), 2439-2443.

118. Fabretto, M.; Zuber, K.; Hall, C.; Murphy, P., High Conductivity PEDOT Using Humidity Facilitated Vacuum Vapour Phase Polymerisation. *Macromol. Rapid Commun.* **2008,** *29* (16), 1403-1409.

119. Kumar, A.; Reynolds, J. R., Soluble Alkyl-Substituted Poly(ethylenedioxythiophenes) as Electrochromic Materials. *Macromolecules* **1996,** *29* (23), 7629-7630.

120. Stéphan, O.; Schottland, P.; Le Gall, P.-Y.; Chevrot, C.; Mariet, C.; Carrier, M., Electrochemical behaviour of 3, 4-ethylenedioxythiophene functionalized by a sulphonate group. Application to the preparation of poly(3, 4-ethylenedioxythiophene) having permanent cation-exchange properties. *J. Electroanal. Chem.* **1998,** *443* (2), 217-226.

121. Bubnova, O.; Khan, Z. U.; Malti, A.; Braun, S.; Fahlman, M.; Berggren, M.; Crispin, X., Optimization of the thermoelectric figure of merit in the conducting polymer poly (3, 4-ethylenedioxythiophene). *Nat. Mater.* **2011,** *10* (6), 429-433.

122. Argun, A. A.; Cirpan, A.; Reynolds, J. R., The first truly all-polymer electrochromic devices. *Adv. Mater.* **2003,** *15* (16), 1338-1341.

123. Jönsson, S. K. M.; Birgerson, J.; Crispin, X.; Greczynski, G.; Osikowicz, W.; Denier van der Gon, A. W.; Salaneck, W. R.; Fahlman, M., The effects of solvents on the morphology and sheet resistance in poly(3,4-ethylenedioxythiophene)–polystyrenesulfonic acid (PEDOT–PSS) films. *Synth. Met.* **2003,** *139* (1), 1-10.

124. Xuan, Y.; Sandberg, M.; Berggren, M.; Crispin, X., An all-polymer-air PEDOT battery. *Organic Electronics* **2012,** *13* (4), 632-637.

125. Kumar, A.; Kumar, A., Single step reductive polymerization of functional 3, 4-propylenedioxythiophenes via direct C–H arylation catalyzed by palladium acetate. *Polymer Chemistry* **2010,** *1* (3), 286-288.

126. Zhao, H.; Liu, C.-Y.; Luo, S.-C.; Zhu, B.; Wang, T.-H.; Hsu, H.-F.; Yu, H.-h., Facile Syntheses of Dioxythiophene-Based Conjugated Polymers by Direct C–H Arylation. *Macromolecules* **2012,** *45* (19), 7783-7790.

127. Padilla, J.; Österholm, A. M.; Dyer, A. L.; Reynolds, J. R., Process controlled performance for soluble electrochromic polymers. *Sol. Energy Mater. Sol. Cells* **2015,** *140*, 54-60.

128. L. D. Stroebel, R. D. Z., *The Focal Encyclopedia of Photography*. 3rd ed.; Focal Press: Boston, MA, USA, **1993**.

129. Kim, B. C.; Hong, J. Y.; Wallace, G. G.; Park, H. S., Recent progress in flexible electrochemical capacitors: electrode materials, device configuration, and functions. *Adv. Energy Mater.* **2015,** *5* (22).

130. Snook, G. A.; Kao, P.; Best, A. S., Conducting-polymer-based supercapacitor devices and electrodes. *J. Power Sources* **2011,** *196* (1), 1-12.

131. Stoller, M. D.; Ruoff, R. S., Best practice methods for determining an electrode material's performance for ultracapacitors. *Energy & Environmental Science* **2010,** *3* (9), 1294-1301.

132. Liu, D. Y.; Reynolds, J. R., Dioxythiophene-based polymer electrodes for supercapacitor modules. *ACS Appl. Mater. Interfaces* **2010,** *2* (12), 3586-3593.

133. Shen, D. E.; Estrada, L. A.; Österholm, A. M.; Salazar, D. H.; Dyer, A. L.; Reynolds, J. R., Understanding the effects of electrochemical parameters on the areal capacitance of electroactive polymers. *J. Mater. Chem. A* **2014,** *2* (20), 7509-7516.

134. Sotzing, G. A.; Reynolds, J. R.; Steel, P. J., Poly(3,4-ethylenedioxythiophene) (PEDOT) prepared via electrochemical polymerization of EDOT, 2,2′-Bis(3,4-ethylenedioxythiophene) (BiEDOT), and their TMS derivatives. *Adv. Mater.* **1997,** *9* (10), 795-798.

135. Li, H.; Fu, K.; Hagfeldt, A.; Grätzel, M.; Mhaisalkar, S. G.; Grimsdale, A. C., A Simple 3,4-Ethylenedioxythiophene Based Hole-Transporting Material for Perovskite Solar Cells. *Angew. Chem., Int. Ed.* **2014,** *53* (16), 4085-4088.

136. Grenier, C. R. G.; Pisula, W.; Joncheray, T. J.; Müllen, K.; Reynolds, J. R., Regiosymmetric Poly(dialkylphenylenedioxythiophene)s: Electron-Rich, Stackable π-Conjugated Nanoribbons. *Angew. Chem., Int. Ed.* **2007,** *46* (5), 714-717.

137. Shen, D. E.; Abboud, K. A.; Reynolds, J. R., Novel Bis-arylPheDOT Synthons for Electrochromic Polymers. *J. Macromol. Sci., Pure Appl. Chem.* **2009,** *47* (1), 6-11.

138. Chen, J.; Chen, B.-X.; Zhang, F.-S.; Yu, H.-J.; Ma, S.; Kuang, D.-B.; Shao, G.; Su, C.-Y., 3,4-Phenylenedioxythiophene (PheDOT) Based Hole-Transporting Materials for Perovskite Solar Cells. *Chem. Asian J.* **2016,** *11* (7), 1043-1049.

139. Spencer, H. J.; Berridge, R.; Crouch, D. J.; Wright, S. P.; Giles, M.; McCulloch, I.; Coles, S. J.; Hursthouse, M. B.; Skabara, P. J., Further evidence for spontaneous solid-state polymerisation reactions in 2,5-dibromothiophene derivatives. *J. Mater. Chem.* **2003,** *13* (9), 2075-2077.

140. Patra, A.; Wijsboom, Y. H.; Zade, S. S.; Li, M.; Sheynin, Y.; Leitus, G.; Bendikov, M., Poly(3,4-ethylenedioxyselenophene). *J. Am. Chem. Soc.* **2008,** *130* (21), 6734-6736.

141. Walczak, R. M.; Leonard, J. K.; Reynolds, J. R., Processable, Electroactive, and Aqueous Compatible Poly(3,4-alkylenedioxypyrrole)s through a Functionally Tolerant Deiodination Condensation Polymerization. *Macromolecules* **2008,** *41* (3), 691-700.

142. Matsidik, R.; Komber, H.; Luzio, A.; Caironi, M.; Sommer, M., Defect-free Naphthalene Diimide Bithiophene Copolymers with Controlled Molar Mass and High Performance via Direct Arylation Polycondensation. *J. Am. Chem. Soc.* **2015,** *137* (20), 6705-6711.

143. Österholm, A. M.; Shen, D. E.; Kerszulis, J. A.; Bulloch, R. H.; Kuepfert, M.; Dyer, A. L.; Reynolds, J. R., Four Shades of Brown: Tuning of Electrochromic Polymer Blends Toward High-Contrast Eyewear. *ACS Appl. Mater. Interfaces* **2015,** *7* (3), 1413-1421.

144. Ponder, J. F.; Österholm, A. M.; Reynolds, J. R., Designing a Soluble PEDOT Analogue without Surfactants or Dispersants. *Macromolecules* **2016,** *49* (6), 2106-2111.

145. Cao, K.; Shen, D. E.; Österholm, A. M.; Kerszulis, J. A.; Reynolds, J. R., Tuning Color, Contrast, and Redox Stability in High Gap Cathodically Coloring Electrochromic Polymers. *Macromolecules* **2016,** *49* (22), 8498-8507.

146. Patra, A.; Bendikov, M., Polyselenophenes. *J. Mater. Chem.* **2010,** *20* (3), 422-433.

147. Hollinger, J.; Gao, D.; Seferos, D. S., Selenophene Electronics. *Isr. J. Chem.* **2014,** *54* (5-6), 440-453.

148. Patra, A.; Bendikov, M.; Chand, S., Poly(3,4-ethylenedioxyselenophene) and Its Derivatives: Novel Organic Electronic Materials. *Acc. Chem. Res.* **2014,** *47* (5), 1465-1474.

149. Zade, S. S.; Bendikov, M., From Oligomers to Polymer: Convergence in the HOMO−LUMO Gaps of Conjugated Oligomers. *Org. Lett.* **2006,** *8* (23), 5243-5246.

150. Li, M.; Sheynin, Y.; Patra, A.; Bendikov, M., Tuning the Electrochromic Properties of Poly(alkyl-3,4-ethylenedioxyselenophenes) Having High Contrast Ratio and Coloration Efficiency. *Chem. Mater.* **2009,** *21* (12), 2482-2488.

151. Wijsboom, Y. H.; Patra, A.; Zade, S. S.; Sheynin, Y.; Li, M.; Shimon, L. J. W.; Bendikov, M., Controlling Rigidity and Planarity in Conjugated Polymers: Poly(3,4-ethylenedithioselenophene). *Angew. Chem., Int. Ed.* **2009,** *48* (30), 5443-5447.

152. Hollinger, J.; Jahnke, A. A.; Coombs, N.; Seferos, D. S., Controlling Phase Separation and Optical Properties in Conjugated Polymers through Selenophene−Thiophene Copolymerization. *J. Am. Chem. Soc.* **2010,** *132* (25), 8546-8547.

153. Gao, D.; Hollinger, J.; Seferos, D. S., Selenophene–Thiophene Block Copolymer Solar Cells with Thermostable Nanostructures. *ACS Nano* **2012,** *6* (8), 7114-7121.

154. Heeney, M.; Zhang, W.; Crouch, D. J.; Chabinyc, M. L.; Gordeyev, S.; Hamilton, R.; Higgins, S. J.; McCulloch, I.; Skabara, P. J.; Sparrowe, D.; Tierney, S., Regioregular poly(3-hexyl)selenophene: a low band gap organic hole transporting polymer. *Chem. Commun.* **2007,** (47), 5061-5063.

155. Hollinger, J.; Sun, J.; Gao, D.; Karl, D.; Seferos, D. S., Statistical Conjugated Polymers Comprising Optoelectronically Distinct Units. *Macromol. Rapid Commun.* **2013,** *34* (5), 437-441.

156. Cihaner, A., Poly(3,4-alkylenedioxyselenophene)s: Past, Present, and Future. *Synlett* **2015,** *26* (04), 449-460.

157. Atak, S.; İçli-Özkut, M.; Önal, A. M.; Cihaner, A., Soluble alkyl substituted poly(3,4-propylenedioxyselenophene)s: A new platform for optoelectronic materials. *J. Polym. Sci. A Polym. Chem.* **2011,** *49* (20), 4398-4405.

158. Karabay, B.; Pekel, L. C.; Cihaner, A., A Pure Blue to Highly Transmissive Electrochromic Polymer Based on Poly(3,4-propylenedioxyselenophene) with a High Optical Contrast Ratio. *Macromolecules* **2015,** *48* (5), 1352-1357.

159. Patra, A.; Agrawal, V.; Bhargav, R.; Shahjad; Bhardwaj, D.; Chand, S.; Sheynin, Y.; Bendikov, M., Metal Free Conducting PEDOS, PEDOT, and Their Analogues via an Unusual Bromine-Catalyzed Polymerization. *Macromolecules* **2015,** *48* (24), 8760-8764.

160. Lai, Y.-Y.; Tung, T.-C.; Liang, W.-W.; Cheng, Y.-J., Synthesis of Poly(3-hexylthiophene), Poly(3-hexylselenophene), and Poly(3-hexylselenophene-alt-3-hexylthiophene) by Direct C–H Arylation Polymerization via N-Heterocyclic Carbene Palladium Catalysts. *Macromolecules* **2015,** *48* (9), 2978-2988.

161. Tamba, S.; Fujii, R.; Mori, A.; Hara, K.; Koumura, N., Synthesis and Properties of Seleno-analog MK-organic Dye for Photovoltaic Cells Prepared by C–H

Functionalization Reactions of Selenophene Derivatives. *Chem. Lett.* **2011,** *40* (9), 922-924.

162. Rampon, D. S.; Wessjohann, L. A.; Schneider, P. H., Palladium-catalyzed direct arylation of selenophene. *J. Org. Chem.* **2014,** *79* (13), 5987-5992.

163. Skhiri, A.; Salem, R. B.; Soulé, J. F.; Doucet, H., Unprecedented Access to β-Arylated Selenophenes through Palladium-Catalysed Direct Arylation. *Chem. Eur. J.* **2017,** *23* (12), 2788-2791.

164. Bubnova, O.; Khan, Z. U.; Malti, A.; Braun, S.; Fahlman, M.; Berggren, M.; Crispin, X., Optimization of the thermoelectric figure of merit in the conducting polymer poly(3,4-ethylenedioxythiophene). *Nat. Mater.* **2011,** *10* (6), 429-433.

165. Kim, G.-H.; Shao, L.; Zhang, K.; Pipe, K. P., Engineered doping of organic semiconductors for enhanced thermoelectric efficiency. *Nat. Mater.* **2013,** *12* (8), 719-723.

166. Qi, Y.; Sajoto, T.; Barlow, S.; Kim, E.-G.; Brédas, J.-L.; Marder, S. R.; Kahn, A., Use of a High Electron-Affinity Molybdenum Dithiolene Complex to p-Dope Hole-Transport Layers. *J. Am. Chem. Soc.* **2009,** *131* (35), 12530-12531.

167. Qi, Y.; Sajoto, T.; Kröger, M.; Kandabarow, A. M.; Park, W.; Barlow, S.; Kim, E.-G.; Wielunski, L.; Feldman, L. C.; Bartynski, R. A.; Brédas, J.-L.; Marder, S. R.; Kahn, A., A Molybdenum Dithiolene Complex as p-Dopant for Hole-Transport Materials: A Multitechnique Experimental and Theoretical Investigation. *Chem. Mater.* **2009,** *22* (2), 524-531.

168. Geiger, W. E., Electrochemistry of Cycloaddition Products of Olefins with Nickel Dithiolenes: A Reinvestigation of the Reduction of the 1:1 Adduct between Ni(S2C2(CF3)2)2 and Norbornadiene. *Inorg. Chem.* **2002,** *41* (1), 136-139.

169. Wang, K.; Patil, A. O.; Zushma, S.; McConnachie, J. M., Ethylene oligomerization using nickel dithiolene complexes Ni(S2C2R2)2 (R = Ph, CF3) and the crystal structure of Ni[S2C2(CF3)2]2. *J. Inorg. Biochem.* **2007,** *101* (11–12), 1883-1890.

170. King, R. B., Organosulfur Derivatives of the Metal Carbonyls. III. The Reaction between Molybdenum Hexacarbonyl and Bis-(trifluoromethyl)-dithietene. *Inorg. Chem.* **1963,** *2* (3), 641-642.

171. Welsh, D. M.; Kumar, A.; Meijer, E. W.; Reynolds, J. R., Enhanced Contrast Ratios and Rapid Switching in Electrochromics Based on Poly(3,4-propylenedioxythiophene) Derivatives. *Adv. Mater.* **1999,** *11* (16), 1379-1382.

172. Rivnay, J.; Owens, R. M.; Malliaras, G. G. The Rise of Organic Bioelectronics. *Chem. Mater*. **2014**, 26, 679−685.

173. Rivnay, J.; Inal, S.; Collins, B. A.; Sessolo, M.; Stavrinidou, E.; Strakosas, X.; Tassone, C.; Delongchamp, D. M.; Malliaras, G. G. Structural control of mixed ionic and electronic transport in conducting polymers. *Nat. Commun*. **2016**, 7, 11287.

174. Neo, W. T.; Ye, Q.; Chua, S.-J.; Xu, J. Conjugated polymer-based electrochromics: Materials, device fabrication and application prospects. *J. Mater. Chem. C* **2016**, 4, 7364−7376.

175. Cai, G.; Wang, J.; Lee, P. S. Next-Generation Multifunctional Electrochromic Devices. *Acc. Chem. Res*. **2016**, 49, 1469−1476.

176. Nielsen, C. B.; Giovannitti, A.; Sbircea, D.-T.; Bandiello, E.; Niazi, M. R.; Hanifi, D. A.; Sessolo, M.; Amassian, A.; Malliaras, G. G.; Rivnay, J.; McCulloch, I. Molecular Design of Semiconducting Polymers for High-Performance Organic Electrochemical Transistors. *J. Am. Chem. Soc*. **2016**, 138, 10252−10259.

177. Patil, A. O.; Ikenoue, Y.; Wudl, F.; Heeger, A. J. Water soluble conducting polymers. *J. Am. Chem. Soc*. **1987**, 109, 1858−1859.

178. Krishnamoorthy, K.; Kanungo, M.; Ambade, A. V.; Contractor, A. Q.; Kumar, A. Electrochemically polymerized electroactive poly(3,4- ethylenedioxythiophene) containing covalently bound dopant ions: poly{2-(3-sodiumsulfinopropyl)-2,3-dihydrothieno[3,4-b][1,4]dioxin}. *Synth. Met.* **2001**, 125, 441−444.

179. Zeglio, E.; Vagin, M.; Musumeci, C.; Ajjan, F. N.; Gabrielsson, R.; Trinh,X.T.;Son,N.T.;Maziz,A.;Solin,N.;Inganaš,O.Conjugated Polyelectrolyte Blends for Electrochromic and Electrochemical Transistor Devices. *Chem. Mater*. **2015**, 27, 6385−6393.

180. Reynolds, J. R.; Sundaresan, N. S.; Pomerantz, M.; Basak, S.; Baker, C. K. Self-doped conducting copolymers: a charge and mass transport study of poly{pyrrole-CO[3-(pyrrol-1-YL)- propanesulfonate]}. *J. Electroanal. Chem. Interfacial Electrochem*. **1988**, 250, 355−371.

181. Haǩansson,A.;Han,S.;Wang,S.;Lu,J.;Braun,S.;Fahlman,M.; Berggren, M.; Crispin, X.; Fabiano, S. Effect of (3-glycidyloxypropyl)- trimethoxysilane (GOPS) on the electrical properties of PEDOT:PSS films. *J. Polym. Sci., Part B: Polym. Phys.* **2017**, 55, 814−820.

182. Shi, P.; Amb, C. M.; Dyer, A. L.; Reynolds, J. R., Fast Switching Water Processable Electrochromic Polymers. *ACS Appl. Mater. Interfaces* **2012,** *4* (12), 6512-6521.

183. Giovannitti, A.; Sbircea, D.-T.; Inal, S.; Nielsen, C. B.; Bandiello, E.; Hanifi, D. A.; Sessolo, M.; Malliaras, G. G.; McCulloch, I.; Rivnay, J. Controlling the mode of operation of organic transistors through side- chain engineering. *Proc. Natl. Acad. Sci. U.S.A.* **2016**, 113, 12017− 12022.

184. Ö sterholm, A. M.; Ponder, J. F.; Kerszulis, J. A.; Reynolds, J. R. Solution Processed PEDOT Analogues in Electrochemical Super- capacitors. *ACS Appl. Mater. Interfaces* **2016**, 8, 13492−13498.

185. Sigg, L. Redox Potential Measurements in Natural Waters: Significance, Concepts, and Problems. Redox: Fundamentals, Processes, and Applications; Schüring, J., Schulz, H. D., Fischer, W. R., Böttcher, J., Duijnisveld, W. H. M., Eds.; Springer: **2000**.

186. Rivnay, J.; Leleux, P.; Ferro, M.; Sessolo, M.; Williamson, A.; Koutsouras, D. A.; Khodagholy, D.; Ramuz, M.; Strakosas, X.; Owens, R. M.; Benar, C.; Badier, J.-M.; Bernard, C.; Malliaras, G. G. High- performance transistors for bioelectronics through tuning of channel thickness. *Sci. Adv*. **2015**, 1, 1−5.

187. Snook, G. A.; Chen, G. Z., The measurement of specific capacitances of conducting polymers using the quartz crystal microbalance. *J. Electroanal. Chem.* **2008,** *612* (1), 140-146.

188. Inal, S.; Rivnay, J.; Leleux, P.; Ferro, M.; Ramuz, M.; Brendel, J. C.; Schmidt, M. M.; Thelakkat, M.; Malliaras, G. G. A High Trans- conductance Accumulation Mode Electrochemical Transistor. *Adv. Mater*. **2014**, 26, 7450−7455.

189. Simon, D. T.; Gabrielsson, E. O.; Tybrandt, K.; Berggren, M. Organic Bioelectronics: Bridging the Signaling Gap between Biology and Technology. *Chem. Rev.* **2016**, 116, 13009−13041.

190. Stavrinidou, E.; Leleux, P.; Rajaona, H.; Khodagholy, D.; Rivnay, J.; Lindau, M.; Sanaur, S.; Malliaras, G. G. Direct Measurement of Ion Mobility in a Conducting Polymer. *Adv. Mater*. **2013**, 25, 4488−4493.

191. Inal, S.; Rivnay, J.; Hofmann, A. I.; Uguz, I.; Mumtaz, M.; Katsigiannopoulos, D.; Brochon, C.; Cloutet, E.; Hadziioannou, G.; Malliaras, G. G. Organic electrochemical transistors based on PEDOT with different anionic polyelectrolyte dopants. *J. Polym. Sci., Part B: Polym. Phys.* 2016, 54, 147−151.

192. Pacheco-Moreno, C. M.; Schreck, M.; Scaccabarozzi, A. D.; Bourgun, P.; Wantz, G.; Stevens, M. M.; Dautel, O. J.; Stingelin, N. The Importance of Materials Design To Make Ions Flow: Toward Novel Materials Platforms for Bioelectronics Applications. *Adv. Mater*. **2017**, 29, 1604446.

193. Reeves, B. D.; Unur, E.; Ananthakrishnan, N.; Reynolds, J. R., Defunctionalization of Ester-Substituted Electrochromic Dioxythiophene Polymers. *Macromolecules* **2007,** *40* (15), 5344-5352.

194. Beaujuge, P. M.; Amb, C. M.; Reynolds, J. R., A Side-Chain Defunctionalization Approach Yields a Polymer Electrochrome Spray-Processable from Water. *Adv. Mater.* **2010,** *22* (47), 5383-5387.

195. Hütter, P. C.; Fian, A.; Gatterer, K.; Stadlober, B. Efficiency of the Switching Process in Organic Electrochemical Transistors. *ACS Appl. Mater. Interfaces* **2016**, 8, 14071−14076.

196. Mawad, D.; Artzy-Schnirman, A.; Tonkin, J.; Ramos, J.; Inal, S.; Mahat, M. M.; Darwish, N.; Zwi-Dantsis, L.; Malliaras, G. G.; Gooding, J. J.; Lauto, A.; Stevens, M. M. Electroconductive Hydrogel Based on Functional Poly(Ethylenedioxy Thiophene). *Chem. Mater*. **2016**, 28, 6080−6088.

197. Duan, C.; Willems, R. E. M.; van Franeker, J. J.; Bruijnaers, B. J.; Wienk, M. M.; Janssen, R. A. J., Effect of side chain length on the charge transport, morphology, and photovoltaic performance of conjugated polymers in bulk heterojunction solar cells. *J. Mater. Chem. A* **2016,** *4* (5), 1855-1866.

198. Grand, C.; Zajaczkowski, W.; Deb, N.; Lo, C. K.; Hernandez, J. L.; Bucknall, D. G.; Müllen, K.; Pisula, W.; Reynolds, J. R., Morphology Control in Films of Isoindigo Polymers by Side-Chain and Molecular Weight Effects. *ACS Appl. Mater. Interfaces* **2017,** *9* (15), 13357-13368.

199. Giovannitti, A.; Sbircea, D.-T.; Inal, S.; Nielsen, C. B.; Bandiello, E.; Hanifi, D. A.; Sessolo, M.; Malliaras, G. G.; McCulloch, I.; Rivnay, J., Controlling the mode of operation of organic transistors through side-chain engineering. *Proc. Natl. Acad. Sci. U.S.A.* **2016,** *113* (43), 12017-12022.

200. Ponder, J. F.; Österholm, A. M.; Reynolds, J. R., Conjugated Polyelectrolytes as Water Processable Precursors to Aqueous Compatible Redox Active Polymers for Diverse Applications: Electrochromism, Charge Storage, and Biocompatible Organic Electronics. *Chem. Mater.* **2017,** *29* (10), 4385-4392.

201. Liu, J.; Kadnikova, E. N.; Liu, Y.; McGehee, M. D.; Fréchet, J. M. J., Polythiophene Containing Thermally Removable Solubilizing Groups Enhances the Interface and the Performance of Polymer−Titania Hybrid Solar Cells. *J. Am. Chem. Soc.* **2004,** *126* (31), 9486-9487.

202. Edder, C.; Armstrong, P. B.; Prado, K. B.; Frechet, J. M. J., Benzothiadiazole- and pyrrole-based polymers bearing thermally cleavable solubilizing groups as precursors for low bandgap polymers. *Chem. Commun.* **2006,** (18), 1965-1967.

203. Bundgaard, E.; Hagemann, O.; Bjerring, M.; Nielsen, N. C.; Andreasen, J. W.; Andreasen, B.; Krebs, F. C., Removal of Solubilizing Side Chains at Low Temperature: A New Route to Native Poly(thiophene). *Macromolecules* **2012,** *45* (8), 3644-3646.

204. Arroyave, F. A.; Reynolds, J. R., 3,4-Propylenedioxypyrrole-Based Conjugated Oligomers via Pd-Mediated Decarboxylative Cross Coupling. *Org. Lett.* **2010,** *12* (6), 1328-1331.

205. Arroyave, F. A.; Reynolds, J. R., Synthesis of π-Conjugated Molecules Based on 3,4-Dioxypyrroles via Pd-Mediated Decarboxylative Cross-Coupling. *J. Org. Chem.* **2011,** *76* (21), 8621-8628.